FABRICATION AND EXPERIMENTAL INVESTIGATIONS ON NANO-PARTICULATES REINFORCED Al7150 METAL MATRIX NANO COMPOSITES

Submitted in partial fulfillment of the requirements

for the award of the degree of

Doctor of Philosophy

by

PAGIDI MADHUKAR

Roll No: 715033

Department of Mechanical Engineering
NATIONAL INSTITUTE OF TECHNOLOGY
WARANGAL – 506004
Telangana State, INDIA.
January – 2020

FABRICATION AND EXPERIMENTAL INVESTIGATIONS ON NANO-PARTICULATES REINFORCED Al7150 METAL MATRIX NANO COMPOSITES

Submitted in partial fulfilment of the requirements

for the award of the degree of

Doctor of Philosophy

by

PAGIDI MADHUKAR
Roll No: 715033

Supervisors:

Dr. N. Selvaraj
Professor

Dr. C. S. P. Rao
Professor

Department of Mechanical Engineering
NATIONAL INSTITUTE OF TECHNOLOGY
WARANGAL – 506004
Telangana State, INDIA.
January – 2020

THESIS APPROVAL FOR Ph.D.

This thesis entitled **"Fabrication and Experimental Investigations on Nano-Particulates Reinforced Al7150 Metal Matrix Nano-Composites"** by **Mr. Pagidi Madhukar** is approved for the degree of Doctor of Philosophy.

Examiners

_____

_____

_____

Supervisors

Dr. N. Selvaraj

Professor
Department of Mechanical Engineering,
National Institute of Technology,
Warangal, Telangana.

Dr. C. S. P. Rao

Professor
Department of Mechanical Engineering,
National Institute of Technology,
Warangal, Telangana.

Chairman

Prof. N. Selvaraj

Head, Mechanical Engineering Department, NIT Warangal

NATIONAL INSTITUTE OF TECHNOLOGY

WARANGAL – 506 004, Telangana State, INDIA

CERTIFICATE

This is to certify the thesis entitled **"Fabrication and Experimental Investigations on Nano-Particulates Reinforced Al7150 Metal Matrix Nano-Composites"** submitted by **Mr. Pagidi Madhukar**, Roll No. 715033, to **National Institute of Technology, Warangal** in partial fulfilment of the requirements for the award of the degree of **Doctor of Philosophy in Mechanical Engineering** is a record of bonafide research work carried out by him under my supervision and guidance. This work has not been submitted elsewhere for the award of any degree.

Dr. N. Selvaraj

Professor
Department of Mechanical Engineering,
National Institute of Technology,
Warangal, Telangana.

Dr. C. S. P. Rao

Professor
Department of Mechanical Engineering,
National Institute of Technology,
Warangal, Telangana.

Place: Warangal.
Date:

.

NATIONAL INSTITUTE OF TECHNOLOGY
WARANGAL – 506 004, Telangana State, INDIA

DECLARATION

This is to certify that the work presented in the thesis entitled "**Fabrication and Experimental Investigations on Nano-Particulates Reinforced Al7150 Metal Matrix Nano-Composites**", is a bonafide work done by me under the supervision of **Prof. N. Selvaraj & Prof. C. S. P. Rao**, Department of Mechanical Engineering, NIT Warangal, India and has not been submitted for the award of any degree to any other University or Institute.

I declare that this written submission represents my ideas in my own words and where ever others ideas or words are included have been adequately cited and referenced with the original sources. I also declare that I have adhered to all principles of academic honesty and integrity and have not misrepresented or fabricated or falsified any idea/data/fact/source in my submission. I understand that any violation of the above will cause for disciplinary action by the institute and can also evoke penal action from the sources which have thus not been properly cited or from whom proper permission has not been taken when needed.

Place: Warangal.
Date :

Pagidi Madhukar
Roll No. 715033

Dedicated to

My Parents & family members

ACKNOWLEDGEMENTS

I would like to express my sincere gratitude and profound indebtedness to **Prof. N. Selvaraj & Prof. C. S. P. Rao**, Department of Mechanical Engineering, National Institute of Technology, Warangal for giving me an opportunity to carry out doctoral work under his esteemed supervision. This work is a reflection of his thoughts, ideas and concepts. **Prof. C. S. P. Rao** looks at things in the right perspective, and it has truly been a learning experience working with him. I owe a lot to him for making me a part of the continuity of the profession.

I extend my sincere gratitude to **Prof. N. V. Ramana Rao,** Director, National Institute of Technology Warangal, India for providing the necessary facilities and encouragement throughout my work.

I am thankful to **Prof. N. Selvaraj**, Head, Department of Mechanical Engineering, NIT Warangal and other faculty members for their encouragement and support extended during this period.

It's my great opportunity to express my deepest gratitude to the Departmental Scrutiny Committee members, **Dr. P. S. C. Bose**, Associate Professor and **Dr. M. J. Davidson**, Associate Professor, Department of Mechanical Engineering, and **Dr. D. Dutta**, Professor, Department of Mathematics for their adeptness and many discussions during the research period.

I am special thankful to **Dr. Veeresh Kumar G.B**, Assistant Professor, Department of Mechanical Engineering, NIT Andhra Pradesh for encouragement and technical support throughout my research.

I am thankful to **Dr. M. Raja Vishwanathan**, Head of Humanities & Social Science Department, NIT Warangal for spending valuable time to proof reading of the papers and useful suggestions during this period

I express my sincere thanks to my co-scholars **Pagidi Aruna** (sister), **M. Vinod Babu,**

Punugupati Gurabvaiah, M. Mohan Babu, K. Rakesh, Suresh Gudipudi and seniors **T. Gopala Rao, Kishore Kumar Kandi, R. Seetharam, D. Harinder** and NIT Warangal for their support and help in completion of this thesis.

I would like to extend my heartfelt thanks to Mr. B. Rangilal, Mr. G. Ilaiah and K. Raju, technicians of Production Engineering Lab, and M.V. Vijay Kumar, MED office and Workshop members of NIT Warangal for their constant help and encouragement.

A special debt of deep gratitude to my parents and family members for their unceasing sacrifices, endeavors and encouragement.

Finally, I would also like to acknowledge the help given by all the persons who have directly or indirectly supported the work.

Pagidi Madhukar

PUBLICATIONS RELATED TO THIS THESIS

Publications in Journals:

1. ***Pagidi Madhukar,*** Selvaraj, N., Raghavendra Gujjala, Chilakalapalli Surya Prakasa Rao, Production of high performance AA7150-1% SiC nanocomposite by novel fabrication process of ultrasonication assisted stir casting. Ultrason. Sonochem. 58, 104665, https://doi.org/10.1016/j.ultsonch.2019.104665 (2019). ***(SCI and SCOPUS indexed with Impact Factor:7.279)***
2. ***Pagidi Madhukar***, Selvaraj, N., Rao, C.S.P., Veeresh Kumar, G.B. Tribological behavior of ultrasonic assisted double stir casted novel nano-composite material (AA7150-hBN) using Taguchi technique. Composites Part B, 175, 107136, https://doi.org/10.1016/j.compositesb.2019.107136 (2019). ***(SCI and SCOPUS indexed with Impact Factor:6.864)***
3. ***Pagidi Madhukar***, N Selvaraj, C S P Rao, G B Veereshkumar, Fabrication and Characterization Two Step Stir Casting with Ultrasonic Assisted Novel AA7150-hBN Nanocomposites, Alloys and Compounds, 152464, https://doi.org/10.1016/j.jallcom.2019.152464, (2019). ***(SCI and SCOPUS indexed with Impact Factor:4.175)***
4. ***Pagidi Madhukar***, N Selvaraj, Gurabvaiah Punugupati, Veeresh Kumar GB, C S P Rao, S K Mishra, Microstructure Studies of AA7150-hBN Nanocomposites, Material Research Express, https://doi.org/10.1088/2053-1591/ab48ad, (2019). ***(SCI and SCOPUS indexed with Impact Factor:1.445)***
5. ***Pagidi Madhukar***, N Selvaraj, C S P Rao, S K Mishra, Gurabvaiah Punugupati, Fabrication of Light Weight Metal Matrix Nanocomposites using Ultrasonic Cavitation Process: A State of Review, Materials Science Forum, Vol. 969, pp. 882-888, https://doi.org/10.4028/www.scientific.net/MSF.969.882 (2019). ***(SCOPUS)***
6. ***Pagidi Madhukar***, Selvaraj, N., Rao, C.S.P. Manufacturing of aluminium nano hybrid composites: a state of review. IOP Conf. Ser.: Mater. Sci. Eng. 149 12114, doi:10.4028/www.scientific.net/MSF.969.882 (2016). ***(SCOPUS)***
7. ***Pagidi Madhukar***, N Selvaraj, Vipin Mishra, CSP Rao, Optimization of Wear Parameters of AA7150-TiC Nanocomposites by Taguchi Technique. Advances in intelligent systems and computing, (NOIEAS -2019), ***(SCOPUS) Accepted for Springer publication.***
8. ***Pagidi Madhukar***, N Selvaraj, C S P Rao, A State of Review of Digital Conjugate Surfaces, Advances in intelligent systems and computing, (NOIEAS -2019), ***(SCOPUS) Accepted for Springer publication.***

Presented in International Conferences:

1. ***Pagidi Madhukar***, C.S.P. Rao, N. Selvaraj, Mechanical and Microstructure Studies of Two Step Stir Casted AA7150-TiC Nanocomposite, Presented on ICSTEM-2019 Conference, Berlin, Germany.
2. ***Pagidi Madhukar***, N Selvaraj, C S P Rao, Ultrasonic Cavitation Process for Aluminium Metal Matrix Nanocomposite: A REVIEW, ISME Conference, 2018, NIT-Warangal
3. ***Pagidi Madhukar***, N Selvaraj, C S P Rao, Effect of Sliding Distance and Applied Load on Double Stir Casted AA7150-1%TiC Nanocomposite, ISME Conference, 2018, NIT-Warangal. Accepted in Book Chapter.

Research Papers under Review/Communicated:

1. ***Pagidi Madhukar***, N Selvaraj, Veeresh Kumar GB, C S P Rao, Effect of Nano B_4C Particles on Mechanical Properties of Vortex-Double Stirred Ultrasonic Assisted Casted AA7150 Nanocomposites, *Submitted to Material Processing Technology, under review (Elsevier)*.
2. ***Pagidi Madhukar***, N Selvaraj, Veeresh Kumar GB, C S P Rao, Enhanced Performance of AA7150-SiC Nanocomposites Synthesized by Novel Fabrication Process, *Submitted to Ceramics International, under review (Elsevier)*.
3. ***Pagidi Madhukar***, N Selvaraj, Veeresh Kumar GB, C S P Rao, Microstructure and mechanical behaviour of AA7150-TiCnp nanocomposites fabricated by advanced novel fabrication process of ultrasonic assisted casting, *Submitted to Composite Part B, with Editor, (Elsevier).*
4. ***Pagidi Madhukar***, N Selvaraj, Veeresh Kumar GB, C S P Rao, Mechanical and Microstructure Studies of TiC Nano-Particulates reinforced metal matrix composites, *Submitted to Materials Letters, under review (Elsevier)*.

ABSTRACT

This research has successfully introduced a novel fabrication process which deals with the combination of vortex, double stir caste, ultrasonic vibration to manufacture AA7150-hBN, AA7150-SiC, AA7150-TiC, AA7150-B4C nanocomposites and AA7150-hBN-B4C hybrid nanocomposites with the nanoparticulate reinforcement varying from 0.0 to 2.0 wt% in the steps of 0.5 wt%. The effect of nanoparticle reinforcement on microstructure, density, microhardness, porosity and ultimate tensile strength was studied. An optical microscope was used to find the grain formation and grain refinement while electron microscopy was used for ceramic nanoparticle distribution studies and factographic studies of fracture surface. Energy Dispersive X-Ray Spectroscopy and X-ray diffraction were used to study the chemical composition of various composites and reinforcement particles. Significant enhancement was observed in mechanical properties at as-cast state of composites with the independent of nano reinforcement particles. Nevertheless, AA7150-1.5 wt% nanocomposite exhibited enhanced performance as compared to base material and other nanocomposites in the present study. Increase in hBN wt%, increased the hardness and strength (151.3-180.2 HV and 141-255 MPa) of the nanocomposites due to uniform distribution, grain refinement and hard phase particles, which promotes load bearing capacity. Further increment in hBN wt% decreases hardness and strength due to voids, clusters and agglomerations. Wear studies on AA7150-hBN nanocomposite were studied and found the wear loss of nanocomposites decreased with the increase in the hBN nanoparticles reinforcement due to hardness enhancement, which leads to seizure and wear resistance. Graphical representation of wear results confirmed that the load has greatest influence on wear loss and temperature due to higher frictional forces. SEM images of wear surface reveals that the wear is an abrasive type with restricted plastic deformation and acted as protective layer at 1.5 wt% hBN, 3 wt% hBN reveals more debris, oxide layer and delamination on wear surfaces.

AA7150-1.5% SiC nanocomposite showed 83.47% reduction in porosity, 23.9% enhancement in microhardness, 60.1% in ultimate tensile strength; Similarly, maximum grain refinement of the TiC nanocomposite is 41.07 μm and minimum porosity is 0.37% which was decreased by 52.37% (86.23-41.04 μm) and 69.87% (1.23-0.37%) as compared to AA7150 matrix alloy material. The microhardness and tensile strength of AA7150-1.5%TiC

nanocomposites at as-cast case enhanced due to novel fabrication process followed by UV treatment effect. These properties of nanocomposites are 177.05 HV and 175 MPa, which are enhanced by 17.40% (150.81-177.05 HV) and 48.31% (118-175 MPa) as compared to AA7150 alloy matrix respectively; In case of AA7150-B_4C, porosity decreases while increasing the B4C nano particle content at the observed minimum of 1.5% B4C (0.11%). Micro-hardness improved by 154.5-192.4 HV (57.7%) Ultimate tensile strength significantly improved by114.7-180.9MPa (24.5%) and found to have optimal properties at 1.5% B4C. Maximum ductility of 16.27% was reported at optimal weight percentage of B4C. Fractographic studies reveal the brittle nature of failure in nanocomposites. In (B4C-hBN) hybrid nanocomposite, porosity decreases while increasing the particle content and observed minimum at 1.5% B4C-hBN (82.03%). Micro-hardness, ultimate tensile, and yield strength significantly improved by 150.81-194.7 HV (29.10%), 94-192 MPa (104.25%), and 35-58 MPa and found to have optimal properties at 1.5% (B4C-hBN). Fractographic studies reveal the failure of AA7150-hBN, AA7150-SiC, AA7150-TiC, AA7150-B4C nanocomposites and AA7150-hBN-B4C hybrid nanocomposites are semi-brittle in nature.

Keywords: *AA7150, hBN, SiC, TiC, B4C, Ultrasonic, Stir Casting, Metal Matrix, Nanocomposites, Nanoparticles, Microstructure, Mechanical Properties.*

TABLE OF CONTENTS

Description **Page No.**

LIST OF TABLE

Page No.

LIST OF FIGURES

Page No.

NOMENCLATURE

AFM	Atomic Force Microscopy
Al	Aluminium
Al_2O_3	Aluminium Oxide
Al-MMCs	Aluminium Metal Matrix Composites
AMC	Al-Matrix Composites
ANOVA	Analysis of Variance
ASTM	American Society for Testing and Materials
B	Boron
B_4C	Boron Carbide
BLA	Bamboo Leaf Ash
BN	Boron Nitride
C	Carbon
CB	Carbon Black
CCA	Corn Cob Ash
Co_3O_4	Cobalt Oxide
Co-dep	Co-deposition
COF	Coefficient of Friction
CTE	Coefficient of Thermal Expansion
Cu	Copper
CV	Cyclic Voltametry
DSC	Differential Scanning Calorimetry;
DTA	Differential Thermal Analysis;
e	Exponential
EDS	Energy Dispersive X-Ray Spectroscopy
EIS	Electrochemical Impedance Spectroscopy
EN31	European Standards 31
Eq	Equation
et.al.	et all

etc	etcetera
FA	Fly Ash
Fe	Iron
$FeAl_2O_4$	Iron Aluminate
g/cc	Gram per cubic meter
GPa	Giga Pascal
Gr	Graphite
hBN	Hexagonal Boron Nitride
HC	Hybrid Composite
HMMC	Hybrid Metal Matrix Composite
HPT	High Pressure Torsion
Hz	Hertz
i.e.	That is
K_2TiF_6	Di-potassium Titanium Hexafluoride
kgs	Kilo Grams
km	Kilo meter
kN	Kilo Newton
kW	Kilo Watts
L/M	Liquid Metallurgy
LSV	Liner Sweep Voltametry
LVDT	Linear Variable Differential Transformer
m/s or ms^{-1}	Meter/Second
MA	Mechanical Alloying
Mg	Magnesium
Mg_2Si	Magnesium Silicide
min	Minutes
MM	Mechanical Milling
mm	Millimeter
MMCs	Metal Matrix Composites
MMNC	Metal Matrix Nano-Composite
Mn	Manganese

MPa	Mega Pascal
N	Newton
NaCl	Sodium Chloride
nm	Nano meter
OCP	Open Circuit Corrosion Potential
OM	Optical Microscope
P/M	Powder Metallurgy
POD	Pin-On-Disc
RHA	Rice Husk Ash
SEM	Scanning Electron Microscope
Si	Silicon
Si_3N_4	Silicon Nitride
SiC	Silicon Carbide
SiO_2	Silicon Dioxide
SPS	Spark Plasma Sintering
T6	Solution Heat-Treated and Artificially Aged
TDIF	Temperature Dependent Internal Friction Measurement
TEM	Transmission Electron Microscope
TGA	Thermal Gravimetric Analysis;
Ti	Titanium
TiB_2	Titanium Diboride
TiC	Titanium Carbide
TiO_2	Titanium Dioxide
UST	Ultrasonic Treatment
UTM	Universal Tensile Machine
UTS	Ultimate Tensile Strength
UV	Ultrasonic Vibration
v	volts
V_f	Volume Fraction
Vol %	Volume percentage
wt	Weight

wt%	Weight Percentage
XRD	X-Ray Powder Diffraction
Zn	Zinc
ZrB_2	Zirconium Diboride
μm	Micro meter
%	Percentage
^oC	Degree Centigrade

CHAPTER -1
INTRODUCTION

This chapter deals with a brief introduction and broad classification of engineering materials and composite materials based on matrix phase as well as Reinforcement Phase (second phase) particles. The discussion was extended to fabrication methods of metal matrix composites and their need for the present industrial demand.

1.1 Engineering materials

Engineering materials are materials that are used to develop various components and structures in engineering sectors. The fundamental objective of an engineering material is to hold and withstand applied loading without much deflection or breaking. The different main parts of engineering materials are: ceramics, metals, polymers and composites. The main classifications of the materials are discussed below in **Figure 1.1.**

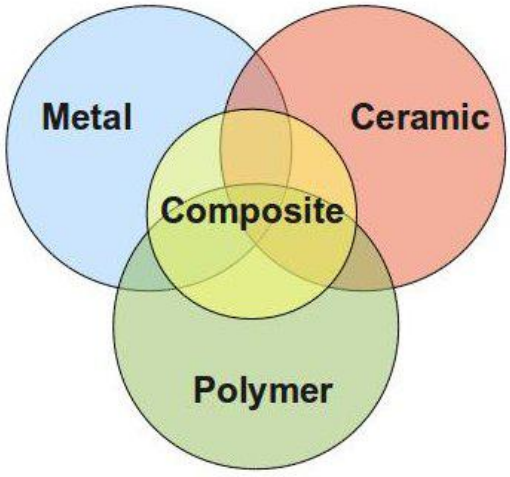

Figure 1. 1 Broad classification of engineering materials.

1.1.1 Metals

It is a material which conducts heat and electricity. Metals are well defined crystal structures and are typically *ductile* or *malleable*. Among several ferrous and non-ferrous metallic materials, Aluminium (Al) is the world's 3rd most natural element and abundant metal comprising 8% of the earths' crust. Pure Al is corrosive resistant, ductile, soft, and has high electrical conductivity. Al material is the lightest engineering metal and has superior

strength to steel due to its high strength to weight ratio coupled with corrosion resistance. Al-alloys play a dominating role in the different engineering sectors and has a quintessential alloying element like Silicon (Si), Copper (Cu), Zinc (Zn), Magnesium (Mg), Manganese (Mn), and Tin (Sn) as minor alloying elements.

1.1.2 Ceramics

It is a solid material involving a non-metallic, inorganic compound of metal which has complex or amorphous crystalline structure with robust ionic bonds. Ceramic materials are hard, brittle and strong in compression but weak in terms of tension as well as shear. These ceramics can also withstand high temperature up to 1500^{o}C.

1.1.3 Polymer

Polymers are “generally long chain of organic macro-molecules with covalent bonds. Each molecule is formed from a large number of unitary molecules known as Monomer and some polymers have molecules which cross link with each other by increasing the strength across the molecules”. Polymers can be stretched & bent easily due to this reason and are bad conductors of heat and electricity with good elasticity and plasticity property.

1.1.4 Composites

A composite is a “material made from two or more constituent materials with significantly different physical or chemical properties that, when combined together, produce a material with characteristics different from the individual components”. This new composite material may be adopted for many reasons such as being less expensive, lighter, stronger, less corrosive and wear.

Composite materials are classified into two categories based on matrix phase and reinforcement phase.

1.1.4.1 Matrix phase

It is a main phase with a continuous nature. It generally holds the reinforcement and increases the load bearing capacity of composites by distributing the loads to dispersed phase. This phase usually contains materials which are less hard and more ductile in nature.

1.1.4.2 Reinforcement or dispersed phase

It is a 2nd phase material which is dispersed in the primary phase in a discontinuous form. This phase is stronger, harder and brittle than the primary phase.

Based on matrix phase, the composites are further classified into three categories such as metal, polymer and ceramic matrix composites. Polymer matrix composites are divided further into two composites like thermoplastics and thermosets. Reinforcement based composites are further divided into structural, fibrous (continuous and discontinuous with aligned or random oriented), and particles reinforced (large particles, dispersion strengthened - micro and nano level size) composites. The detailed classification is shown in **Figure 1.2**.

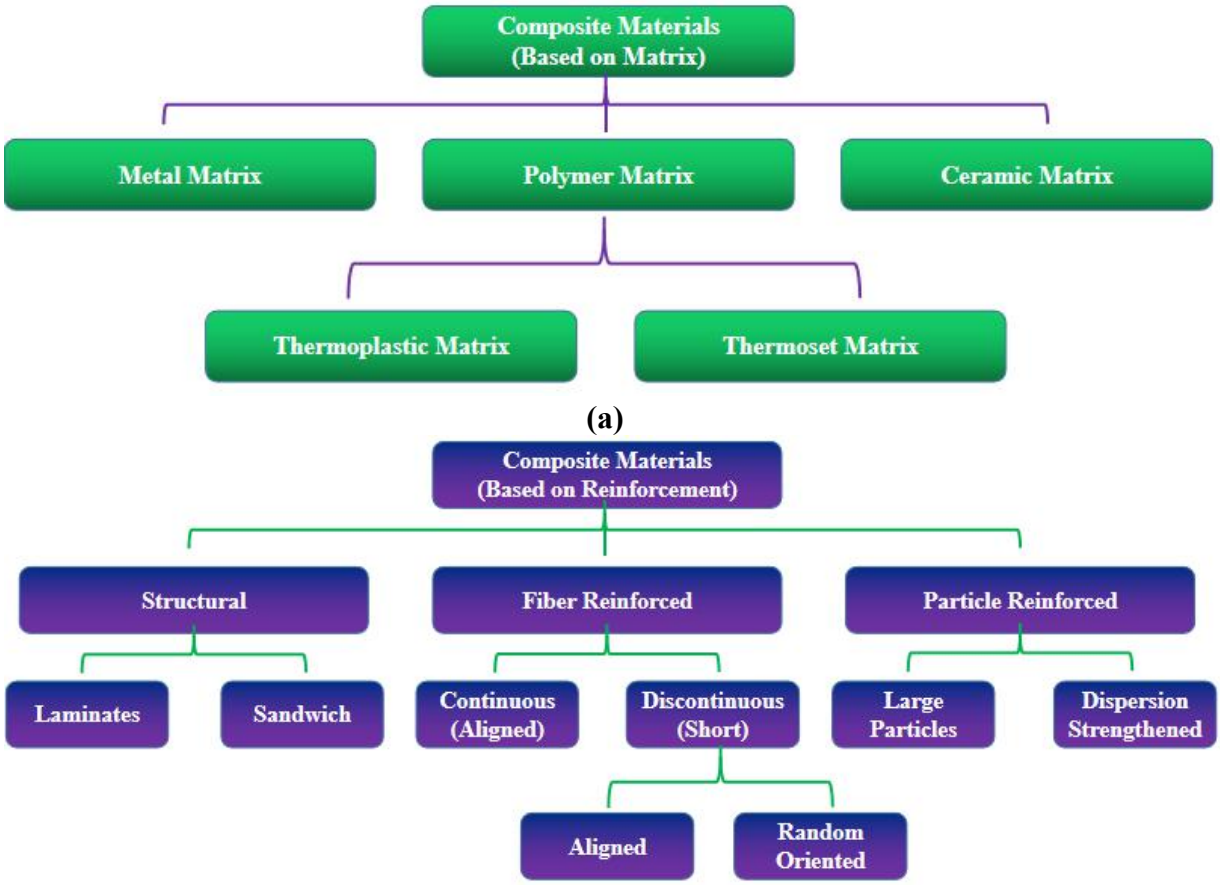

Figure 1. 2 Classification of composites based on (a) matrix and (b) reinforcements.

Nano-particles reinforced composite materials are different from micro-particles reinforced composites and alloys due to their superior surface area to volume ratio. Nanocomposites are special purpose materials with a nanostructure. Reinforcement particles may be made of fibers (electrospun fibers or nanotubes) or particles such as Titanium Carbide

(TiC), Boron Carbide (B_4C), Titanium Diboride (TiB_2), Silicon Nitride (Si_3N_4), Silicon Carbide (SiC), Hexagonal Boron Nitride (hBN), Titanium Dioxide (TiO_2), Silicon Dioxide (SiO_2), Graphite (Gr), Aluminium Oxide (Al_2O_3), etc,. In conventional composites, interfacing area between reinforcements and matrix are typically less than that of nanocomposites and properties of matrix material are significantly affected by the nature and size of reinforcements. A small amount of nanoparticles create a large amount of surface area which can affect the macro-scale properties of composite materials. For example, incorporation of nanopowder as a reinforcement into matrix material. Nanoparticles may result in enhanced mechanical properties such as enhanced strength, stiffness, corrosion, wear and fatigue resistance. The addition of a certain percentage of nano-sized reinforcement into the matrix during the fabrication process is low (percentage by weight of nanoparticles is the order of 0.5% to 5.0%) due to low filler percolation threshold.

A Metal Matrix Composite (MMC) is a "composite material with at least two constituent parts, one being a metal and the other non-metal, ceramic material such as TiC, SiC, B_4C, or organic Rice Husk Ash (RHA), Bamboo Leaf Ash (BLA), Fly Ash (FA), Carbon compound are most commonly used. When more than one reinforcement materials are added into the matrix then, it is called a "hybrid composites". The detailed graphical represented in **Figure 1.3**.

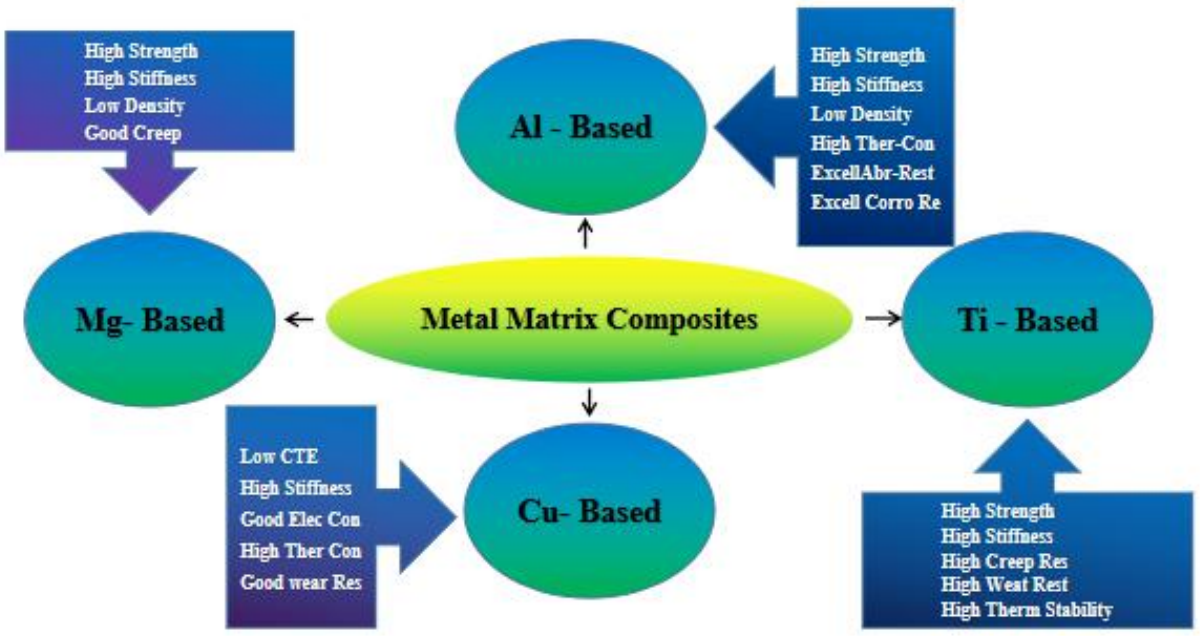

Figure 1. 3 Classification of MMCs.

Al-Matrix Composites (AMC) are a large group in MMCs. These composite matrices vary from 1XXX to 9XXX alloy series and are fabricated by Powder Metallurgy (P/M) and Liquid Metallurgy (L/M) methods in which, liquid metallurgy method via stir casting technique is most widely adopted owing to its various benefits in the fabrication of particulate reinforced MMCs. The typical advantages of AMCs are high stiffness, strength and thermal conductivity, low density and excellent abrasion resistance. It has a wide range of applications in automobile industry, as brake rotors for high speed trains, core wires in electric cables and aerospace (wings, fuselage frames, seat rails) industry.

1.2 Manufacturing methods for MMCs

MMCs are fabricated through various methods such as In-situ, Co-deposition (Co-dep), Solid and Liquid states techniques. The detailed fabrication techniques and further classifications are shown in the following **Figure 1.4**.

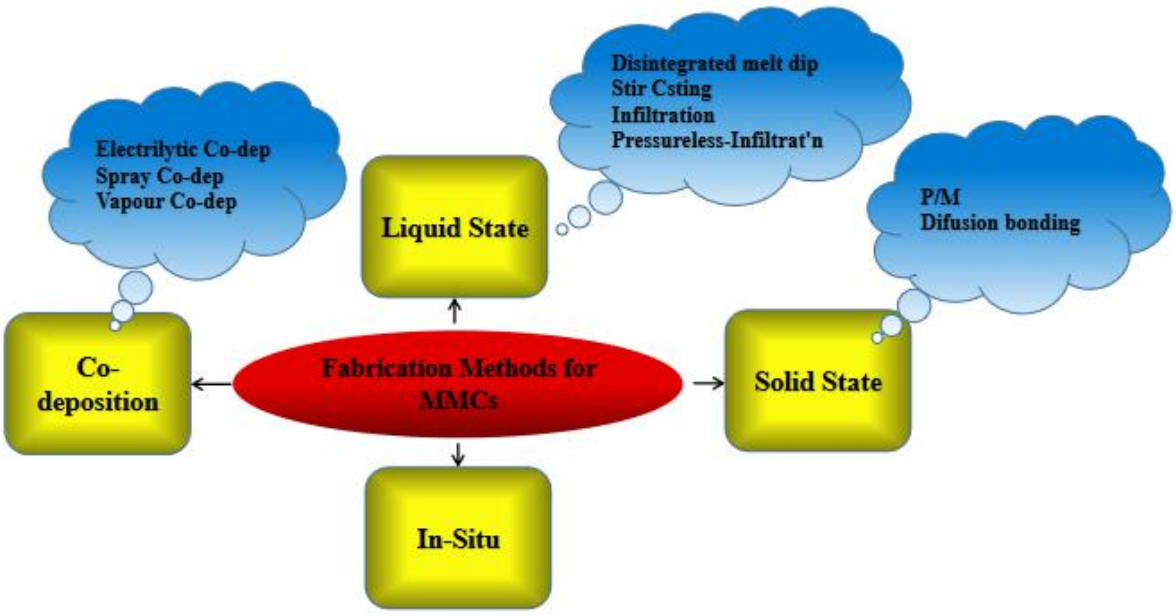

Figure 1. 4 Different fabrication methods for MMCs.

Stir casting is a recommended technique to manufacture MMCs because of its ease with which the MMCs are fabricated, economical as well as mass production is possible. This process contains a mechanical impeller to stir the molten liquid metal continuously. During this process, there is an opportunity to oxidation of the matrix phases. Oxidation plays a crucial role on the metal surface and reduces the wettability, which results in improper mixing of secondary phase particulates. To avoid formation of metallic oxidation during the process an inert gas (argon, helium, krypton, xenon) is used along with wettability agents (Borax, Di-

potassium Titanium Hexafluoride (K_2TiF_6), and Mg) to improve wettability between dispersion phase and matrix phase. Apart from these problems, uniform distribution of reinforcements in the molten liquid phase is another challenge typically faced during the stir casting method., which is controlled by stir casting process parameters. Therefore, stirring parameters such as blade diameter, angle, stirring speed, and stirring time as well as position of stirrer in a molten liquid play a critical role in uniform distribution of second phase particles in the matrix phase (Madhukar et al., 2016).

1.2.1 Ultrasonic vibration assisted casting

Homogeneous distribution of second phase particles is an important aspect in molten phase to produce quality composites. It is very difficult to produce due to high viscosity of molten liquid and poor wettability which leads to agglomeration/cluster formation. Mechanical rotary stirring may be required for homogeneous mixing of particles and improving the quality of composite but it increases the cost of fabrication process in the case of nanoparticles. To minimize the cost and improve the quality of composite, ultrasonic probe assisted fabrication process has been used (Xia Zhou et al., 2014). The following **Figure 1.5** shows the stir casting and ultrasonic fabrication processes for the nano-particulates reinforced MMCs. During the fabrication process, atmospheric air interacts with the reinforcement particles and forms the metallic oxides, because of Al is very much prone to oxidation in normal atmosphere which form slag, clusters/agglomerations that lead to poor wettability and also, degrade the properties of MMCs. To avoid such problems, an argon-controlled atmosphere was used to fabricate Al-MMCs.

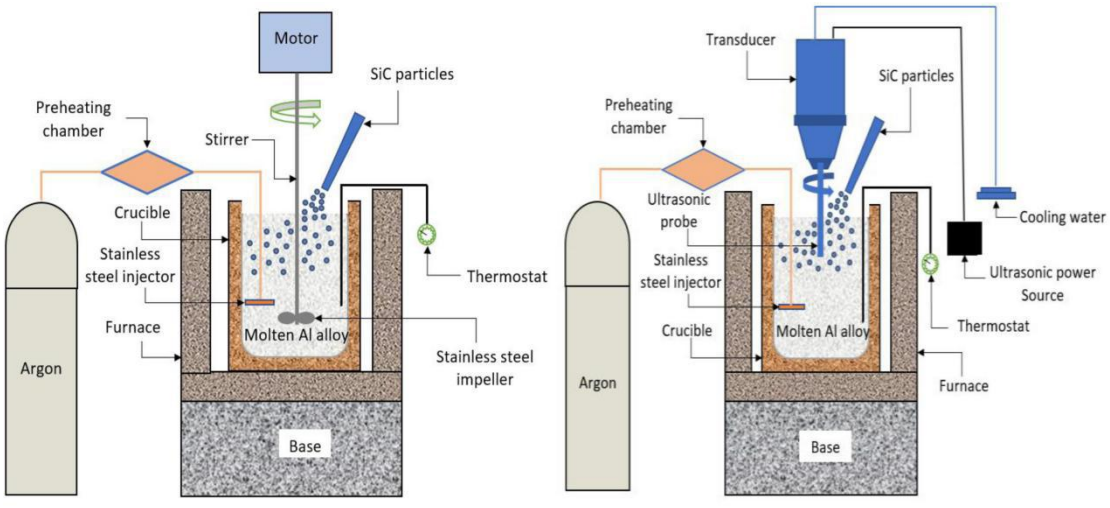

Figure 1. 5 Fabrication of MMCs (a) Stir casting method (b) Ultrasonic treatment method.

1.3 Material characterization and testing methods

Characterization of material is defined as the study of *composition* and *structure* (including defects) of a material that are significant for a particular preparation, study of properties, or use, and suffice for reproduction of material". The detailed characterization for a material is graphically shown in **Figure 1.6**.

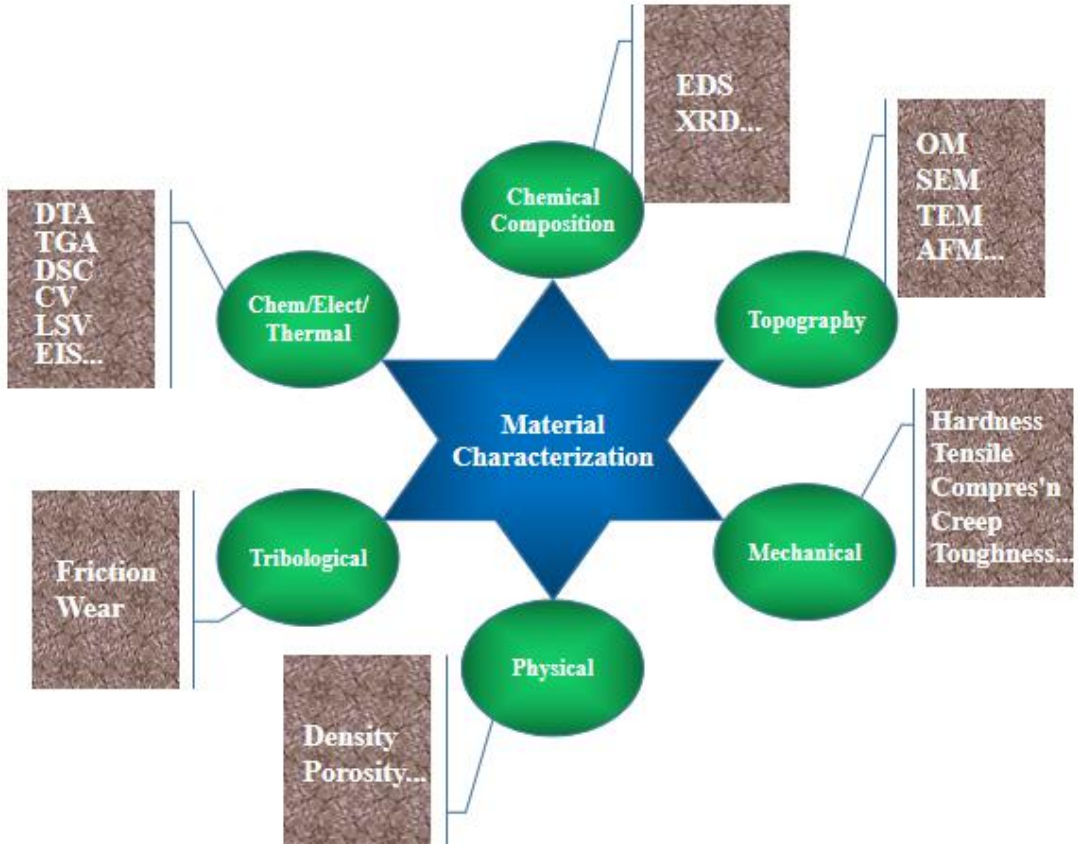

Figure 1. 6 Characterization of materials and testings.

**Chem/Elect/Thermal= Chemical/Electrical/Thermal Properties; DTA=Differential Thermal Analysis; TGA= Thermal Gravimetric Analysis; DSC=Differential Scanning Calorimetry; CV= Cyclic Voltametry; LSV= Liner Sweep Voltametry; EIS=Electrochemical Impedance Spectroscopy; OM= Optical Microscope; SEM=Scanning Electron Microscope; TEM= Transmission Electron Microscope; AFM= Atomic Force Microscopy; EDS= Energy Dispersive X-Ray Spectroscopy; XRD=X-Ray Powder Diffraction*

1.4 Need of composite materials

The main advantage of a composite material over conventional material is the combination of different properties which are not often found in the conventional materials. Nowadays, nanocomposites are becoming more popular due to tremendous advantages they bring and the number of applications they promise. Leading manufacturing industries are thus concentrating on as well as spending lots of money on nano material research and

development. A composite material is "composed of at least two materials, which combine to give superior to those individual constituents". The major reason for choosing the composite material is due to its light weight relative to its strength and stiffness. For example; a composite reinforced with carbon fiber is 5 times stronger than steel (Grade:1020) with $1/5^{th}$ the weight of steel. Al6061 alloy is very close to the weight of carbon fiber reinforced composite and somewhat heavier but the composite has 7 times strength and 2 times the modulus. Therefore, demands for composites across the globe is increasing and composite industries are being set up for designing new materials for industrial applications like aerospace, automobile, marine and other engineering domains.

1.5 Summary

This chapter deals with the nanocomposites and their benefits over micro-composites as well as monolithic materials. The chapter also discusses broad classification of engineering materials and composite materials based on matrix phase as well as second phase particles. The discussion was extended to fabrication methods of metal matric composites and their classification, especially Al-MMCs and stir casting process.

CHAPTER -2
LITERATURE REVIEW

This chapter represents the literature review of the research work carried out by the researchers on MMCs from the past two decades and discussed liquid state manufacturing processes and characterization of MMCs in detailed.

2.1 Introduction

From the last two decades, researchers are aiming for Al and Mg alloys because of their high strength to weight ratio. The traditional fabrication methods for lightweight MMCs involve mechanical stirring, P/M, squeeze casting and semisolid stirring. In recent years, ceramic particles have been scaled up to nano-size such as nano Al_2O_3, SiC, B_4C, hBN, TiC, TiB_2, etc, for use as reinforcements to form Metal Matrix Nano-Composite (MMNC). There are several ways to produce MMNCs, two popular methods being P/M and L/M routes. The casting process is a liquid phase method to manufacture a component with highly complex shapes. But getting uniform dispersion and distribution of ceramic particle in a metallic liquid is highly difficult and challenging task, due to its poor wettability, gravity segregation, oxidation of matrix materials, high viscosity as well as huge ratio of surface to volume. Since the fabrication of MMNCs through P/M route is very costly and also, involves series of processes like, selection of proper size and distribution of particulates of both matrix and reinforcements, blending, mixing, lubrication, compaction, sintering and secondary processes post fabrication, considering these challenges, in the present investigation the fabrication of MMNCs is planned by fallowing liquid metallurgy method via stir casting route.

2.2 Fabrication methods through liquid casting

2.2.1 Stir casting route

Rotor and ceramic crucible reservoir are used to distribute the reinforcement particles into molten matrix materials by mechanical stirring. It contains heating furnace with electric resistance coil to melt the base metal, feeding mechanism for ceramic nanoparticles and a mechanical stirrer connected to an electrical motor to mix the preheated nanoparticles in matrix liquid. Researchers have fabricated hybrid MMCs through stir casting method

(Thirumalai Kumaran S et al., 2015; Jaswinder Singha et al., 2015; Rajmohan T et al., 2013; Thirumalai T et al., 2014) and conducted experiments to analyze it in various aspects; in one such attempt, Radhika et al., 2013, studied Hybrid Composite (HC) of AlSi10Mg reinforced with Al_2O_3 & Gr and unreinforced alloy specimens they performed microstructural analysis as well as examined mechanical properties such as tensile strength, double shear strength and hardness of HC with that of unreinforced alloy. They found that hybrid MMCs had higher values than that of unreinforced alloy. The tribological behavior of HCs was studied using Pin-On-Disc (POD) test machine, and it was concluded that the HCs had higher wear resistance compared to unreinforced alloy and wear debris; worn out surfaces analyses were studied by SEM. Pradeep Sharma, et al., 2016, developed HC of AA6082-Si_3N_4 & Gr, and investigated mechanical properties and micro structure with analysis done using SEM, and XRD. Both micro as well as macro hardness and tensile strength of HCs were examined and notice the enhancement in the properties.

2.2.2 Compo casting (Two step stir casting) method

A recent interesting development involves matrix material heating above its melting temperature and then cooling it to a certain temperature between liquid-solidus points. At this stage, preheated nano reinforcement particles are added and mixed. The slurry is heated again to get it to liquid state and stirred thoroughly. It was used to prepare HCs by different nano reinforcement particles such as Bamboo Leaf Ash (BLA) & Al_2O_3 (Alaneme K K et al., 2014) in the Al–Mg–Si alloy (Prakash C H et al., 2011) as a base material; in such connections, through two-step stir casting (Dora Siva Prasada et al., 2014) was used to enhance various properties. Kenneth Kanayo Alaneme et al., 2014 investigated the wear and corrosion behavior of Al–Mg–Si alloy material reinforced with rice husk and SiC particles, which was fabricated through double stir casting technique. Potentio dynamic polarization measurements and open circuit corrosion potential (OCP) were used to steady corrosion behavior. The corrosion resistance was improved by reinforcement of SiC and RHA; SiC had great corrosion as well as wear resistance.

Kenneth Kanayo Alaneme et al., 2013 investigated the wear and corrosion behavior of Al–Mg–Si alloy material reinforced with RHA and Al_2O_3 particles, which was fabricated through double stir casting technique. The results indicated that Al-Mg-Si/10wt.% Al_2O_3 single reinforced composites were superior to hybrid MMCs in Sodium Chloride (NaCl) 3.5%

solution. Corrosion rate increased with increasing Weight Percentage (wt.%) RHA in the HCs while wear rate also increases with the addition of wt.% RHA.

2.2.3 Ultrasonic assisted stir casting method

The experimental set up consists of a heat furnace with resistance to melting base metal, a gas protection system, a feeding mechanism with nanoparticles and ultrasonic process system. The equipment has mild steel crucible of 127 mm height and 114 mm inside diameter, which is used for melting base metal matrix. In ultrasonic process, a probe, which is made up of Niobium C-103 alloy and Ti alloy, is used due to its high-temperature resistance property and because it does not react with molten liquid during the sonication process, to produce maximum 4 kw power output and 17.5-20 kHz frequency for melting process; the niobium probe, 39cm in length and 35mm in diameter, is dipped into the melt pool and in case of Ti alloy probe, 115 mm in length and 20 mm in diameter to achieve effective sonication. The ultrasonic processing melt temperature is about 700-800 degree centigrade ($^{\circ}$C). This process is performed after adding pre-heated ultra-fine (nano) ceramic particles through steel tube into the matrix melt and the process can refine grain size of matrix material significantly and disperse as well as distribute homogeneously after finishing the ultrasonic test in molten matrix; the processed liquid is than poured into a preheated (about 500°C) permanent steel mold cavity to cast the MMNCs.

2.2.4 The effect of ultrasonication

The treatment of ultrasonic for liquid metals is a dynamic, cost-effective and environmentally friendly process. Since the 1950s, Ultrasonic Treatment (UST) has been implemented and it shows ultrasound application during the solidification process of liquid metals, this technique is introduced to produce a broad area of MMNCs. In the current UST process, the strongest non-linear effects are generated in molten metal alloy based on great intensity of ultrasonic waves, namely, acoustic streaming and transient cavitation. Additionally, the transient miniaturized scale problem areas with a temperature of around 5000 K, and pressure of above 1000 atm can be settled. The solid effect of combination with confined elevated temperature can clear the molecule surface, break nanoparticles groups, enhance their wettability and circulate nanoparticles inside the molten metal. Ultrasonic probe vibrations carried out at the time of solidifying liquid metal results in the following (Jin Ho Bang et al., 2012):

I. Reduction in porosity by degassing
II. Particle and grain refinement of primary phase
III. Grain duplication because of dendrite fragmentation and increase in nucleation because of initiation of substrates through wetting
IV. During the debacle of cavitation bubbles exertion of large acoustic pressures which cause reduction in segregation and agglomeration
V. Dispersion as well as distribution of immiscible or solid form through natural process as well as acoustic micro-streaming

2.2.4.1 Dispersion of nanoparticles

It is very tricky to circulate nano-sized particles in a liquid medium because of their higher surface to weight ratio as well as poor wettability; these nanoparticles form clusters because of their surface property when mixed with a liquid medium or when they are exposed to the atmosphere and cluster formation as shown in **Figure 2.1** with and without sonication. So, the new fabrication method gets rid of nano-clusters to get uniform distribution. In this process, uniform distribution and breaking of nano-clusters take-place because of acoustic streaming phenomena.

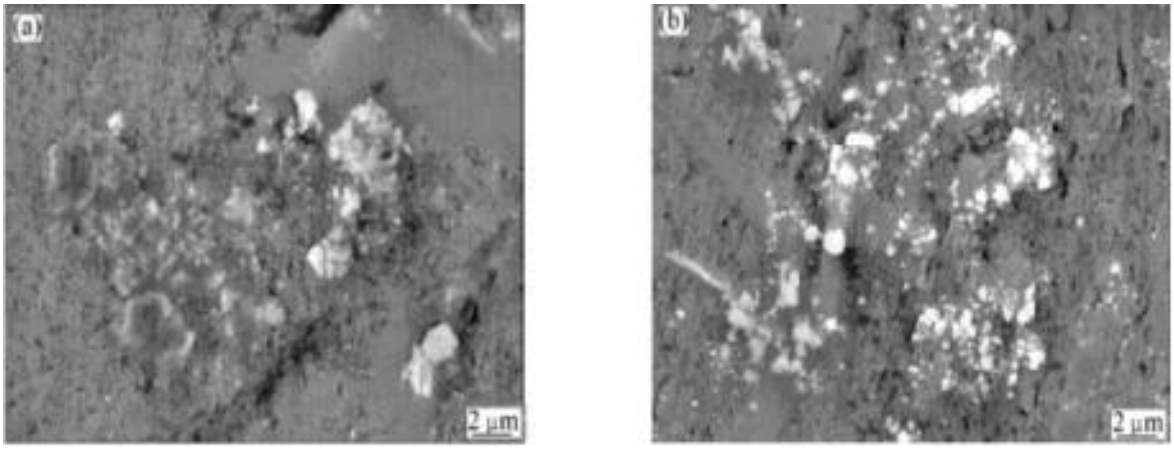

Figure 2. 1 SEM image (a) Without high-energy ultrasonic field (b) With high-energy ultrasonic field (Song-Li Zhang et al., 2014).

2.2.4.2 Acoustic streaming

Lan J et al., 2010, found that in contrast with conventional energy sources, ultrasonic illumination stipulates fundamentally odd response conditions (a brief span of too many high temperatures and in addition pressures in fluids) that can't be acknowledged by different strategies strikingly, and such exceptional situations are not obtained in a straightforward

fashion from ultrasound vibration. Acoustic wavelengths are significantly greater than sub-atomic measurements. Rather, acoustic cavitation (i.e., the development, enlargement as well as the implosive failure of air bubbles in fluids) is determined through the chemical impact of ultrasound by high-intensity ultrasound represents. At the point when fluids are illuminated through ultrasound, broad and compressive acoustic waves produce bubbles (i.e., cavities). The faltering air pockets can increment ultrasonic energy efficiently while developing a specific range in microns (μm). Under normal circumstances, an air pocket (bubbles) can increase and collapse subsequently, discharging moving energy saved in the rise inside a bubble within fraction of seconds (with a cooling as well as heating rate of >1010Ks-1). This cavitation implosion is extremely confined with 1000 bar pressure, and transient at 5000 K temperature. This heightened energy is adequate to break groups of clusters and scatter nanoparticles in different directions.

2.2.5 The effect of the ultrasonic probe (horn)

Li X et al., 2007, noticed that at a particular frequency, the natural vibration forms a represented shape of mode with specially designed tools such as sonotrodes (ultrasonic horns) as well as boosters. The axial-mode half-wavelength sonotrode is the easiest example of the existence of predominant direction of vibrational motility together with the axis of sonotrode. Half-wavelength is defined as the variation of vibration amplitude along the length with zero-point (axial) motion in the middle. The ultimate function of the horn is to amplify the frequency of the tool to the level required for efficient machining assistance, although it serves as a means of transmitting the vibrational energy from the transducer and helps the better dispersion of reinforcement particles in the liquid.

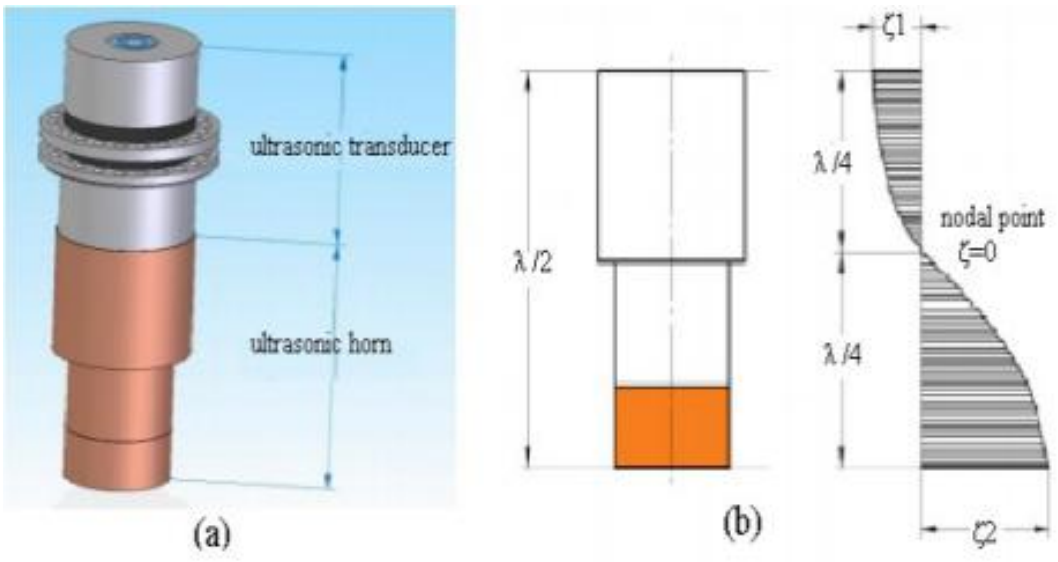

Figure 2. 2 (a) Ultrasonic chain: (b) Stepped ultrasonic horn (correlation l - λ and amplitudes) (Alexandru Sergiu Nanu et al., 2011).

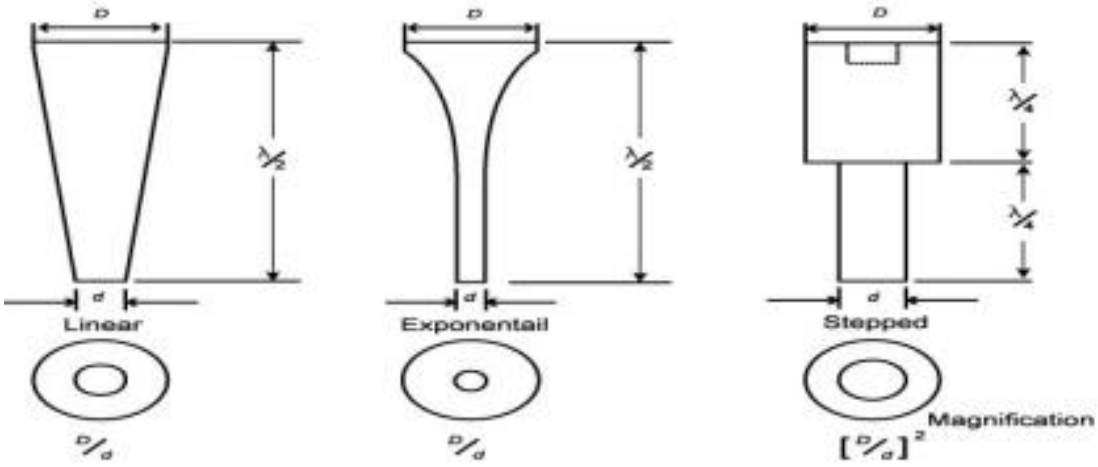

Figure 2. 3 Horn designs (Alexandru Sergiu Nanu et al., 2011).

Figure 2.2 represents the relation between length-frequency and amplitude of the stepped horn (Alexandru Sergiu Nanu et al., 2011). In the ultrasonic treatment process, we insert the stepped horn in the molten metal. When it starts vibrating the horn releases acoustic waves into the molten metal. **Figure 2.3** represents a few horn designs which were used in the casting industries for ultrasonic treatment.

Wang X J et al., 2014, fabricated Mg-SiC (micro 5-20 wt.%) MMCs by Ultrasonic Vibration (UV) assisted stir casting processing. They were revealed that there exists an optimal time in favor of sonication and that too long or too short times for the process, resulted in non-homogeneous particles circulation and they proved that ultrasonic is essential

to attain uniform particle circulation and the grain size of the composite decreased along with increase of particle content, resulting in increase of yield strength, ultimate strength as well as elastic modulus. They concluded that ultrasonic treatment apparently improves the mechanical properties of composite compared with traditional stir casting.

Harichandran R et al., 2015, added B_4C particle reinforcement of nano and micro size particles to the Al matrix. They fabricated the composite by conventional stir casting assisted by ultrasonic cavitation casting process. The researcher investigated mechanical properties when B_4C nanoparticles were added to the base metal. The mechanical property of the tensile test results revealed that 6% B_4C with nanoparticles showed better properties than micro particles. This article also includes impact energy and ductility analysis of micro and nanocomposites. The micro B_4C reinforced composites were shown to be fewer compared to nano. The performance of nanocomposite wear resistance notably increased with B_4C particle amount and increased up to 8 wt.%. Dinesh Kumar Koli et al., 2015, fabricated Al 6061- nano Al_2O_3 (40 nm) composite by mechanical stirring assisted by the ultrasonic cavitation casting process. They prepared different wt.% compositions (1-4 wt.% of reinforcement with a variation of 0.5%). They investigated microstructure of nanocomposites. The microstructure analysis indicated that uniform distribution in Al matrix by ultrasonic frequency at 20 kHz and they conducted mechanical tests to find out properties like hardness, tensile and compressive strength. The test resulted in an increase in mechanical properties.

Jufu J et al., 2015, fabricated nano-sized SiC / Al-7075 matrix composite by ultrasonic dispersion technique. They examined the mechanical and microstructural properties of the prepared composite. The effect of acoustic streaming as well as cavitation of the ultrasonic experiment was studied while mixing nano SiC in the molten liquid. They carried out heat treatment process for the campsite and they compared the values of mechanical properties before heat treatment and after heat treatment. The heat treatment led to an improvement in mechanical properties. Ravindra Singh Rana et al., 2014, fabricated Al-5083/ 10 wt.% nano-SiC composite by mechanical stirring assisted by ultrasonic cavitation machining and they performed a wear test using Taguchi technique. The experiments were conducted at different factors and levels. The results were analyzed using Analysis of Variance (ANOVA). The results showed that the highest influencing parameters are applied load along with speed and distance on the nanocomposite.

2.3 Investigative studies on properties of MMCs

2.3.1 Microstructure evaluation

The primary task of fabrication process is to produce the composites with uniformly distributed particulates in the matrix and secondary, is to avoid the clusters/ agglomerations during the fabrication process. Qiang & Qiu., 2018, and Jayakrishnan et al., 2016, UV process introduced in molten liquid and investigated degassing phenomena, nanoparticles distribution, and grain refinement. Easton et al., 2011 investigated the grain refinement of material during the fabrication process and achieved the grain refinement by novel experimentation which deals with semisolid casting process, electromagnetic stirring and UV treatment. Yang et al., 2017, found that UV treatment was also a highly effective technique to distribute ceramic nanoparticles in molten liquid because of acoustic streaming and cavitation effect. The ultrasonic energy introduces cavitation bubbles which develop micro level "hot spots" containing high temperature and pressure. Hence, these can break up the agglomerations and enhance the wettability of nanoparticles in the molten liquid of Al alloy. In the meantime, acoustic streaming stimulates homogeneous mixing of ceramic nanoparticles in the metal pool.

Yong Yang and Li, 2007, fabricated nanocomposites through ultrasonic assisted process and achieved homogeneous dispersion of nano SiC particles. From the results, it was noticed that the enhancement of material properties was achieved due to the incorporation of SiC particles. Puga et al., 2009, studied the effect of parameters such as power, processing time and temperature of melt during ultrasonic degassing process in Al melt. The results suggested that the UV treatment has an important role to improve the degassing effect in molten liquid. Du Yuan et al., 2019, studied the effect of squeeze casting and UV techniques for reinforcement and the effect of SiC nanoparticle distribution of A356-2wt.%SiC nanocomposites. It is observed that UV treatment reduces secondary dendritic arm spacing of α-Al by 49% while it also reduces squeeze casting by 55% compared to base A356 alloy.

Helder Puga et al., 2009, studied the intensity of UV effect on degassing of $AlSi_9Cu_3$ alloy melt. The different parametric influence of ultrasonic, processing time and temperature were investigated on degassing efficiency and found that the degassing efficiency strongly influenced by the processing time, power of ultrasonic and melting temperature of matrix. Harichandran and Selvakumar, 2016, in their process, high energy ultrasonic waves were introduced in the melt pool to generate nonlinear effect called transient cavitation and acoustic

streaming. Acoustic streaming as well as transient cavitation process involves to form the cavitation bubbles and to develop energy levels, which is highly greater than the energy levels produced by mechanical stirring process; therefore, these transient cavitations and macroscopic streaming have a tendency to disperse nanoparticles to prevent agglomeration, and enhance the wettability of reinforcement in molten liquid.

2.3.2 Physical properties

In general, the density of composite material increases when the ceramic particulates reinforced in to alloy during fabrication. Nevertheless, the mixing of low-density ceramic particulates, reduces the density of composites (Miracle D.B., 2005; Alanemea et al., 2013; Olugbenga et al., 2010). Boopathi et al., 2013, calculated the experimental density values of Al/FA, Al/SiC, and Al/SiC/FA composites. It was noticed that the experimental density of composites decreased with increase of FA content due to its low density. Similar results are also notice, i.e., the density decreases with increase of FA reinforcement content and the same phenomenon also been noticed for FA particulates reinforced composites studied by Gnjidi et al., 2010 and Rao et al., 2001.

Rajmohan et al., 2013, reported that the experimental density of mica reinforced Al-Mica HCs was higher than that of ceramic reinforced composite density. It was also reported that the density of the composite increased with increase in mica reinforcement. The Sahin, 2003, experimental results are also in line and found that the experimental density increased by increase in the particulate contents of reinforcement. The enhancement of material density indicates that the breakage of particle may not have any influence on the composite material and the interfacial bonding between the matrix and particulates. The existence of porosity levels may be due to pull out of particles, improper mixing and casting, clusters/ agglomerations. As per Alaneme et al., 2013, slight porosity in the composite material due to SiC and BLA reinforcements. It was also noticed that the porosity level does not increase with multiple reinforcements. These porosity levels are very much lower than that of acceptable range in composite materials (Kok M, 2005; Alaneme K.K et al., 2012).

In another report, Alaneme K.K et al., 2013, discussed that the density was decreased by 6% in the HCs which is fabricated with RHA & Al_2O_3 and it is also compared with ceramic particulate reinforced composites. The density of composite significantly decreases as the contents of RHA increased due to its lower density. The reliability of the composite can be

in line with a lower porosity level and it is a good sign for the quality of manufacturing process (Kok M, 2005; Alaneme K.K., 2012). Prasad et al., 2012, noticed that the experimental density of hybrid Al-x%SiC-x%RHA (x=0-8 wt.%) composite decreased with increased particles content. It was mainly due to the lower density values of RHA particles. It was also noticed that the porosity of the composite enhanced with increase of particles content due to gas involvement during the mixing and shrinkage of the material during solidification process.

2.3.3 Mechanical properties

2.3.3.1 Hardness

Low aspect ratio of ceramic particle reinforcement is very much important as far as hardness of the composites material is concerned. According to Hutching, 1987, reinforcement particles like Al_2O_3, and SiC enhance the hardness of MMCs. Miyajima et al., 2003, noticed that the composite fabricated through ceramic particles were much harder than that of fiber & whisker reinforced MMCs. The effect of reinforcement particles on microhardness of Al-MMCs have been reported by several researchers and their contribution discussed below:

Boopathi et al., 2013, noticed that the reinforcement particle increases the hardness of the MMCs. It was significantly enhanced with increase of weight fraction of particle content and also observed the maximum hardness for Al-10%SiC-10%FA composite due to the FA reinforcement which leads to enhance the interfacial bonding between matrix and particles. Rajmohan et al., 2013, successfully fabricated HC (Al-x%mica-10SiC; x=0-8wt.%) and estimated the microhardness of the composite. It was noticed that the microhardness of Al-10SiC-3%mica shown better than that of Al-10SiC-6%mica HC material. Improving of machining characteristic of the HMMCs concern, the lower hardness values are plays an important role. Songmene et al., 1999, observed that the brittle material required more energy for machining operation than that of ductile materials due to more forces required to shear the material. It was also reported that the hardness of HMMCs increased with the mica content.

Prasad and Shoba, 2014, noticed that the microhardness of the A356.2-x%RHA-x%SiC was significantly enhanced as compared to pure A356.2 alloy. the microhardness of the monolithic enhanced with mixing of particles reinforcement content because of hard phase

ceramic particulates. It was also reported that the hardness was enhanced with incorporating of particle reinforcements up to 8wt.%. Uvaraja and Natarajan, 2012, investigated the effect of B_4C (3 wt.%) & SiC (0–15 wt.%) ceramic particles on the microhardness of base metal. The microhardness of HMMCs achieved more hardness than the monolithic material due to hard ceramic phase and minimum dislocation movement. It was also noticed that the monolithic and Al-5SiC-3B_4C reinforced HC showed similar results of microhardness but Al-15SiC-3B_4C shown significant improvement in microhardness and low toughness as compared to Al-10SiC-3B_4C HC due to higher % of ceramic particles is closely related to superior microhardness. During the investigation, the maximum wt.% of reinforcements was suggested for optimal hardness and strength of HMMCs. Alaneme K K et al., 2013, studied microstructure, corrosion behaviour and mechanical properties of Al-HMMCs (Al-SiC-BLA) which were fabricated through stir casting method. Experimental investigation for these composites were done, while results indicated that hardness of hybrids decrease with increase in BLA reinforcement and the same trend was observed with Prakash C H et al., 2011.

Alaneme K K et al., 2013, fabricated HMMCs by RHA & Al_2O_3 (RHA: Al_2O_3 = 0:10, 2:8, 3:7 & 6:4) reinforcements. The microhardness of HCs was decreases (4.58%, 8.14% & 10.94% is compared to monolithic) with increase of RHA content. The same trend was also noticed with SiO_2 in RHA. The SiO_2 has lower hardness value as compared to ceramics reinforcements (Courtney, T.H., 2006; Alaneme K.K., 2013). Hence, RHA particles have noticeable effect on the microhardness of the Al-MMCs. Arun Kumar M et al., 2011, prepared HCs (Al6061-eGlass-FA) with different wt.% by L/M method. Specimens were machined as per test standards and casting defects were found using ultrasonic flaw detector, some of the mechanical properties had been calculated and compared with Al-MMCs. The researchers were reported the improvement of hardness in HC and also increased with increases in wt.% of FA particles. Devaraju A et al., 2013, developed surface-based HCs with reinforcement of (SiC & Gr) and (SiC & Al_2O_3) nano sized particles through friction stir casting process. Microstructure of both composites were investigated with various tests, and based on the results they concluded that the hardness of both HCs was improved, when compared with average Vickers Hardness (HV) 104 of the matrix material. The composite (Al-SiC-Gr) showed less hardness due to the Gr content and (Al-SiC-Al_2O_3) showed superior hardness.

Devaraju A et al., 2013, prepared surface HC with reinforcements such as SiC and Gr to the Al alloy matrix through friction stir process. Taguchi method was used to find the optimal parameters such as rotational speed and Volume percentage (Vol %) of reinforcements for enhancing the mechanical and tribological properties of hybrid surface composites. It was observed that the microhardness of HC increases due to the presence of SiC particles. Venkat Prasad S et al., 2013, tried to produce HCs with low cost reinforcements such as FA and Gr to improve the mechanical properties. HCs (AlSiMg-Gr-FA) were fabricated by stir casting technique. It showed superior hardness when correlated with unreinforced composite. Adding Gr particles to the matrix material decreases the hardness of hybrid.

Nayak D et al., 2014, fabricated Cu-HMMCs with reinforcement of Gr and TiC through P/M route and used factorial method to analyze the tribological performance and found that the addition of Gr, reduced the hardness of HC and addition of TiC increases hardness. Radhika N et al., 2013, manufactured HMMCs (AlSi10Mg reinforced with Al_2O_3-Gr) by stir casting technique where unreinforced alloy specimens were also fabricated for comparison. Investigation was done for microstructure as well as mechanical properties; it was found that HMMCs showed higher microhardness values then that of unreinforced alloy.

2.3.3.2 Tensile strength

Mechanical properties of composites are much important and play a key role in the application point of view. Chen et al., 1997, observed that the composite strength increased with particle content due to the strong interface between the particulates and matrix. Further, Thakur S.K., 2001, noticed the improvement of interfacial strength because of proper distribution of ceramic particulates (preheated) in the composite material. In Al-MMCs, two types of strengthening mechanisms have been noticed; i.e., indirect and direct strengthening mechanisms. As per Chawla N et al., 2001, the direct strengthening occurs when the hard phase ceramic particulates involved with the soft phase matrix. Which results, load baring capacity of a composites increase due to transfer of load from matrix to ceramic particles and resistance offered by the composite material increases. M.K. Surappa, 2008, the indirect strengthening arises due to Coefficient of Thermal Expansion (CTE) mismatch between the monolithic and particle reinforcements while solidification process which leads thermal stresses and dislocation movement. The effect of size and reinforcement content place a

critical role in the indirect strengthening. The strength of MMCs increases with decreases in particulate size or increase particulate content due to dislocation density and larger contact area for punching of dislocation in composite material. Various findings for the material strength of MMCs are discussed below.

Mitrovic S et al., 2012, carried out research on HCs to make it lightweight often resistance to wear and improve the mechanical properties. The chosen material matrix was based on Zn-Al and reinforced with Gr and SiC particles. The results showed that HCs had higher tensile strength compared with pure alloys. Essam R.I M et al., 2010, carried out investigation on fabrication process and wear behaviour of HCs (Al1050 with SiC & Al_2O_3). It was carried out on pure Al sheet by reinforcement mixture of SiC & Al_2O_3 by friction stir process, and various tests were used to evaluate the strength. The average COF decreased with increment of Al_2O_3 particles in relative ratios. Wu H F et al., 1995, studied the failure characteristics of straight-sided and dog bone-type specimens and analyzed fiber/metal hybrid laminates through stress analysis in part I, it was found that the UTS is significantly different at 5% significance level. The authors recommended straight-sided specimen of fiber-reinforced Al_2O_3 laminates as being better than dog bone type specimens for tensile testing. Wu H F et al.,1994, discussed the study of tension test specimens, with a comparison of size and alignment effects between straight-sided and dog bone-type specimens. The effect of size (width) on tensile strength in fiber or metal laminates is insignificant over the range of specimen width investigated for a constant strain rate.

Attharangsan S et al., 2012, investigated influence of Carbon Black (CB)/ RHA ratio on tensile properties, curing characteristics and fatigue life of the composite. They found that the inclusion of carbon black in hybrid decreases curing and scorch time but increases the torque. As the carbon % increases the modulus, fatigue and tensile strength increase whereas elongation decreases at break. Pradeep Sharma, et al., 2016, developed HC of AA6082-Si_3N_4 & Gr, and investigated mechanical properties and micro structure with analyzed using SEM, and XRD. Both micro as well as macro hardness and tensile strength of HCs were examined and notice the enhancement in the properties. Thirumalai Kumaran S et al., 2015; Jaswinder Singha et al., 2015; Thirumalai T et al., 2014, fabricated hybrid MMCs through stir casting method and conducted experiments to analyze it in various aspects. They performed microstructural analysis as well as examined mechanical properties such as tensile strength,

and hardness of HC with monolithic. They found that the hybrid MMCs had higher values than that of monolithic alloy.

Oluwagbenga Babajide Fitile et al., 2014, investigated mechanical behaviour and microstructure analysis of Al-Mg-Si alloy MMCs which were reinforced with SiC and Corn Cob Ash (CCA) nanoparticles, and fabricated through 2 step stir casting process. Density measurements, percentage porosity, tensile strength, micro hardness measurements and microstructure characterization were done to characterize the HCs; based on the results, the author concluded that mechanical properties such as UTS, hardness of HC gradually decrease with CCA content. Complementing reinforcement for the development of high performance, low cost Al-HCs. Ravindran P et al., 2013, investigated through experimental study hybrid Al-MMCs with SiC & Gr reinforcement particles through P/M method while investigation was done for the tribological and mechanical properties. It was found that the strength improved by increasing Gr reinforcements particles. It was noticed the greatest achievement with the combination of 5wt.% SiC-10wt.% Gr in HCs when compared to matrix material. Wong W L E et al., 2005, studied mechanical characteristics of Mg based HC (Mg-5 vol.% of micron and nano Al_2O_3 particulates), fabricated through P/M technique. Different experimental tests were done and it was concluded that addition of micro and nano sized particles to the composites increases in elastic modulus, strength as well as hardness and decreases ductility when compared to pure Mg. There was increase in the vol% of Al_2O_3 nano size particles reinforcement from 0.75 to 1.0 vol%, while the overall mechanical properties of the HCs also improved.

2.4 Mechanical property evaluations of Al-MMCs based on nano reinforcement particles

Al-MMCs exhibit better mechanical properties with particulate (p) reinforcements because of their high strength and improved wear resistance than unreinforced Al alloy (Veeresh Kumar GB et al., 2012). From the recent past nanocomposites have been attracting the attention of researchers because they have low density, high strength and other properties such as high thermal conductivity, low CTE and dumping properties (Chen Baiming et al., 2008). The production of nanocomposites is a very difficult process and faces several hurdles like random distribution of reinforcement particles, poor wettability, porosity, clusters and agglomerations formation during the fabrication. An ultrasonic-assisted stir casting method

may overcome the above-mentioned difficulties and also improve the uniform distribution of particles and wettability (Yang Y et al., 2007). Double stir casting (compo casting) technique was adopted to improve the uniform distribution of nanoparticles during the fabrication of Al-MMNCs (Ezatpour H R et al., 2013). In a study of Al-Graphene MMNCs, the nano-grains during the reheating process significantly enhanced the yield strength. The graphene sheets with onion shape decreased the agglomeration of SiC nanoparticles. Wrapping graphene sheet, resulted in lessening the porosity, thereby enhancing the tensile properties of Al-MMNCs (Fadavi Boostania A et al., 2018).

Shusen Wu et al., studied the microstructure and mechanical properties of nano-SiC/Al-MMNCs by diluting the molten Al under UV via squeeze casting and noticed that the nano-SiC are uniformly distributed in the Al-SiC MMNCs and the tensile strength of the MMNCs improved compared to Al356 alloy matrix (Shulin Lü et al., 2018). In a study of γ-Al_2O_3/A356 MMNCs the UTS and elongation of the MMNCs enhanced and the improvement was attributed to the homogeneous distribution of the nanoparticles and refinement of the grains (Xu Tuo et al., 2019). The Al-Cu MMNCs with Magnesium Silicide (Mg_2Si)-nanoSiC were subjected to microstructure and mechanical properties studies. The UTS and yield strength results indicated higher values than the other composites with good ductility. The improvement in the properties was attributed to the refined eutectic Mg_2Si phases in Mg_2Si-SiC/Al-Cu MMNCs (Li Jianyu et al., 2019). The Al6005-TiB_2 MMNCs fabricated via Mechanical Alloying (MA) and hot extrusion was showed good distribution of the nano-reinforcement through optical studies and nano-indentation test shows an increment in hardness values with TiB_2 reinforcement in the Al6005 alloy (Abu-Warda A et al., 2018).

Al6061-Zirconium Diboride (ZrB_2) MMNCs properties like hardness, strength and elongation were significantly improved due to the ZrB_2 nano-dispersoids and a quantitative calculation indicated that as ZrB_2 content increased, Orowan strengthening contributed to improved yield strength (Zhang ZY et al., 2018). The P/M route developed Al-B_4C MMNCs, showed that the hardness of the Al-B_4C MMNCs were higher than Al whereas the density and electrical conductivity of Al-B_4C MMNCs were lower than pure Al. This behavior has been explained by Hall–Petch Model and Orowan strengthening (Javad Nasr Isfahani Mohammad et al., 2019). Al-TiC MMNCs were synthesized by MA with nano-diamonds as precursors. The DSC showed that the composite developed was stable within a wide range of temperatures, which permit its application in casting technologies (Popov Vladimir A et al.,

2018). Shimaa A et al., prepared Al/Ni-SiC MMNCs with nano-Ni and SiC as reinforcements by P/M process and concluded that an enhancement in the CTE with increasing Ni-SiC percentage (Elkady Omayma A et al., 2019). For Al6061-SiC-Gr hybrid MMNCs, the influence of nano SiC and Gr content resulted in improved wear resistance, lower COF and superior surface compared to Al6061 (Manivannan I et al., 2018). In a microstructural study of Gr-B_4C hybrid reinforced ZA27 MMNCs fabricated via Mechanical Milling (MM) and hot pressing, the optical results revealed that MM method can be utilized for homogeneous distribution of the nano-sized additives in the matrix alloy (Dalmis R et al., 2018). Al6061 was reinforced with TiC, Al_2O_3 and hybrid (TiC & Al_2O_3) nanoparticles, the wear tests indicated that the wear rate increased with the load and sliding velocity. Hybrid Al6061 MMNCs had lower wear rate and COF compared with the other MMNCs investigated (Jeyasimman D et al., 2014).

Beitallah Eghbali et al., fabricated the Al2024-SiO_2-TiO_2 hybrid MMNCs, where the structural and mechanical properties were examined; this indicated an increase in the hardness, tensile and yield strength of hybrid MMNCs. The Al7075-SiC MMNCs were fabricated through stir casting technique to provide significant benefits compared to other methods in terms of enhanced mechanical characteristics compared with unreinforced Al7075 (Suresh S et al., 2019). In a study of P/M synthesized Cu-B_4C MMNCs on the microstructure and abrasive wear performance, the MMNCs with 1.5 wt.% of B_4C revealed superior micro-hardness and wear resistance (Poovazhagan L et al., 2019). In a study of Graphene reinforced Cu-MMNCs, optical studies confirmed even distribution of the reinforcement phase in the matrix with nano-crystalline microstructure and strong interfacial bonding between Cu and graphene with improved hardness and Young's modulus. The increment in strength was attributed to the microstructural refinement and dislocation pinning at the strong matrix-reinforcement interface (Roy Debdas et al., 2019).

Prasanta S et al., 2018, studied the effect of Tungsten Carbide (WC) nano-particles on tribological behaviour of Mg-based MMNCs on the Vicker's micro-hardness and wear behaviour of MMNCs and concluded that the micro-hardness and wear resistance of composites increased with increase in the WC nano-particles in the matrix. Jinling Liu et al., 2018, investigated the dry sliding wear behavior of Mg based nanocomposites using the ball-on-disk wear tester. The COF of Mg-SiC reinforced nanocomposites were much higher than pure Mg and Mg-AZ31B alloy. Analysis on the surface and debris suggested that the

dominant wear mechanism of the Mg-SiC nanocomposites was oxidation by analyzing the surface morphology and debris.

Pallav Gupta et al., 2018 reported the dependence of wear behavior on sintering mechanism for iron (Fe) –Al_2O_3 MMNCs fabricated via P/M technique. They indicated that the XRD pattern of sintered nanocomposite showed the formation of Iron Aluminate ($FeAl_2O_4$) phase. Wear and COF behavior of nanocomposite specimens were investigated and it was found from the studies that the wear properties in nanocomposite specimen depends on the sintering temperature and time respectively. Mehrdad S et al., 2019, studied the AA2024-SiO_2-TiO_2 hybrid nanocomposites, fabricated via stir casting process and their structural and mechanical properties were examined. The results indicated that the analysis of mechanical properties showed an increase of hardness, tensile strength and yield strength. The larger amounts of nanoparticles, SEM studies showed that there were more quantities of nanoparticles agglomerates in the structure, reducing the mechanical properties of the nanocomposite, as compared to the nanocomposite with 0.5 vol.% of SiO_2 nanoparticles. The main strengthening mechanisms were estimated to be Hall-Petch strengthening, Orowan strengthening, and the CTE mismatch and elastic modulus mismatch between the reinforcements and metal matrix. There was also some evidence showing some of the singular and agglomerated nanoparticles in the matrix on the fractured surfaces of the nanocomposites. Liangchi Zhang et al., 2019, aimed to develop a microstructure-based model to describe the material deformation and fracture of the particulate reinforced MMCs. The most important factors, such as particle morphology, distribution, matrix deformation, fracture, and particle-matrix debonding, were comprehensively integrated into the modelling. It was found that such a microstructure-based model can capture the major material deformation and failure mechanisms. Particle fracture happens near its sharp corners, while matrix failure initiates around the particle crack tips and propagates to connect the microcracks caused by particle fracture, or through the area with high stress/strain concentration, leading to the fracture of the whole workpiece. Tuo Xu et al., 2019, in their study, showed that the nanometer in-situ γ-Al_2O_3 particles reinforced Al-MMCs were successfully fabricated by the A356 alloy and Cobalt Oxide (CO_3O_4) powder at 850^{o}C by means of in-situ reaction in the high temperature melt. It was found that the UTS and elongation of the 0.6 vol% γ-Al_2O_3/A356 composites had enhanced in comparison to the matrix and this was attributed to the homogeneous distribution of the nanoparticles, the refinement of the grains and the modification of the eutectic Si phases.

Fadavi Boostania et al., 2018, revealed that the semi-solid deformation of Al-MMNCs by restricting the growth of the nano-grains during the reheating process to significantly enhance the yield strength of the fabricated composites. The graphene sheets with onion shape have also shown the unique capability in alleviating the agglomeration of SiC nanoparticles, attributed to the manipulated Hamaker constant of these particles as a result of wrapping graphene sheets, which has resulted in diminishing the porosity and stimulating multi-scaled micro/nano grains, thereby significantly enhancing the tensile properties of the fabricated composites. Sandra V et al., 2019, studied and developed a model to predict the wear rate of the Al356 reinforced with SiC nanoparticles which were produced by compo-casting process. The tribological tests were performed on block-on-disc tribometer under wet conditions. A model was developed for prediction of wear rate, by using regression model and Taguchi analysis and it was concluded that the predicted values were close to the experimental values. Abu-Warda A et al., 2018, fabricated Al6005-TiB_2 composites through MA route. Hot extrusion was employed as a consolidation process. The obtained results through the optical studies and micro-hardness tests showed a good distribution of nano-reinforcement within the Al matrix. Nano-indentation test shows an increment in hardness values with TiB_2 reinforcement in the A6005 alloy.

Debdas Roy et al., 2019 studied the graphene reinforced Cu MMNCs fabricated by High Pressure Torsion (HPT) process. The optical studies confirmed even distribution of the reinforcement phase into the matrix with nano-crystalline microstructure and strong interfacial bonding between Cu and graphene with improved hardness and Young's modulus. The increment in strength was attributed to the microstructural refinement and dislocation pinning at the strong matrix-reinforcement interface. Further, the results indicated that HPT consolidation is an efficient mean for synthesizing Cu-graphene nanocomposite with improved strength with negotiable conductivity.

2.4.1 Review on hBN reinforcement based MMCs

h-BN is a layered material and isostructural to Gr, also called graphitic-BN, h-BN, g-BN, and α-BN. h-BN is an insulator with bandgap ~ 5.9 eV. Boron reinforced materials find nuclear applications due to their capability for neutron absorption and better suits in MMCs because of the unique properties as well as crystal structure (Duan X et al., 2016). The structure of hBN is the same as that of Gr and each B-N atom exhibits covalent bond as well

as “Weak Van der Waals Forces” in their adjacent layers. Hence, it acts as a solid lubricant material.

Lava Kumar Pillari et al., 2018, investigated Al-hBN composites fabricated through P/M route. The high energy ball mill was performed to convert micro particles to ultrafine nanoparticles of hBN. Al-2% hBN and Al-5% hBN composites were green compacted at a pressure of 250 MPa and 500^{o}C temperature under nitrogen environment. The authors observed that the milling time effectively worked upto 10 hrs and beyond this time, the composites showed agglomerations. 2% hBN reinforced composite enhanced the microhardness and reduced the melting point. Palanivel R et al., 2016, fabricated Al-TiB_2, Al-TiB_2-hBN, Al-hBN composites by Friction Stir Process (FSW). Author noticed that the uniform distribution of TiB_2 and hBN particles through the composite. It is also observed that the wear loss of Al-TiB_2-hBN composite was minimum as compared to individual composite materials. Firestein K L et at., 2015, fabricated Al-hBN nanocomposites through Spark Plasma Sintering (SPS) method and studied the microstructural behaviour, distribution of nanoparticles, damping and mechanical properties. The samples were analyzed through TEM, SEM and Temperature Dependent Internal Friction Measurement (TDIF). It was noticed that the strength of nanocomposite improved at elevated temperature (300^{o}C) and at room temperature respectively. Jeyasimman et al., 2015, investigated the effect of hBN nanoparticles reinforcement on dry sliding wear behavior of pure Mg and Mg-MMNCs synthesized by P/M technique, and followed by a hot extrusion process. The obtained wear test results show that the Mg-MMNCs wear level rises with higher sliding speeds and loads. Mg-MMNCs shows lower wear rates and COF compared with other MMNCs.

2.4.2 Review on B_4C reinforcement based MMCs

B_4C is the 3rd hardest material with a melting point of 2450^{o}C, great mechanical properties, corrosion and wear resistance and also more neutron absorption capacity. Knoop hardness of B_4C (ρ=2.52 g/cc) at hot press material is 29.0±1.5 GPa. Due to these attractive properties, B_4C has a wide range of applications including as grinding tool, blasting nozzle, high weight armour plating, cutting tool, and neutron absorption material. Recently, research focused towards the Al-B_4C based MMCs due to the attractive enhancement of mechanical properties.

Mohammad J N I et al., 2019, developed Al-B_4C nanocomposites by P/M technique and investigated the structural, mechanical and electrical properties and concluded that the hardness of Al-B_4C nanocomposites were higher than Al whereas the density and Electrical conductivity of Al-B_4C nanocomposites were lower than pure Al. The behavior has been explained by Hall–Petch Model and Orowan strengthening. Guo H et al., 2019, investigated the influence of ball milled B_4C_{np} on the Al-B_4C nanocomposites. Morphological studies on Al-B_4C nanocomposites were done through TEM, SEM and XRD analysis. The results are showed that the increase in B_4C reinforcement content increases the grain refinement of nanocomposite even at low dislocation densities and lattice strain.

Poovazhagan L et al., 2019, studied the behaviour of Copper (Cu)-B_4C nanocomposites on the abrasive wear performance and microstructure of Cu nanocomposites synthesized by solid state P/M technique. Abrasive wear experiments were carried out by sticking the abrasive sheets of 400 grit SiC onto disc of POD wear tester. It was concluded that the nanocomposites with 1.5 wt.% of B_4C possess the superior micro-hardness and maximum wear resistance property. Dalmis R et al., 2018, concentrated on the effect of MM on Gr & B_4C hybrid reinforced ZA27 nanocomposites were fabricated via a combination of MM and hot-pressing techniques. The nanocomposites were investigated for microstructural and mechanical properties. The results showed that MM method can be utilized for homogeneously distributing the nano-sized additives. Flake-shape morphology negatively influences physical and mechanical properties.

2.4.3 Review on SiC reinforcement based MMCs

SiC is also known as carborundum containing “Si” (50%) and “C” (50%). Si-C has very strong tetrahedral covalent bonds and each carbon atom contains 4-Si atoms and vice versa. “It is also characterized by its high-temperature strength, high thermal conductivity, resistance to chemical reaction, low thermal expansion, and ability to function as a semiconductor. Jianya Li et al., 2019, developed nano-sized SiC particles and in-situ Mg_2Si particles reinforced Al-Cu composites. The microstructure and mechanical properties were studied. The eutectic Mg_2Si phase in the Mg_2Si/Al-Cu composites were refined in Mg2Si-SiCnp/Al-Cu composites, which is uniformly distributed inside Al_2Cu phases that precipitated at the grain boundary. The UTS and yield strength of the composites results indicated higher values than those of Mg_2Si/Al-Cu composites while maintaining good ductility. Omayama A et al., 2019, prepared Al/Ni-SiC composites with 10 wt.% nano-Nickel along with SiC

particulates as reinforcements by P/M process. The CTE was measured and they concluded there was an enhancement in CTE with increasing Ni-SiC percentage.

Manivannan I et al., 2018, in their investigation, fabricated Al6061 reinforced with nano SiC and fixed quantity of micro Gr hybrid nanocomposites which were prepared by ultrasonic assisted stir casting method. The influence of nano SiC & Gr content on the mechanical and tribological properties of Al6061 hybrid nanocomposites was studied. The obtained results of Al/SiC/Gr hybrid nanocomposites showed improved wear resistance, lower COF and showed superior surface smoothness compared to Al6061 alloy. Suresh S et al., 2019, aimed to fabricate Al7075- nano-SiC powder reinforced nano-MMCs through stir casting technique and to provide significant benefits compared to other methods. The mechanical characteristics like tensile, micro-hardness and wear behaviour were examined and revealed that the characteristics were enhanced with the increase wt.% of nano-SiC powder in the Al7075 compared with unreinforced Al7075.

2.4.4 Review on TiC reinforcement based MMCs

TiC is an extremely hard material (Mohs 9–9.5), and similar to WC. It shows excellent chemical and thermal stability, wear resistance, high melting point, and extensively used for cutting tools. Investigation of nano TiC particle reinforced Al-MMCs has not been adequately studied and it has come into popularity only recently due to its low CTE, high melting point, superior hardness and wear resistance (Wang Y et al., 2001; Salem H et al., 2009). The size of the particles which ranges from micro to nano level scale, increases the mechanical properties but it tends to increase the clusters and agglomerations (Hanada K et al., 1997; Tan M J et al., 1998; Fagagnolo J B et al., 2006). It is also an important task to produce homogeneous distribution of nano scale reinforced particles in dense liquid metals to attain the required properties (Khakbiz M et al., 2009).

Vladimir A Popov et al., 2018, presented the work showing that the in-situ synthesis of TiC nanoparticles in the Al matrix during DSC is possible when nano-diamonds are used as a precursor. They concluded based on DSC that the composite developed is stable within a wide range of temperatures, which allow its application in casting technologies. Jayasimman D et al., 2014, aimed to investigate sliding wear behaviour of AA6061 MMNCs reinforced with TiC, Al_2O_3 and hybrid (TiC & Al_2O_3) nanoparticles. The wear tests were performed on a POD wear tester at room temperature and indicated that the wear rate increased with the load

and sliding velocity. Hybrid nanoparticles reinforced AA6061 MMNCs had lower wear rate and COF compared with the other nanocomposites investigated.

2.5 Research gap analysis

After extensive of the existing literature survey, it is found that limited research work was carried out for nano-particulates reinforced MMCs. Mixing of nanoparticles is very difficult through conventional mechanical rotary impeller due to high surface area to volume ratio of nanoparticles. Limited work is available on the MMCs fabricated through stir casting route with ultrasonic assisted dispersion of particulates in the matrix alloy. It was also found that very meager information available in the literature related to AA7150 matrix alloy reinforced with B_4C, hBN, SiC, and TiC ceramic nanoparticles. Based on these findings, the recent literature was discussed Al-MMCs and nano-particulate reinforcements.

❖ **Applications of AA7150**

It finds applications in aerospace industry and used in the manufacturing of fuselage, stringers, floor beams, airline passenger seat tracks, upper and lower wings is shown in **Figure 2.1**.

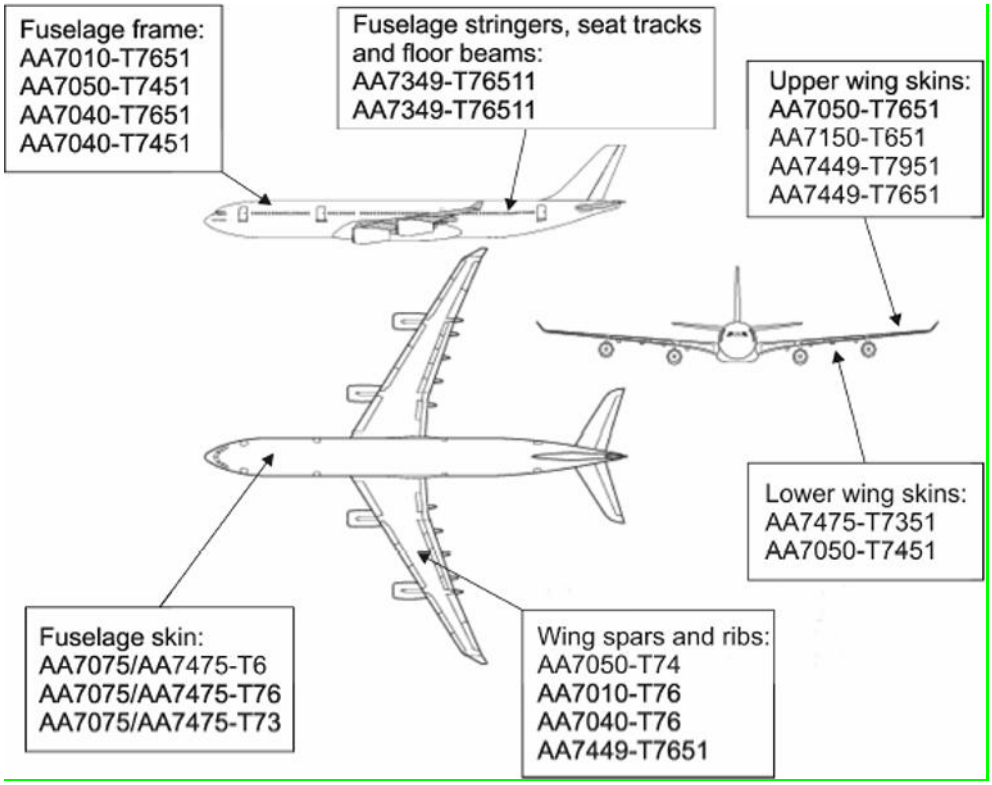

Figure 2. 4 Applications of 7 series

2.6 Objectives of the research work

Aerospace and automobile sectors are always in search of new materials with higher grade mechanical and wear properties along with ease of fabrication and the ability to vary composition so that a range of desired properties may be attained. Lightweight, high stiffness, and high strength make Al-Zn-Cu-Mg alloy MMCs a suitable candidate material for aerospace, military and automobile applications. Ceramic micro-particulates are injected into Al alloy to enhance its mechanical and wear properties but in recent years, nanoparticles have been introduced to fabricate MMCs and these exhibit far better properties than micro composites which has been confirmed by positive results, especially with respect to strength, corrosion resistance, wear resistance, fatigue life of the material and temperature creep resistance. AA7150 finds applications in aerospace industry and used in the manufacturing of fuselage, stringers, floor beams, airline passenger seat tracks, upper and lower wings.

- To study the effect of ultrasonication over a double stir casting process on AA7150-SiC Nanocomposite.
- To study the effect of individual nano sized hBN, B_4C, TiC, SiC, hybrid particulates & ultrasonication on mechanical, microstructure and fracture studies of AA7150 metal matrix nanocomposites.

2.7 Problem statement

In the present investigation is aimed at the development of hBN, B4C, TiC, SiC, hybrid nano-particulates reinforced AA7150 metal matrix nanocomposites through a novel fabrication process by combining a sequence of vortex, two step stir casting and ultrasonication techniques to investigate the homogeneous distribution of nanoparticles, leading to refinement of microstructure in the nanocomposites.

2.8 Overall work plan

The consolidated work plan for the fabrication of AA7150 based nanocomposites through ultrasonic assisted stir casting was given below for the better understanding the process.

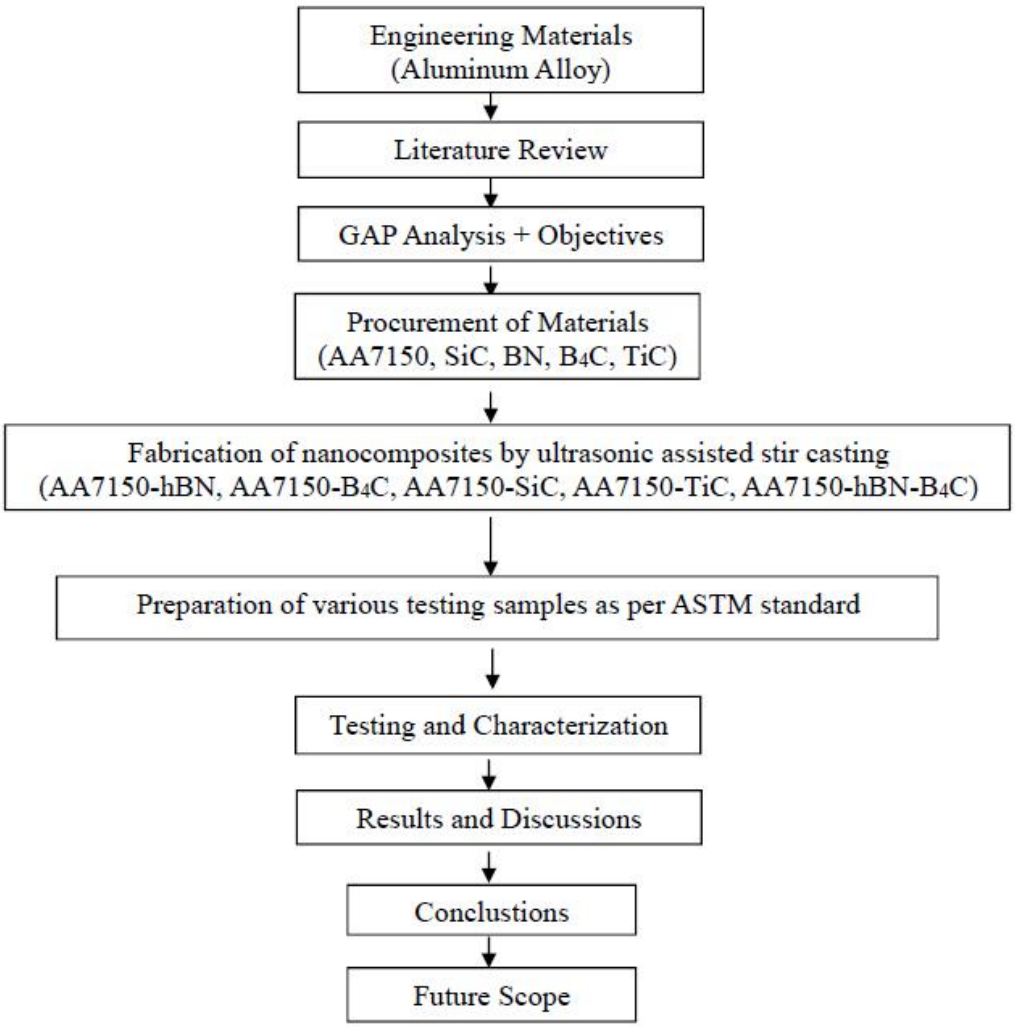

Figure 2. 5 Flow chart of the overall work plan.

2.9 Summary

This chapter deals with the literature review related to the introduction and fabrication methods of liquid casting which includes stir casting, compo casting and ultrasonic assisted casting. In the ultrasonic assisted casting, the effect of cavitation and acoustic streaming on nanoparticles dispersion. The literature is mainly focused on fabrication methods, matrix materials, reinforcement particles, nanocomposites, mechanical properties and microstructure characterization as well as testing processes followed. It also deals with the research gap analysis, objective of the work, problem statement and overall research plan.

CHAPTER -3
MATERIALS AND METHODS

This chapter deals with materials required to fabricate ceramic particle reinforced nanocomposites, fabrication method, and various testing methods for characterization.

3.1 Materials

AA7150 ingot was chosen as matrix material and bought from Venuka Engg. Pvt. Ltd., Hyderabad, India. The chemical composition is shown in **Table 3.1**. B_4C, SiC and TiC were procured from Platonic Nanotech Pvt. Ltd., Jharkhand, India. SiC with a density of 3.216 g/cc, >99.9% purity and Average Particle Size (APS) of 40-60 nm, TiC with a density of 4.91 g/cc, >99.5% purity and APS of 40-50 nm, B_4C with a density of 2.52 g/cc, >99% purity and APS of 40-60. Nanoparticles of hBN were purchased from Sisco Research laboratories private limited, India with an average particle size of 70 nm, density of 2.1 g/cc, and >99.9% purity. Hexachloroethane (C_2Cl_6) and Mg were selected as degassing agent as well as flux and purchased from Taranath Scientific & Chemical Company, Hanamkonda. Mechanical stirrer was coated with ZrO_2 (melting point: 2,715 ^{0}C) to improve the temperature resistance of stirrer blade.

Table 3. 1 Chemical composition of AA7150 in weight percentage.

Chemical Composition	Mg	Zn	Cu	Fe	Zr	Si	Mn	Al
AA7150	2.56	6.37	2.25	0.12	0.11	0.08	0.009	Balance

Table 3. 2 Mechanical properties of matrix and reinforcement particles.

Material	Elastic Modulus (GPa)	Density (g/cc)	Hardness (VH)	Tensile Strength (MPa)
AA7150	71	2.83	140	160
hBN	64.8	2.21	3800	83.3
B_4C	472	2.52	3200	569
TiC	451	4.91	2400	258
SiC	410	3.21	2500-3500	290

The microstructure and XRD patterns of purchased materials (AA7150, hBN, B_4C, SiC, and TiC) were examined to confirm material, purity and the good peak arrangement with reported values of "Joint Committee on Powder Diffraction Standards (JCPDS), X'Pert HighScore Plus" and shown in **Figure 3.1**.

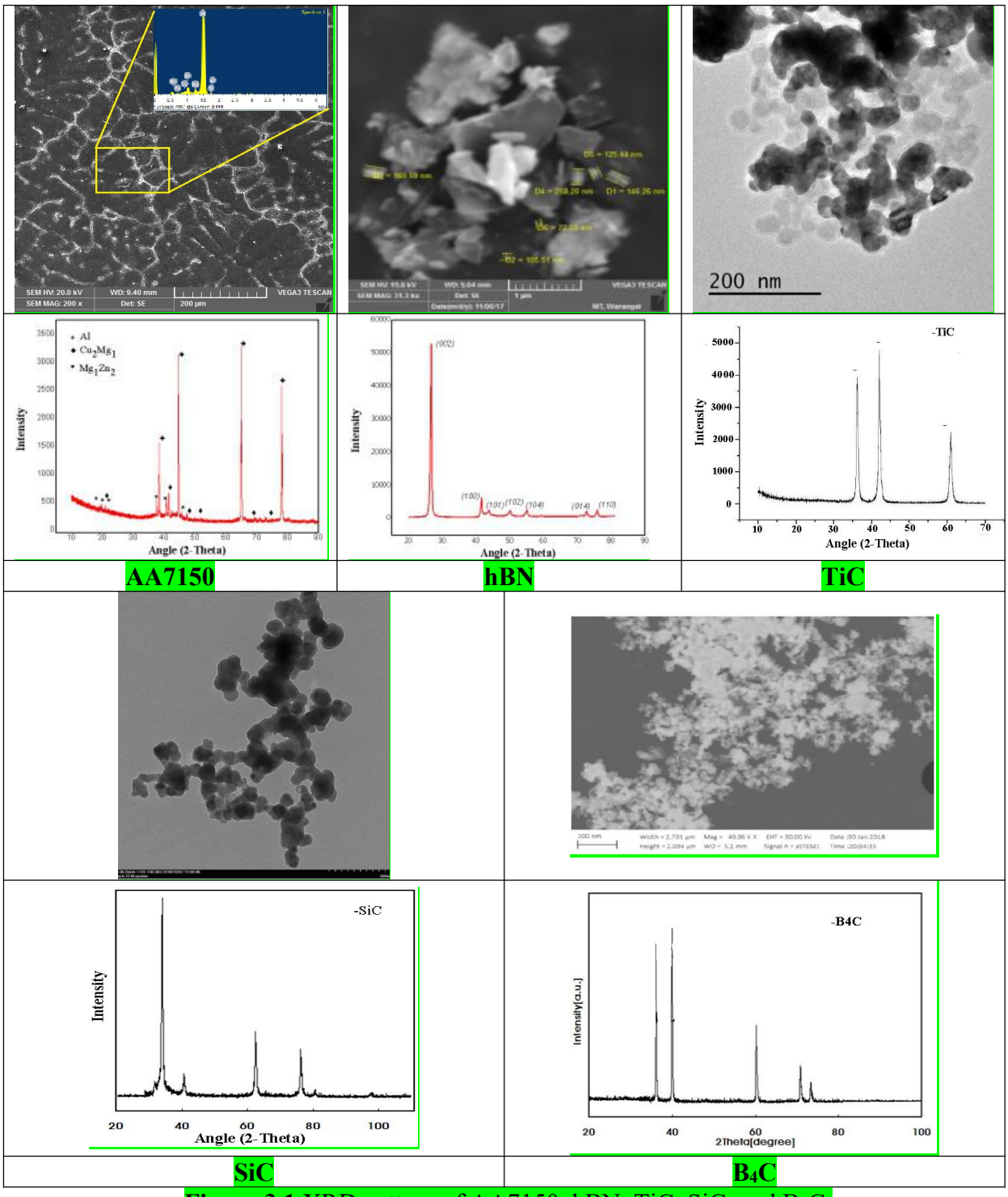

Figure 3.1 XRD pattern of AA7150, hBN, TiC, SiC, and B_4C

3.2 Fabrication process

The experimental setup for the fabrication process is shown in **Figure 3.2** and the respective flow chart is shown in **Figure 3.3**. AA7150 ingot was melted and maintained at 750°C for an hour to achieve uniform melting throughout liquid. A Zirconium Oxide (ZrO_2) coated mechanical stirrer was used for stirring process and the stirring action was performed for 20 minutes in two steps. While stirring, 1 wt.% Mg powder was added to improve the wettability of reinforcement and C_2Cl_6 for degassing. Preheated (500°C) reinforcements (0.5, 1.0, 1.5, 2.0 wt.%) were individually added in the melt pool to prepare individual nanocomposites. In case of B_4C, preheated temperature was about 300°C and K_2TiF_6 for wettability enhancement. Double stir casting process was performed followed by UV test of 10 min. The fabricated molten liquid was poured into preheated (500°C) mold and allowed to cool for 24 hrs at room temperature.

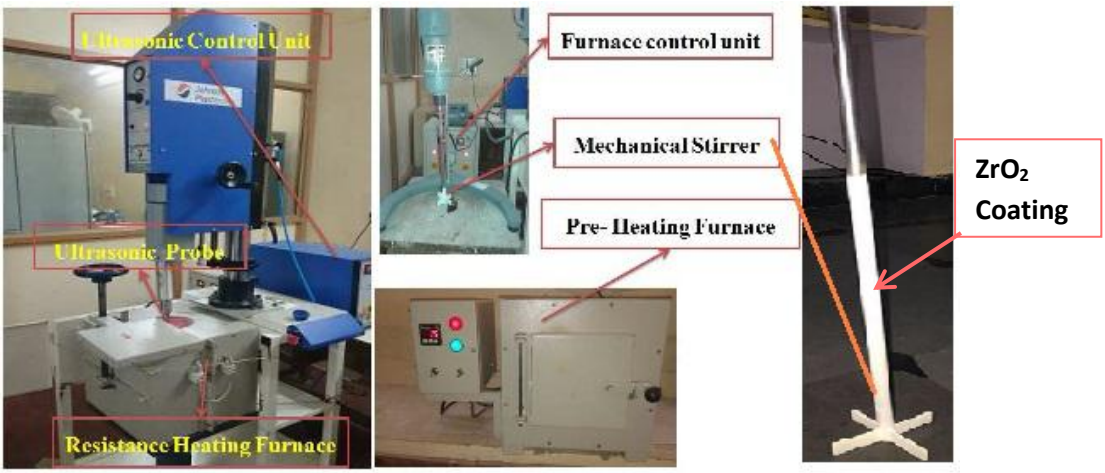

Figure 3. 2 Experimental setup for UV assisted stir casing.

In case of hybrid nanocomposites, the reinforcement particles were added (50-50%) one after another through stirring action and followed by flux to improve the wettability between metal liquid and nanoparticles. Then double stir casting process for 20 min in two steps as well as UV process for 10 min as a part of fabrication process.

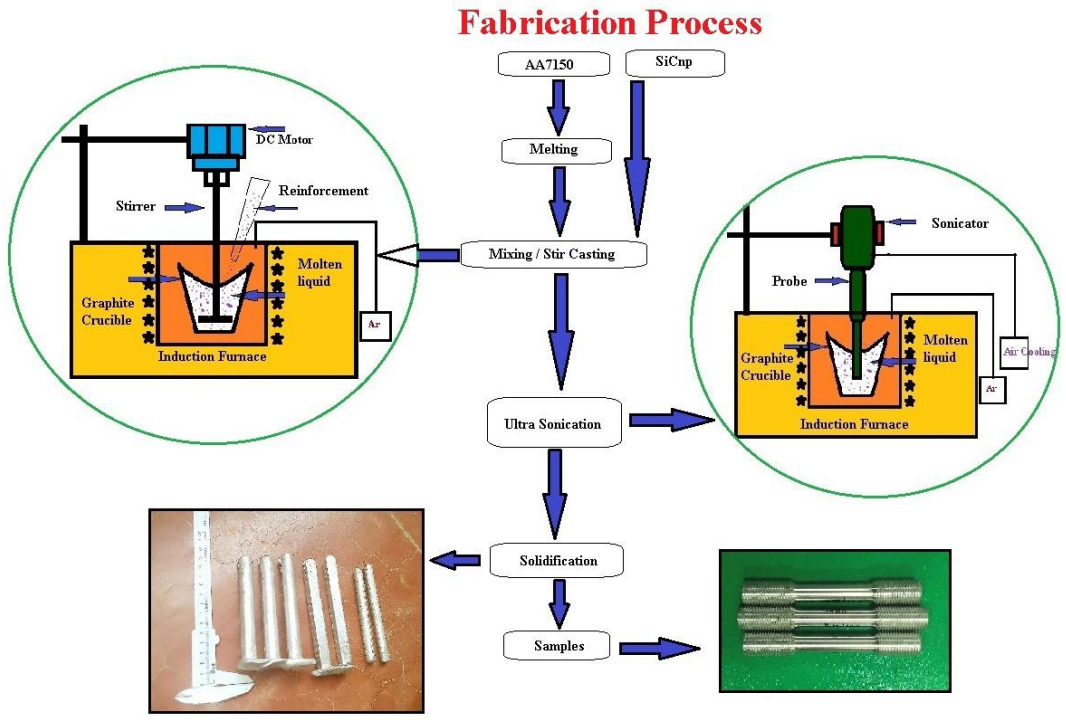

Figure 3. 3 Fabrication process with materials, stirring, sonication and spacemen.

3.3 Detailed mechanism for novel fabrication process

A novel fabrication process was developed to produce homogeneous mixing of nanoparticles throughout the Al melt pool and the schematic line diagram is represented in **Figure 3.4**. This fabrication process involves a combination of three techniques, namely vortex method, double stir casting method and UV method. Vortex method was conducted at 750^{o}C temperature (above liquidus) to increase the flowability of liquid as well as the particles redirected into liquid metal. Double stir casting method was a two-step stirring process that used a mechanical rotary impeller. Each step involved 10 min of stirring process. ***Step-I:*** It was performed at 650^{o}C for 10 min leading to reduction in the agglomerations due to high viscosity of material at low temperature. This led to break up of the agglomeration because of high frictional forces between the reinforcements and matrix. Then molten liquid was then allowed to become semi-solid. ***Step-II:*** It was performed at 750^{o}C (above liquidus) temperature and it allowed the distribution of ceramic nanoparticles due to the liquid property of high flowability and low viscosity at high temperatures. Finally, ultrasonic vibration was performed on the above liquidus temperature because of high flowability of the nanoparticles with low viscosity, where ultrasonic energy waves transferred effectively through liquid pool leading to the creation of cavities and acoustic streaming. The cavitation bubbles are produced

at high temperature (>5000 K) along with high pressure (>1000 atm). Due to the transient difference in pressure and temperature, the bubbles collapse and break the nano agglomerations. Meanwhile, the acoustic stream spreads the nanoparticles into liquid metal and the combined effect of streaming and cavitation process encourages uniform distribution of nanoparticles.

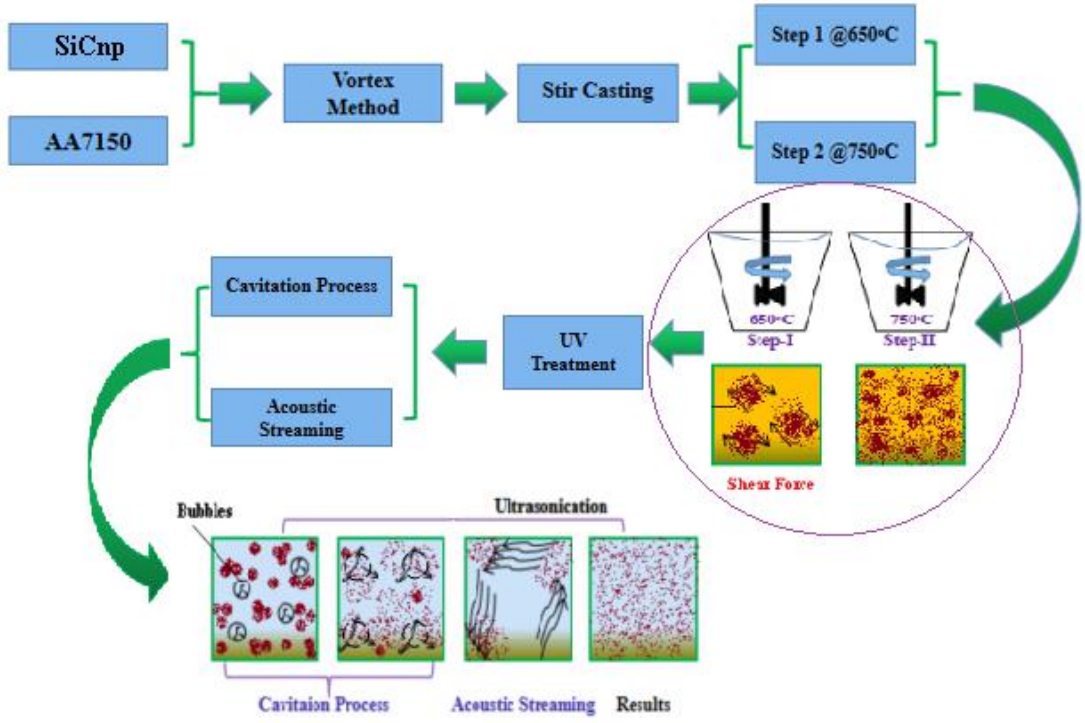

Figure 3. 4 Schematic diagram for detailed mechanism of novel fabrication process.

The fabricated samples were machined as per ASTM standard. The prepared test specimens were used for tensile, fracture and microstructure studies. Density, microhardness and tensile tests were repeated 6 times and mean value of each test was consider to analysis the results. Samples were polished on four different grades of emery paper, where disc polishing, etching, and cleaning were the steps followed to prepare the sample for OM and SEM analysis. Initially the samples were hand polished. Then disc polished for 10 minutes where Al_2O_3 powder was used for better surface finish and then etched. Now the samples were ready for SEM and OM analysis.

3.4 Microstructure analysis

3.4.1 Sample preparation

Samples were polished on four different grades of emery paper followed by disc polishing and etching. To study the microstructure analysis through OM/SEM initially, samples were polished manually on I/0, II/0, III/0, and IV/0 standard emery papers. The direction of polishing changes from one grade to other. Alternatively, perpendicular directions were selected to eliminate all the hatching lines on the surface of the specimen. Then samples were disc polished for 10 minutes, where Al_2O_3 powder was used for better surface finish while mirror-like finish was obtained after disc polishing. Polished samples (**Figure 3.5**) were etched with a solution of Kellar etchant which elevates grain boundaries (25-27 minutes) on the surface and the samples were than cleaned with acetone. OM images were used to investigate the grain refinement of different nanocomposites and SEM for particle distribution as well as fracture surface analysis.

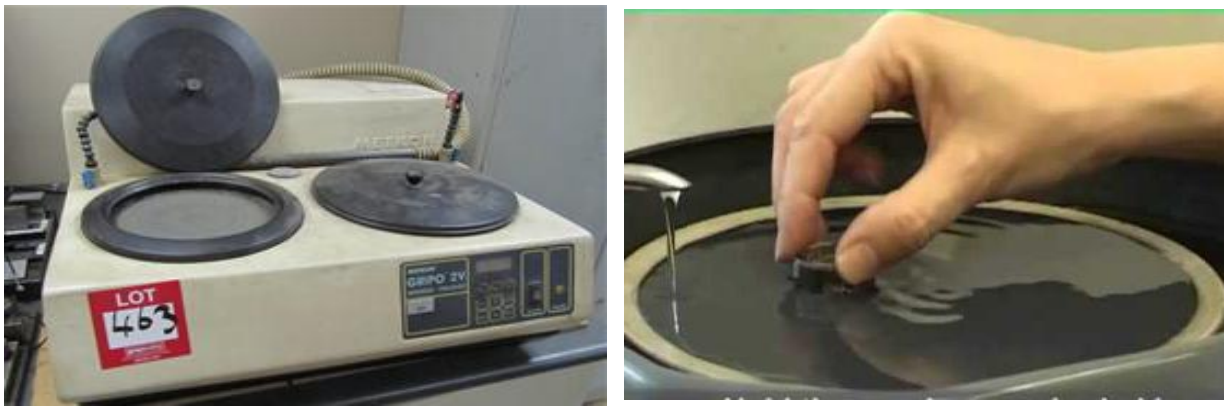

(a) **(b)**

Figure 3. 5 Sample preparation (a) Disc polishing machine (b) Sample polishing.

3.4.2 Optical microscopy

OM studies were carried out on various nanocomposites. The optical microscope is a type of microscope which uses visible light and a system of lenses to show surface morphology (i.e., formation of grain distribution) at different magnification views and the typical diagram is shown in **Figure 3.6**. Microscopic analysis was done for all the samples, and the images were taken at different magnification values.

Figure 3. 6 Optical Microscope.

3.4.3 Scanning electron microscopy

SEM instrument was used to investigate the distribution pattern of particle and fracture surface. EDS was used for elemental analysis and a typical diagram is shown in **Figure 3.7**. Nanocomposite microstructure analysis was performed by SEM (Vega 3 LMU Model, Tescon Make) and elemental analysis was carried out with the help of EDS (Oxford Instruments, U.K).

Figure 3. 7 SEM for microstructure analysis.

3.4.4 X-Ray diffraction

XRD technique is a non-destructive and universal technique to identify phase formation, chemical composition, and crystallographic structure of the specimens. XRD (Model: PANALYTICAL XPERT POWDER) was used to examine the monolithic and

nanocomposites and this has also confirmed the presence of base metal as well as reinforced particulates in elemental analysis. The XRD machine setup (work place: NIT-Warangal, India) is shown in **Figure 3.8**.

Figure 3. 8 XRD for material characterization set up.

3.5 Material properties

3.5.1 Density

The density of monolithic and various weight percentage reinforced composites was calculated using "*Archimedes*" principle, which involves weight in air as well as weight in water. The calculation process of experimental density (Ex-Density) is explained below:

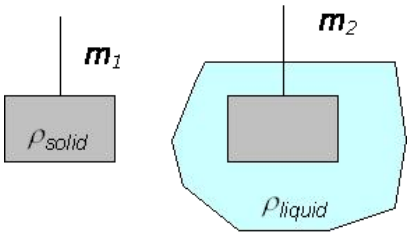

Figure 3. 9 Density calculation using Archimedes principle

$$\rho_{mmc} = \frac{m_1}{m_1 - m_2} \text{-----(3.1)}$$

Where m_1 is the sample mass in air, m_2 is the sample mass in distilled water.

The theoretical density can be calculated using the rule of mixing formula as given below:

$$\rho_{th} = \rho_m V_m + \rho_r V_r \text{ -----} (3.2)$$

Where, ρ_m, V_m, ρ_r, V_r are the density and volume fraction of matrix, and reinforcement particles respectively. The volume faction of each % is calculated through the following equation.

$$V_r = \frac{W_r \rho_m}{\rho_r + W_r(\rho_m - \rho_r)} \text{ -----} (3.3)$$

Where, ρ_m, and ρ_r are the density of matrix and reinforcement particles respectively, and W_r is the weight percentage of reinforcement particles.

3.5.2 Porosity

Porosity plays a critical role to determine the properties of material in the casting process. While porosity levels are normal, when incorporating the particles, the atmospheric air interacts with particles, resulting in porosity. Avoiding porosity is very difficult but it can be minimized and controlled during the process.

3.5.3 Hardness

Hardness of monolithic and particle reinforced nanocomposites were evaluated using Vickers microhardness tester (ECONOMET VH 1MD, 2 kgf), as per ASTM G92 standard (10X10 mm^2 block). The experiment was performed on test surface by applying 200g load for 15sec dwell time and the experimental set up of vickers micro-hardness is shown in **Figure 3.10**.

Figure 3. 10 Micro-hardness tester.

3.5.4 Tensile strength test

Tensile tests were conducted on cast samples of monolithic and nanocomposites using UTM (Make: BLUE STAR WDW-100 S) with a cross-head speed of 0.5 mm/min at atmospheric temperature and the fracture surfaces were captured with SEM. It is also tested heat treated ("T6 heat treatment in which solution treatment is carried out at around 530°C followed by ageing at temperatures in the range 150–180°C") nanocomposites at particular reinforcement to know the influence of temperature over green casting.

Figure 3. 11 UTM for strength prediction

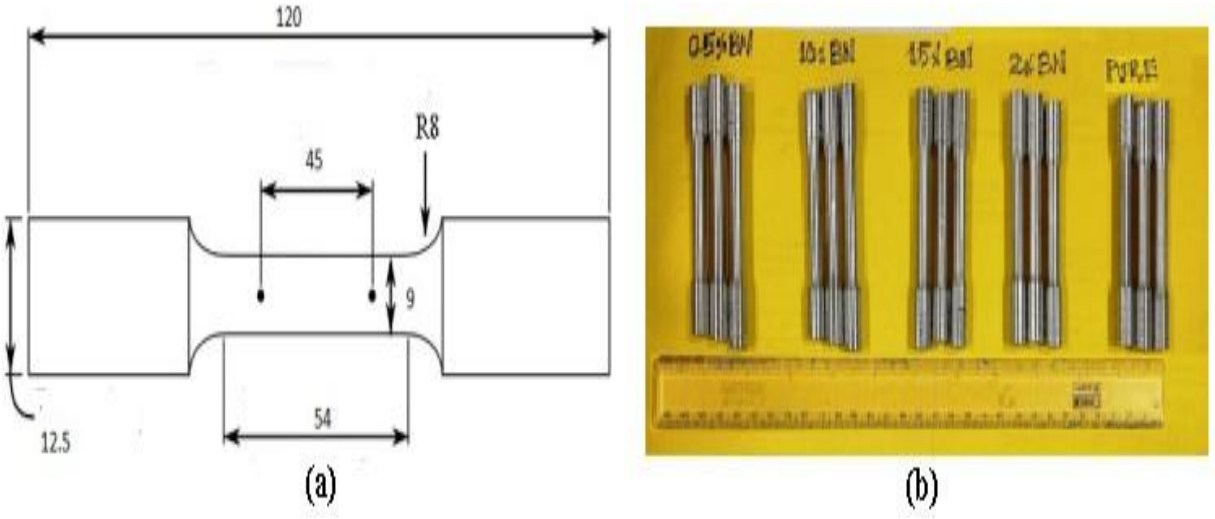

Figure 3. 12 (a) Tensile test schematic diagram and (b) Samples as per ASTM E8.

The tensile behaviour of various nanocomposites was tested as per ASTM E8M standard. The sample size had 9 mm gauge diameter, 45 mm gauge length and 100 mm of total length. The schematic diagram as shown in **Figure 3.12**. For each combination, the test was repeated 6 times.

3.5.5 Wear test

The tribological experiments were carried out at room temperature on POD tribometer by varying the different input parameters such as wt% of reinforcement (0.5-2.0%), applied load (10-40N) against EN 31 stainless steel having 60HRC hardness. The output responses such as COF, Wear loss, and Temperature (^oC) were noted from the Linear Variable Differential Transformer (LVDT). hBN nano particulate reinforced composites were tested for wear parametric influence.

Figure 3. 13 Wear test machine and wear track

3.6 Summary

This chapter deals with the materials such as AA7150, TiC, SiC, B_4C and hBN. Chemical compositions and properties of the matrix and reinforcement particles are discussed. This chapter also explains the experimental procedures like UV process and flow chart for fabrication of individual and hybrid nanocomposites. The detailed mechanism of double stir casting and ultrasonic effect for particle distribution in-terms of ultrasonic cavitation and acoustic streaming was also presented. The material testing and characterization methods were also explained for the composite materials in detailed.

CHAPTER -4

EFFECT OF DOUBLE STIR CASTING AND ULTRASONICATION ON NANOCOMPOSITE

This chapter deals with the fabrication of AA7150-1 wt.% SiC nanocomposite through novel fabrication process and compared with the existing double stir casting technique. The experimental results were displayed through graphical and tabular form.

4.1 Introduction

Ceramic particle reinforced Al-MMCs are widely used in aerospace and automobile industries. Al-Zn-Mg-Cu alloys are used especially in upper and lower wings, fuselage and stringers of aeroplane due to high specific modulus and strength to weight ratio. SiC particles are primary choice as ceramic reinforcement for lightweight alloy matrix due to their exceptional characteristics like high hardness, high melting point, good thermal stability, low CTE, high corrosive resistance and low density. The strength of Al-MMCs depends on the size of reinforcement and interparticle spacing. Micro ceramic particulates incorporated as reinforcement into liquid metal matrix, and show significant improvement in strength of composite material at the cost of declined ductility. Recently nano ceramic particles were introduced to fabricate MMCs and was proved that the size of ceramic reinforcements are playing a crucial role in the MMCs properties and distinctly enhance the base material properties while ensuring beneficial elongation as well as high resistance to creep. The quality of MMNCs fully depends on the ceramic nanoparticle distribution and dispersion into the liquid matrix metal. UV is widely used technique in Al-MMCs to ensure uniform dispersion of micro/nano-sized particles as well as to ensure wettability between the matrix to ceramic reinforcements with reduced porosity.

4.2 Materials and methods

Matrix material was AA7150 (Al-Mg-Zn-Cu Alloy) ingots and nano SiC ceramic particles having 40-60 nm average particle size and >99.9% purity which were used as reinforcements. The density of AA7150 and SiC nanoparticles is 2.83 g/cc and 3.92 g/cc. Mg was used for improving the wettability for matrix and reinforcement, while C_2Cl_6 tablet was used for degassing Al melt pool.

4.3 Experimental results and discussions

4.3.1 Microstructure analysis

4.3.2.1 Optical microscope analysis

Figure 4.1a-c shows the OM images of monolithic and reinforced composite developed by double stir casting as well as novel fabrication methods. The novel process of manufacturing AA7150-1% SiC nanocomposite was evident from the image **(Figure 4.1c)** as the grains were significantly refined when compared to monolithic material and double stir cast AA7150-1% SiC nanocomposites. The Average Grain Size (AGS) can be measured using Linear Intercept Method (LIM) and Planimetric (Jeffries) Method. In this article, LIM was used to find the AGS on principle planes (Transfer and Longitudinal directions) of each microphotograph with the help of "*ImageJ software"*. The measured values were determined using a formula ($\text{AGS} = \frac{\text{Length of the line}}{\text{Number of grains}}$) to get the size of grain. The grain size of nanocomposite decreases with increase of weight fraction of nanoparticles in decrease of nanoparticle size. **Figure 4.1c** also shows that the agglomerations and clusters which were minimized due to novel process nanocomposite compared to double stir casted nanocomposite due the UV effect, which breaks the clusters and agglomerations. The AGS of unreinforced and reinforced materials was calculated using liner intercept technique. The AGS is the ratio of linear length of line to number of grains in a line. The length of line was calculated through "ImageJ Software" and the values of AGS of each material are reported in **Table 4.1.** Fine grain refinement was observed with 24 µm (i.e., 64.7% reduction) in the novel process for manufacturing AA7150-1% SiC nanocomposite compared with base material and 29 µm (i.e., 17.2% reduction) with double stir cast AA7150-1% SiC nanocomposite (Double Stir is 57.3% reduction with base material). The graphical representation of grain refinement is shown in **Figure 4.1d.**

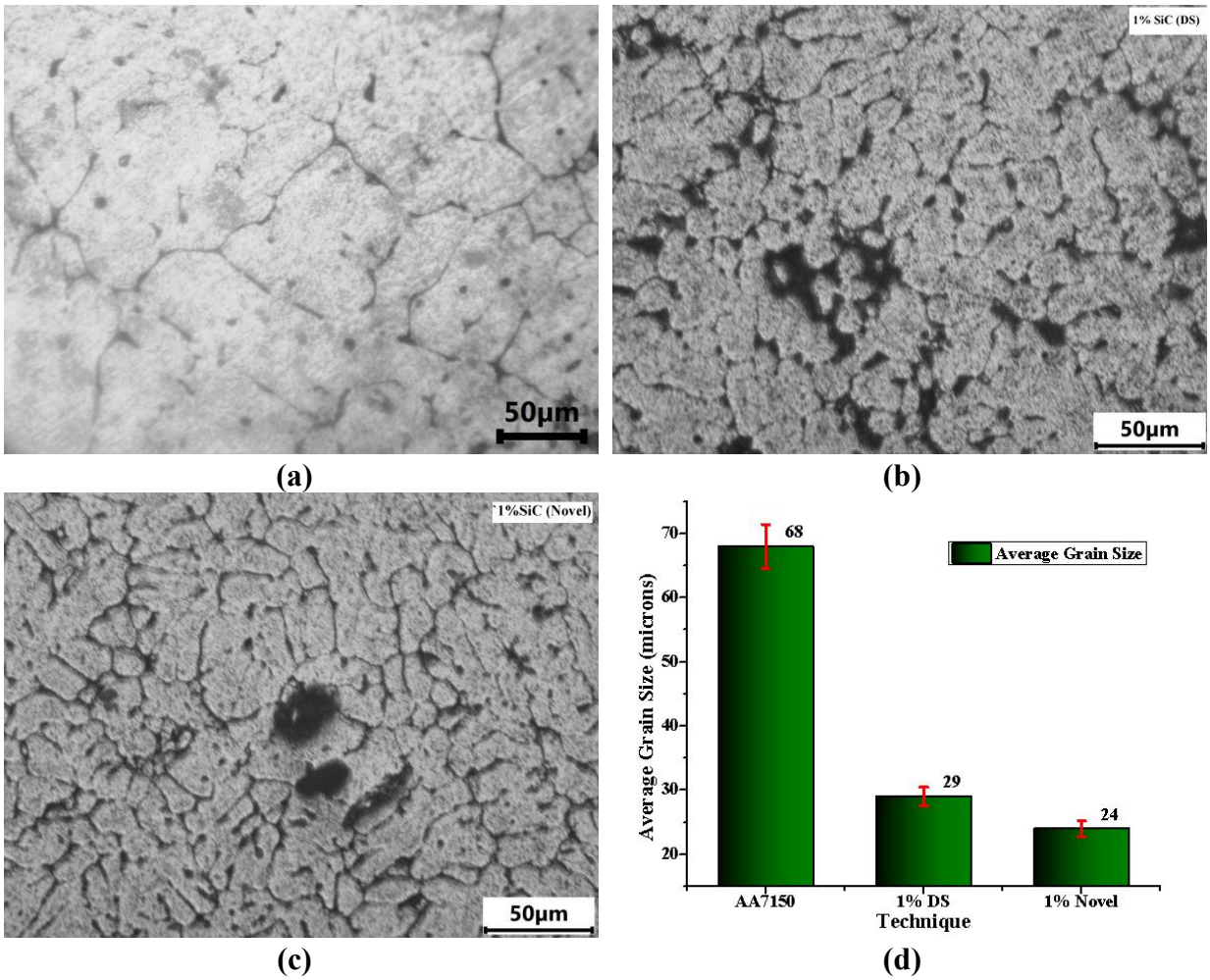

Figure 4. 1 Optical Micro-images of (a) AA7150 (b) Double Stir casting AA7150-1% SiC (c) Novel AA7150-1% SiC (d) AGS of different materials

4.3.2.2 SEM and EDS analysis

Figure 4.2 shows the SEM photographs of 2 µm magnification. Novel fabrication process of AA7150-1% SiC nanocomposite shows uniform distribution of nanoparticles and low porosity as compared to double stir casting process of AA7150-1% SiC nanocomposite. The particle distribution depends on the viscosity of liquid metal. At temperature lower than 650^{o}C, the viscosity of the molten liquid is high and the friction between ceramic reinforcements to matrix material is more while the mechanical stirring. The viscosity of melt decreases with increase in temperature which reduces the friction between molten metal and ceramic nanoparticles. Therefore, mechanical stirring at lower temperature increases particle distribution and reduces agglomerations/cluster size due to more friction. UV treatment at high temperature provides better distribution of mixture due to less viscosity leading to transmission of high energy ultrasonic waves. These waves break the nanoclusters/ agglomerations as well as spread the nanoparticles homogeneously throughout the melt.

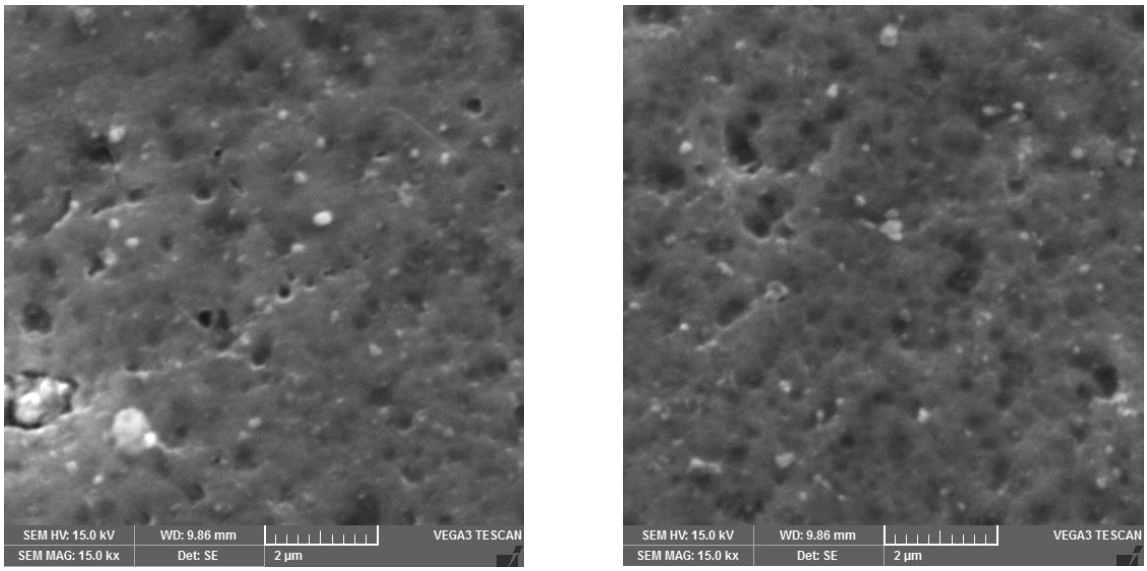

(a) **(b)**

Figure 4. 2 SEM photographs for particles distribution of (a) Double Stir AA7150-1% SiC (b) Novel AA7150-1% SiC

Figure 4.3 shows the SEM photographs with EDS spectroscopy for monolithic as well as 1% SiC nanocomposite at 9µm magnification level. EDS spectroscopy confirms the chemical composition of major elements such as Al, Mg, Zn, Cu for AA7150 and Al, Mg, Zn, Cu. Si, C for 1% SiC nanocomposite.

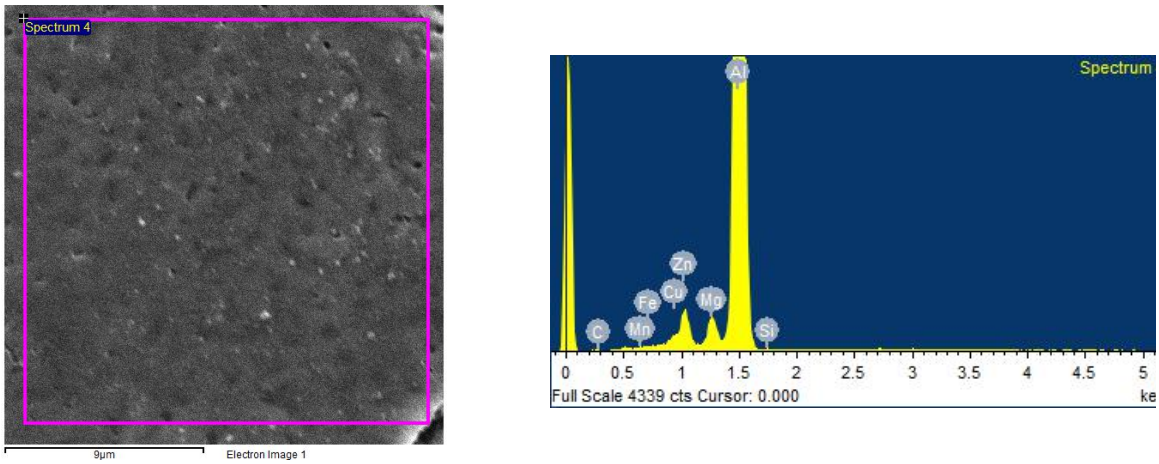

Figure 4. 3 EDS spectrum for elemental analysis at AA7150-1% SiC.

4.3.2 Material properties

4.3.1.1 Density and porosity

Table 4.1 represents the measured density, and porosity of the matrix material, and double stir casting process composite as well as novel fabrication process composites. The density of AA7150-1% SiC composite increased by 3.67% while porosity decreased by

74.1% due to the effect of ultrasonic degassing as compared to the base material. Double stir casting of AA7150-1% SiC composites increased 2.53% while porosity decreased by 51% compared to the base material. The corresponding bar chart for porosity is represented in **Figure 4.4**.

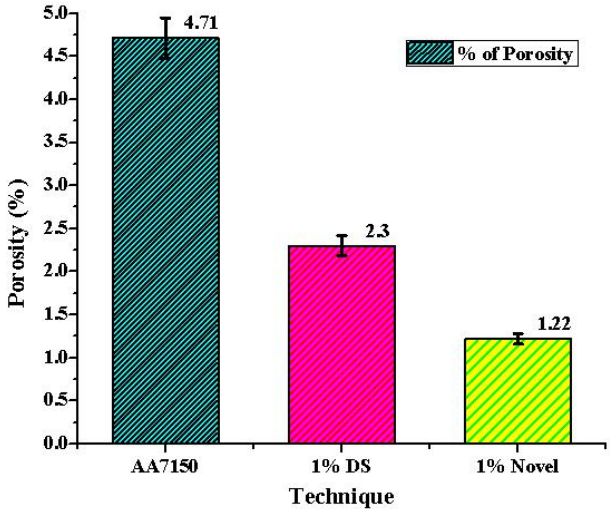

Figure 4. 4 Porosity graph for AA7150, Double Stir process AA7150-1% SiC, and Novel process AA7150-1% SiC

4.3.1.2 Hardness and tensile strength

Figures 4.5, and 4.6 shows the mechanical properties of monolithic and 1% SiC reinforced nanocomposite with different techniques. Uni-axial load was applied gradually and the corresponding results were generated. This load was gradually transferred from particle lacking place to particle-rich place in nanocomposite due to the hard phase SiC particles, because of which load-bearing capacity of the composite increased. The microhardness and strength of novel fabrication process composite was more than that of the counterparts. These improvements were due to decrease in porosity, uniform distribution and grain refinement. The reduction of porosity and increase in grain boundary density reduces dislocation movement resulting in better strength of the composite.

Table 4. 1 AGS and mechanical properties of AA7150 and nanocomposites

Composition	Density (g/cc)	Porosity		Hardness		UTM	AGS	
		(%)	Error	(HV)	Error	(MPa)	(µm)	Error
AA7150	2.6967	4.71	0.235	154	7.725	114.4	68	3.4
AA7150-1% SiC Double Stir	2.7678	2.3	0.115	165.9	8.295	120.6	29	1.45
AA7150-1% SiC Novel	2.7984	1.22	0.061	170.7	8.535	144.2	24	1.2

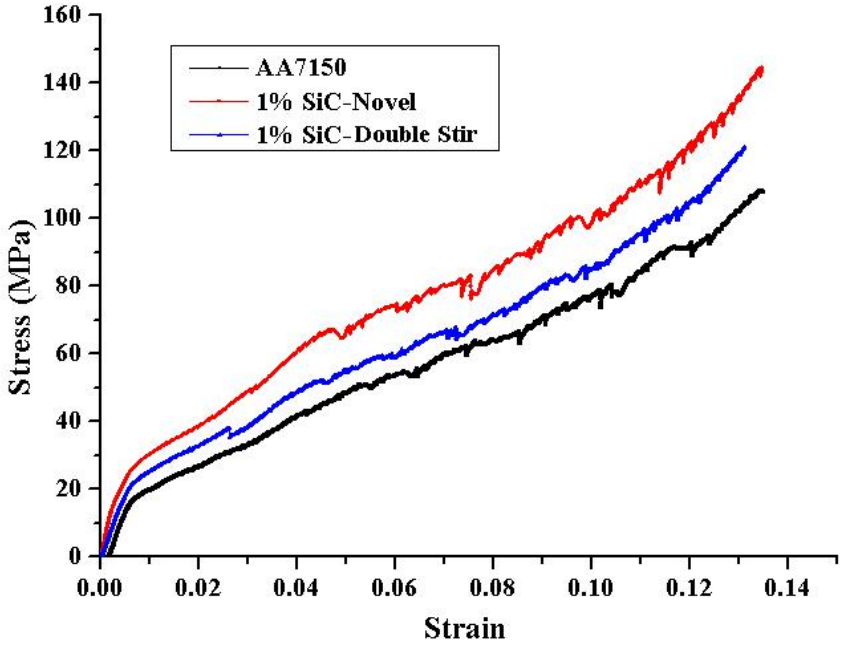

Figure 4. 5 Stress-Strain of AA7150, Double Stir AA7150-1 wt.% SiC and Novel AA7150-1 wt.% SiC

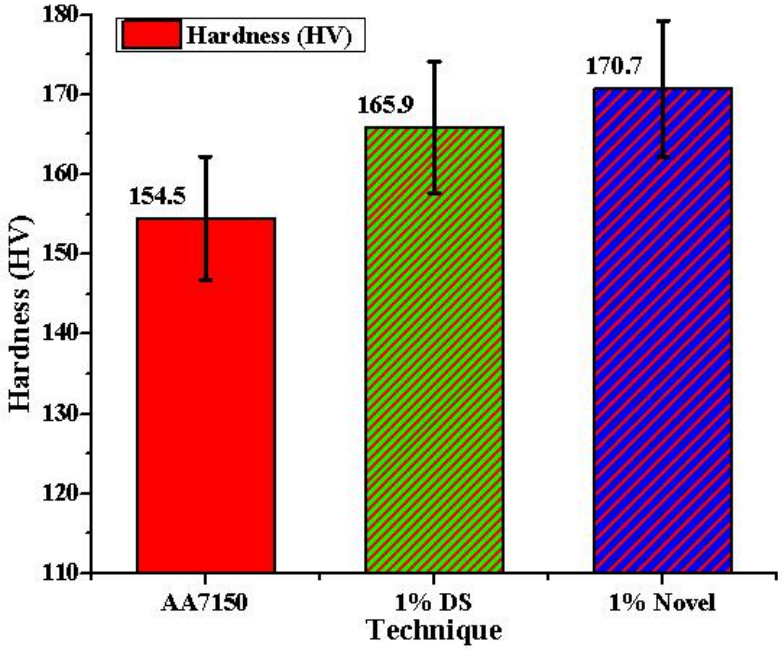

(b)

Figure 4. 6 Hardness graph for AA7150, Double Stir AA7150-1% SiC and novel AA7150-1% SiC

4.3.2.3 Fracture surface analysis

The fracture surface of the novel method fabricated AA7150-1% SiC nanocomposite is shown in **Figure 4.7**. An analysis of fracture surfaces reveals that the failure mechanism is a combination of naturally occurring locally ductile and brittle fracture in the nanocomposite due to soft and ductile nature of Al matrix as well as hard phase ceramic SiC particles. Failure of the composite because of microcracking, voids, and decohesion is evident on the fracture surface. The behaviour of the fracture is governed by ceramic SiC particle mismatch to matrix alloy. It diminishes the strain carrying capacity among the hard phase particles to soft Al-alloy matrix. Therefore, it promotes stress concentration effect of SiC nanoparticles and clusters/agglomerations from the next alloy matrix.

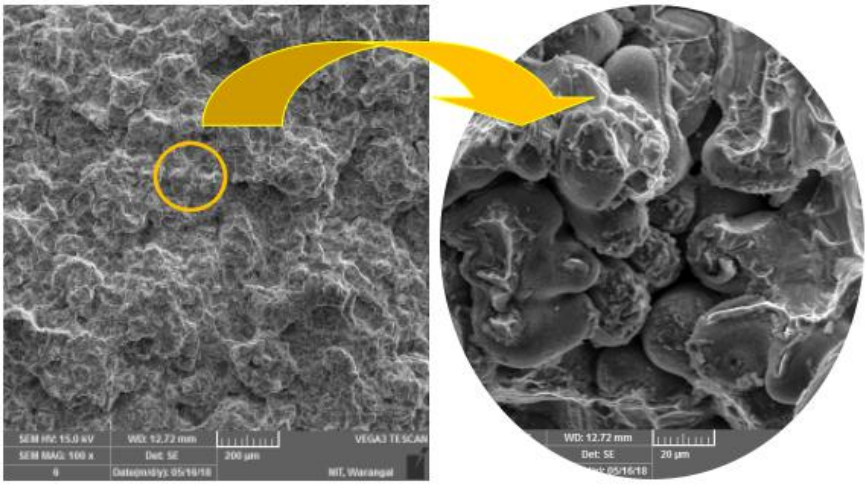

Figure 4. 7 Fracture surface of AA7150-1%SiC nanocomposite.

Based on the analysis of results and discussions, it can be observed that SiC nanoparticle distribution also plays a vital role to improve the mechanical properties. Generally, particle clusters are initial source of crack formation, which leads to load failure of composite materials. The existence of clusters/agglomerations in the composite material is necessary for crack initiation and propagation resulting in the reduction of mechanical properties. Therefore, the novel fabrication process has been introduced successfully to produce AA7150-1% SiC nanocomposite with uniform distribution and better mechanical properties compared to double stir casting process.

4.4 Summary

AA7150-1% SiC nanocomposite was successfully fabricated through a novel fabrication process by combining vortex, double stir casting, and UV techniques. Microstructure and mechanical properties were investigated for novel fabrication process and compared with double stir casting process and base material. The following conclusions are stated below.

1. Grain refinement was observed more in the novel fabrication process than any other process and the AGS of novel process was 24 μm (64.7% reduction) while it was 29 μm (57.3% reduction) for double stir casting process when compared to the base material (68 μm).
2. Double stir casting of AA7150-1% SiC nanocomposite showed 5.42% increase in tensile strength, 7.73% increase in microhardness and 64.7% reduction in porosity compared to base alloy.
3. Novel fabrication process shows improvement in mechanical properties of AA7150-1% SiC with 144.2 MPa (26.05% increase) in tensile strength, 170.7 HV (10.85% increase) in microhardness and 74.1% reduction in porosity as compared to base alloy.
4. SEM photographs confirm that the novel fabrication process led to uniform distribution of nanoparticles and minimum porosity (47% reduction) compared to double stir casting process.
5. SEM photographs of fracture surface of nanocomposites confirm mixed kind of ductile and brittle failure mechanism.

As discussed above and from the obtained results it is confirmed that the novel method of fabrication is very well suited to fabricate nano particulate reinforced metal matrix composites. The same procedure was adopted to fabricate the AA7150 Nanocomposites with hBN, B_4C, TiC, and SiC ceramic particulates as reinforcements. The various tests performed on the fabricated nanoparticulate reinforced metal matrix composites along with the obtained results were discussed in the next chapter.

CHAPTER -5

MICROSTRUCTURE AND MECHANICAL CHARACTERIZATION OF NANOCOMPOSITES

This chapter deals with microstructure and mechanical properties of nano particulates reinforced AA7150 MMCs fabricated using novel fabrication process. Microstructure of nanocomposites were analysed by OM and SEM. The mechanical characterization was done using microhardness tester and UTM. The properties microstructure was evaluated for the following nanocomposites.

1.) AA7150-hBN Nanocomposites

2.) AA7150-B_4C Nanocomposites

3.) AA7150-SiC Nanocomposites

4.) AA7150-TiC Nanocomposites

5.1 AA7150-hBN nanocomposites

5.1.1 Microstructure studies of AA7150-hBN nanocomposites

Figures 5.1.1a-f, show the OM images of monolithic and nanocomposites. In the OM; images it can be noticed that the elements are segregated at the boundaries for matrix materials and the size of the grains reduces (grain refinement) with the content of hBN reinforcement resulting in improvement in mechanical properties.

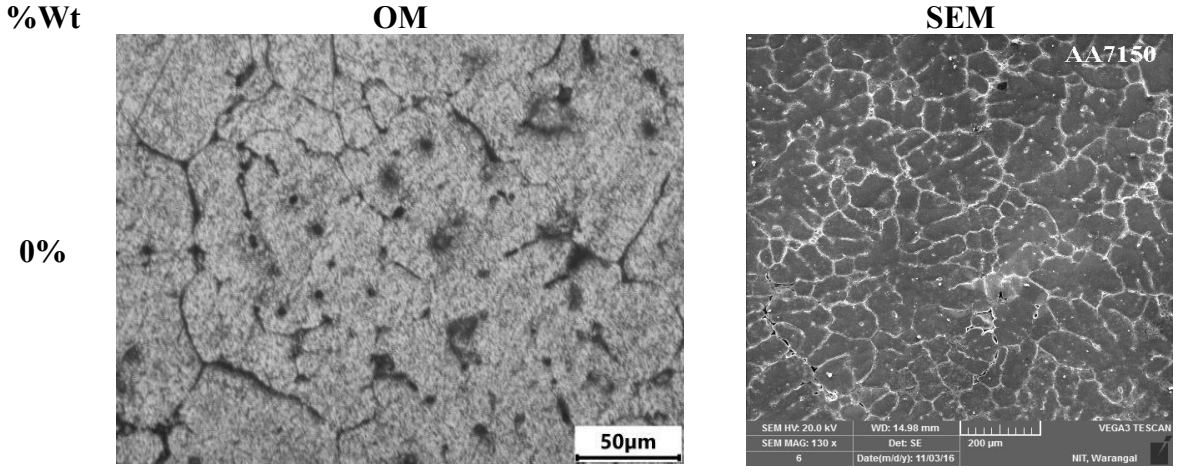

(a) **(g)**

0.50%

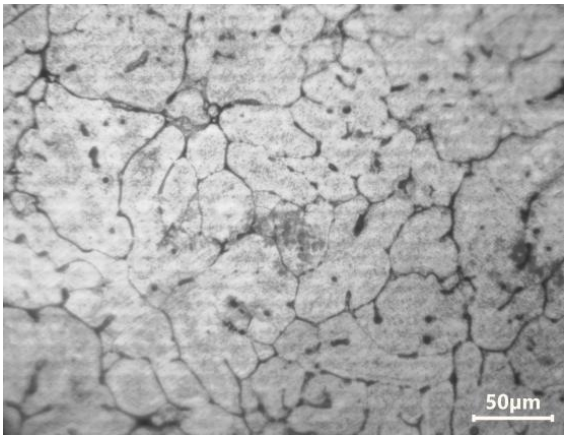

(b)

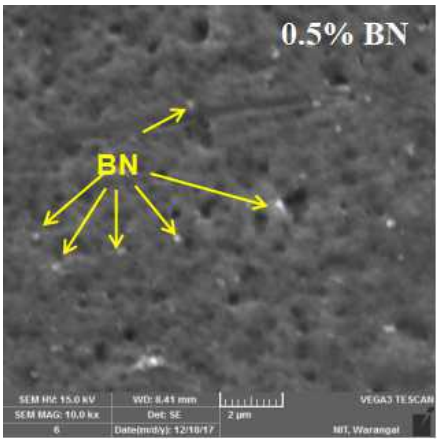

(h)

1%

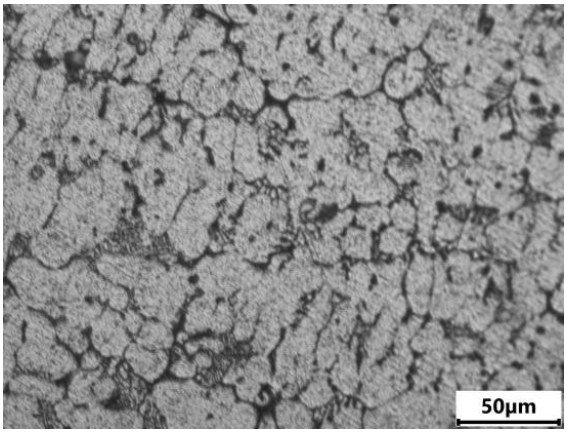

(c)

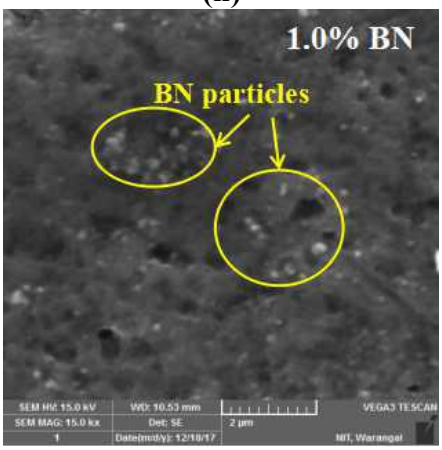

(i)

1.50%

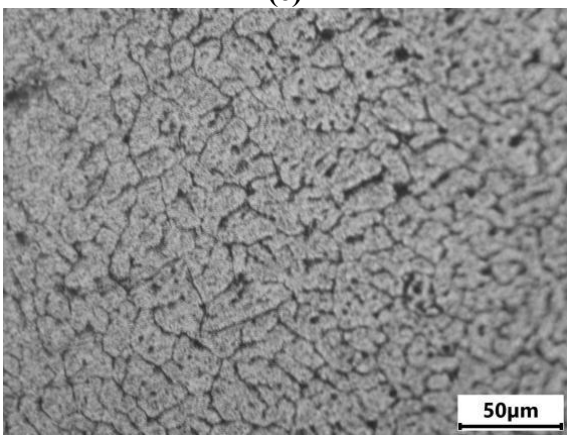

(d)

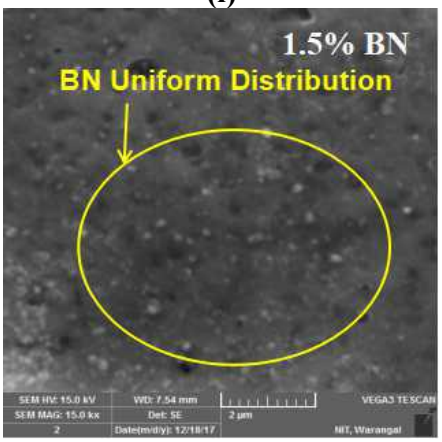

(j)

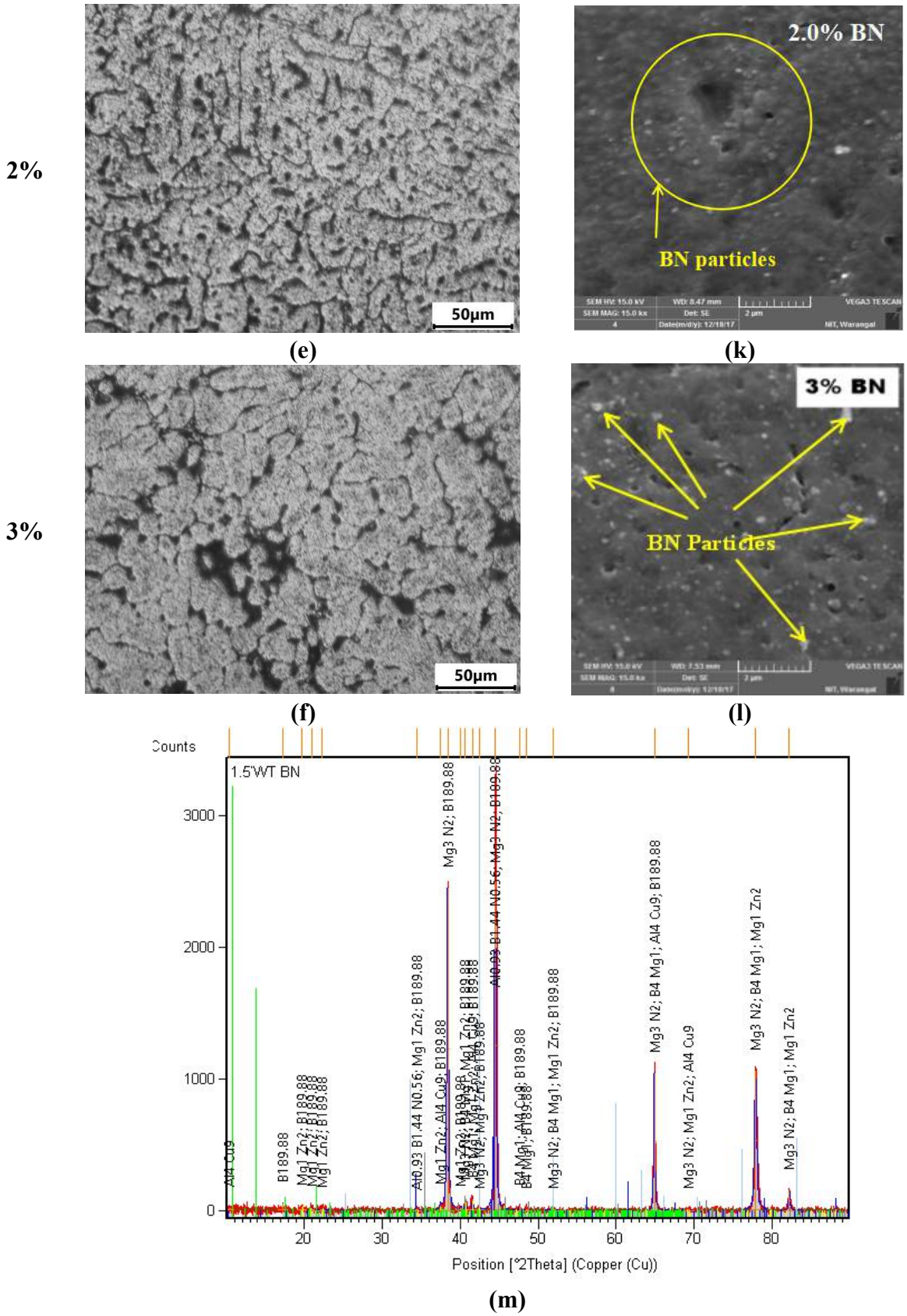

Figure 5.1. 1 (a)-(f) OM images, (g)-(l) SEM images of AA7150, 0.5 wt.%, 1.0 wt.%, 1.5 wt.%, 2.0 wt.%, 3.0 wt.% hBN reinforcement particles, and (m) XRD analysis for chemical composition at 1.5 wt.% hBN.

SEM images in **Figures 5.1.1g-i** show particle distribution of reinforced and unreinforced composites and it may be concluded that (**Figure 5.1.1j)** 1.5% hBN shows uniform distribution, fewer voids and better grain refinement compared to 2% & 3% of hBN, which leads to better mechanical properties. According to Hall-Petch effect, the grain refinement and fine grains show better properties for uniformly distributed particles.

There are several techniques to support the strengthening of MMCs. Each technique is individual and does not depend on a unique technique but several act simultaneously. The current article used grain refinement and fracture surface analysis to predict the strength. From **Figures 5.1.1a-f**, it is observed that there is grain refinement at each composition. The calculated results for monolithic and nanocomposites are presented in **Table5.1.1**. From the results, the finer grain size was confirmed in 1.5%hBN nanocomposite when compared to its counter parts. Hence, it is understood that 1.5%hBN shows superior mechanical properties for Al7150. **Figure 5.1.1m** shows the XRD analysis to analyse the phase interactions of optimal reinforcement. It is observed that the Aluminium Boride Nitride ($Al_{0.93}B_{1.44}N_{0.56}$), Magnesium Nitride ($Mg_3N_2$), Magnesium Boride ($B_4Mg$), Magnesium Zinc ($MgZn_2$), Aluminium Copper ($Al_4Cu_9$), Boron phases are present in the composite.

5.1.2 Mechanical properties of AA7150-hBN nanocomposites

The graphs for both experimental density and porosity are shown in **Figure 5.1.2**. The theoretical density is decreasing with increasing hBN reinforcement particles due to its low density (2.21 g/cc). Theoretical density was calculated using the rule of mixing while experimental density was calculated by "*Archimedes Principle*". From the experimental results, it was observed that the density decreasing with increasing hBN reinforcement due to lower density value of hBN and ultrasonic degassing effect which minimizes the porosity and % of porosity decreases due to ultrasonic cavitation effect as well as closely packed uniform distribution of nanoparticles due to ultrasonic streaming effect.

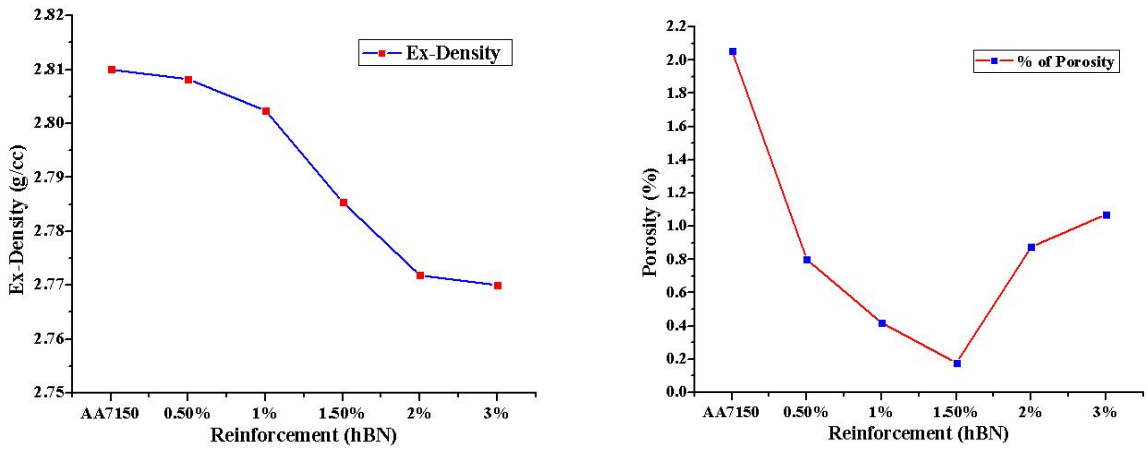

(a) **(b)**

Figure 5.1.2 (a)Ex.Density, (b) % porosity vs different wt.%.

The graphical trend of microhardness is shown in **Figure 5.1.3**. The microhardness of hBN reinforced nanocomposites increases with increasing the wt.% of particle content due to hBN hard phase particles and tight adhesion between hBN as well as matrix material. This limits the movement of dislocation, even distribution of load from matrix to reinforcement particulates and hence increase in hardness.

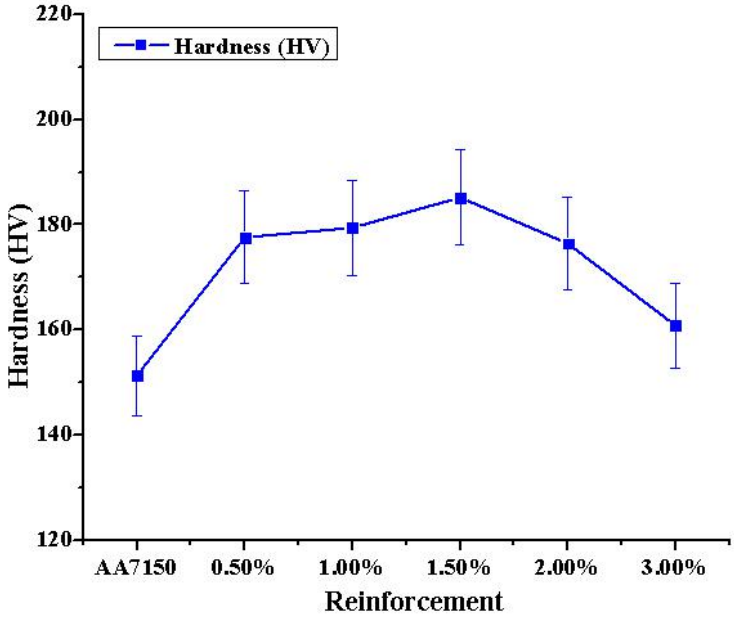

Figure 5.1. 3 Hardness vs different wt.% hBN.

From the figure it is clear that there is increase in hardness with the increase in the wt.% of hBN nano-reinforcement from 0.5 wt.% to1.5 wt.%, further the hardness decreased with the increase in the wt.% of hBN nano-reinforcement. The decrease in hardness of the

NMMCs beyond 1.5 wt.%, hBN was reasoned to the formation of agglomerations, nonuniform distribution and formation of clusters of hBN nano-reinforcement particulates.

Table 5.1.1 shows the results of hardness, ultimate, % elongation and AGS of monolithic and nanocomposites with error values as well. The fracture surface of tensile specimens was studied through SEM pictograph. **Figure 5.1.4** shows the results of Stress-Strain, UTS and % elongation of monolithic and reinforced nanocomposites of hBN particles at T6 condition. It is also compared with the room temperature as shown in **Figure 5.1.5**. Heat treated composites shown better strength and found to be 38.14% enhancement at 1.5% hBN due to grain refinement and fine precipitates at grain boundaries of heat-treated composites. These precipitates can be act as barriers to dislocations, so the UTS of nanocomposites increases. The observations were made based on the results that the UTS increases with increasing wt.% of hBN content by upto 1.5% due to higher dislocation between nanoparticles as well as base material along with the larger surface area of hard hBN phase particles, which bear higher load transformation by matrix during loading and grain refinement. Further improvement in hBN content leads to diminishing strength due to voids, clusters and agglomerations, which advance the failure. The % of elongation also follows the same trend for up to 1.5%hBN and then decreases and is shown in **Figure 5.1.4a**.

Table 5.1. 1 Mechanical properties and AGS of each composition

S. No.	Sample	Hardness		UTS (T6)		% Elongation		AGS (µm)
		(HV)	Error	(MPa)	Error		Error	
1	AA7150	151.3	7.565	141	7.05	4.03	0.2015	76
2	AA7150+0.5%hBN	177.6	8.88	223	11.15	7.684	0.3842	53
3	AA7150+1.0%hBN	179.4	8.97	230	11.5	10.86	0.543	33
4	AA7150+1.5%hBN	***185.2***	9.01	***255***	12.75	***11.78***	0.589	***17***
5	AA7150+2.0%hBN	176.4	8.82	243	12.15	10.30	0.515	26
6	AA7150+3.0%hBN	160.8	8.04	216	10.8	7.22	0.361	34

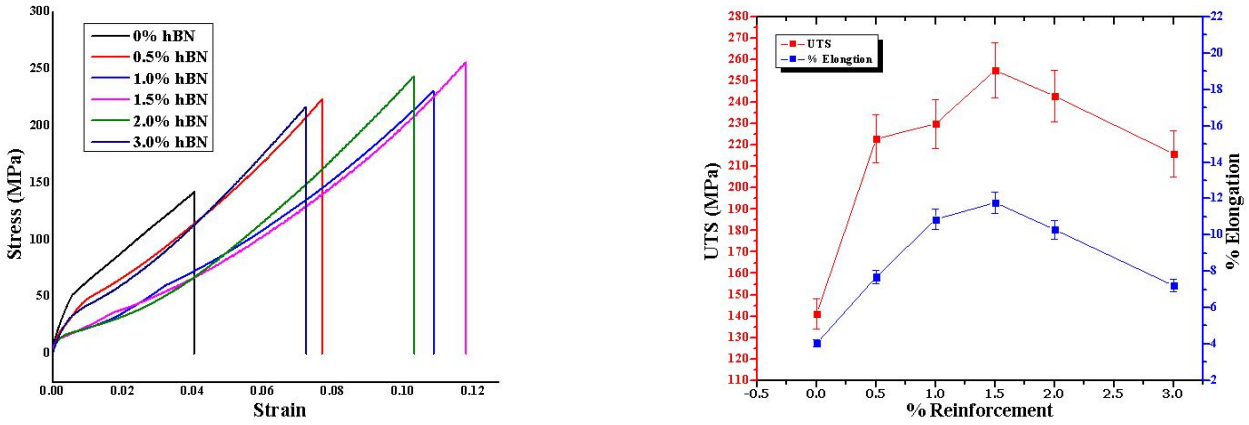

(a) (b)

Figure 5.1. 4 (a) Stress vs Strain curve of monolithic and reinforced nanocomposites (b) UTS, %Elongation vs wt.% at T6.

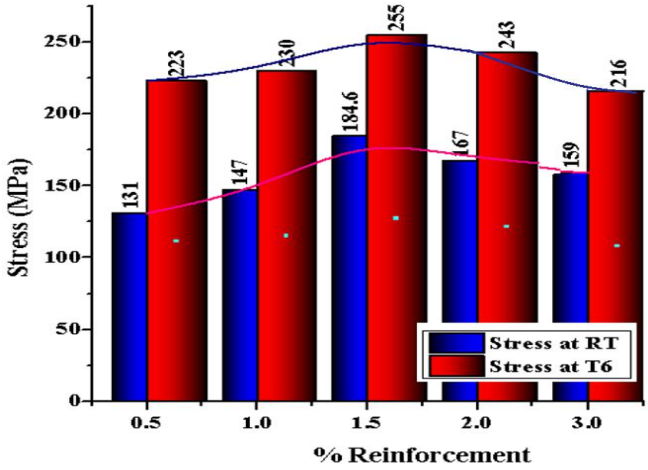

Figure 5.1. 5 UTS of monolithic and reinforced nanocomposites at RT and T6 conditions.

5.1.3 Fracture studies of AA7150-hBN nanocomposites

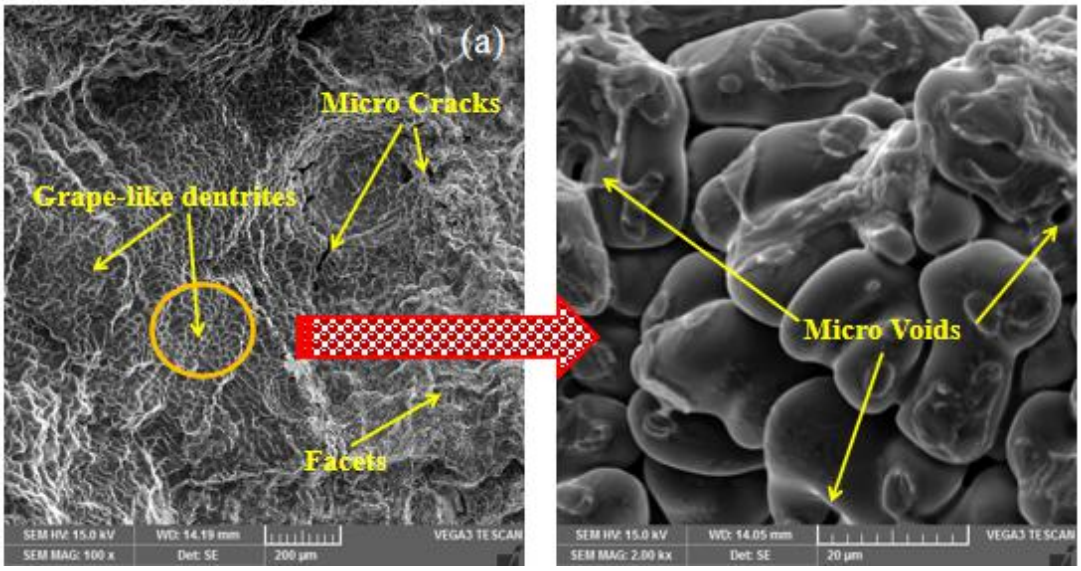

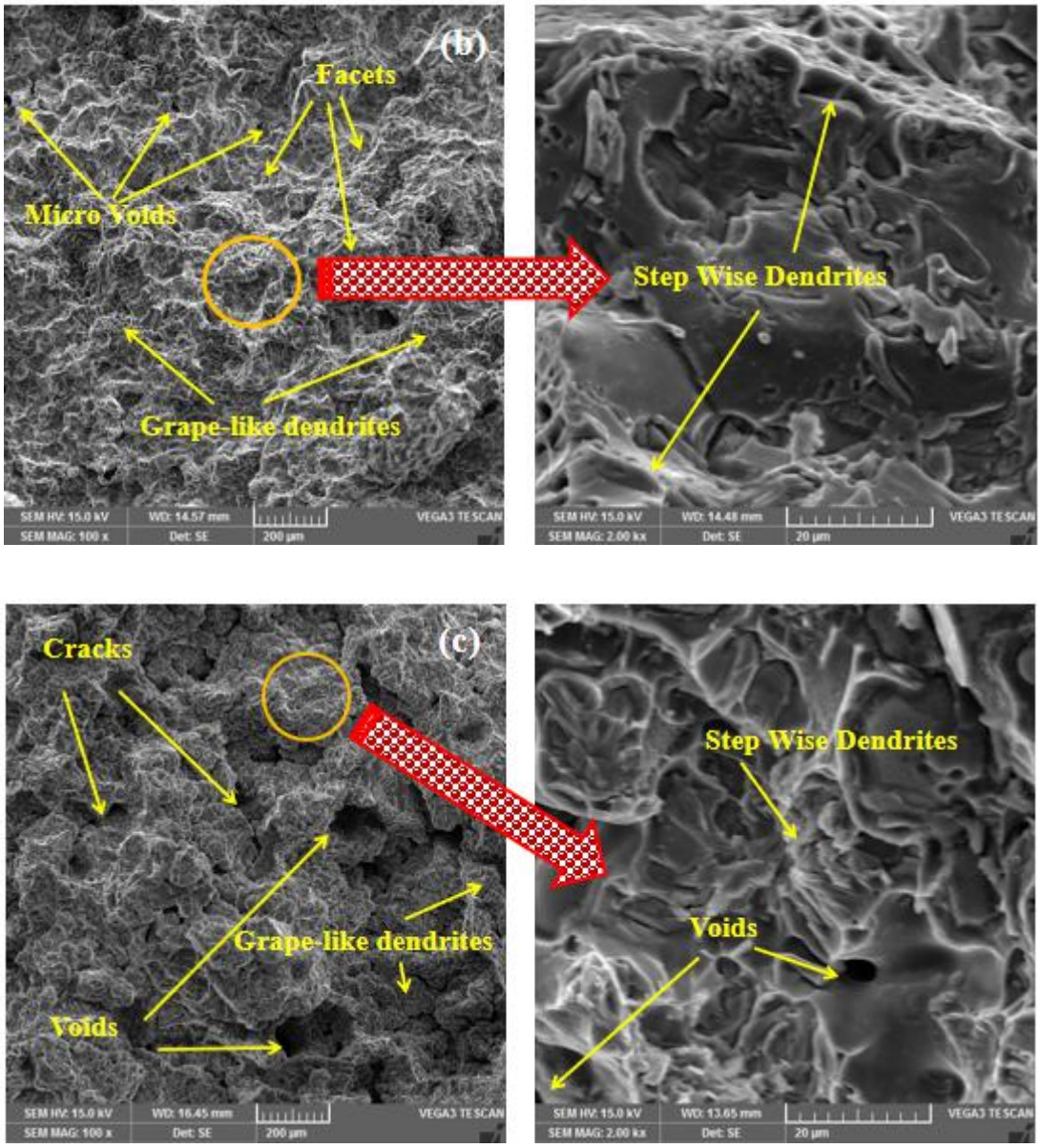

Figure 5.1. 6 SEM images of tensile fracture surface (a) AA7150 (b) AA7150+1.5 wt.% hBN (c) AA7150+3 wt.% hBN.

SEM images of tensile fracture surface at 200-micron scale for monolithic, 1.5 wt.% hBN and 3.0 wt.% hBN reinforced nanocomposites are shown in **Figure 5.1.6** and also enlarged for analysis. **Figure 5.1.6a** represents many voids, cracks and grape-liked dendrites, and the enlarged picture attributes of the grains are caused due to grain detachment; these are confirmed as brittle fracture in nature. **Figure 5.1.6b** represents the image at 1.5 wt.% hBN reinforced nanocomposite, which results in superior properties, with fewer voids, cracks, facets and grape-like dendrites. The enlarged scale shows the facets, step-wise dendrites and its attributes in B-N bonding strength between adjacent layers of crystal structure, which

elevate the surface energy as well as the interface friction required for particles to detach. 3wt.% hBN reinforced SEM image comes with larger voids and cracks (**Figure 5.1.6c**)compared with other two, which confirmed with the declination in properties.

5.1.4 Wear behaviour of AA7150-hBN nanocomposites

The tribological studies related to the fabricated materials were conducted on a fully computerized tribometer at room temperature under dry sliding conditions, the wear experiments at a load of 10-40 N while the sliding distance 3000 m was maintained and sliding speed of 2 m/s was considered and maintained constant. ASTM G-99 standard was followed for the conduction of the tribo experiments with cylindrical specimens of dimensions 8 mm in diameter and 30 mm in length was used for the tribo experiments. The weight loss of the samples was measured in microns for different loads, wt.% of hBN and other output responses with LVDT. The average surface roughness of the Al7150 alloy and its composites pin and disc were maintained at 0.1 µm Ra.

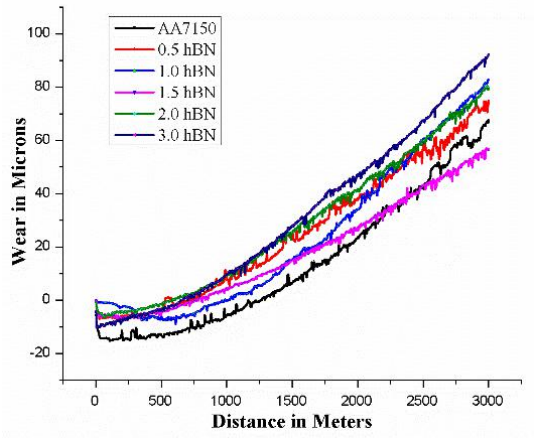

(a)

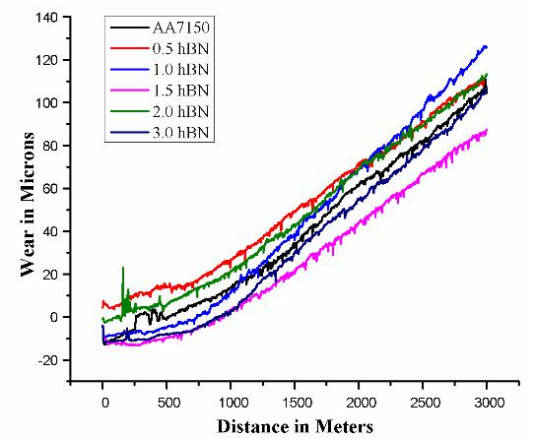

(b)

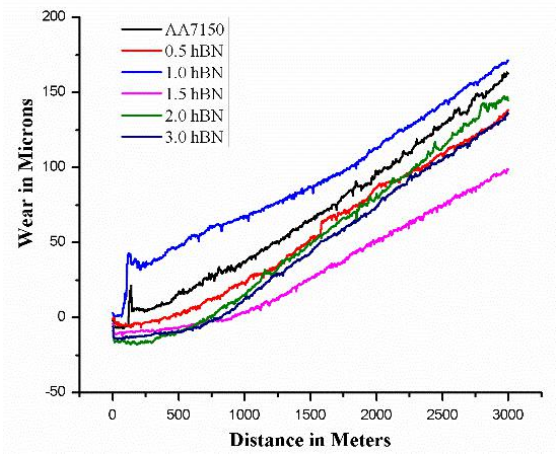

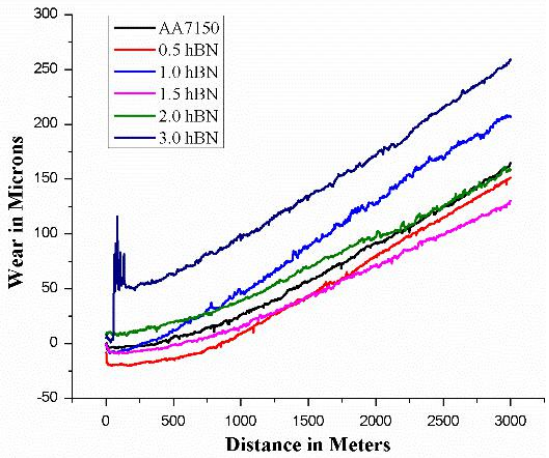

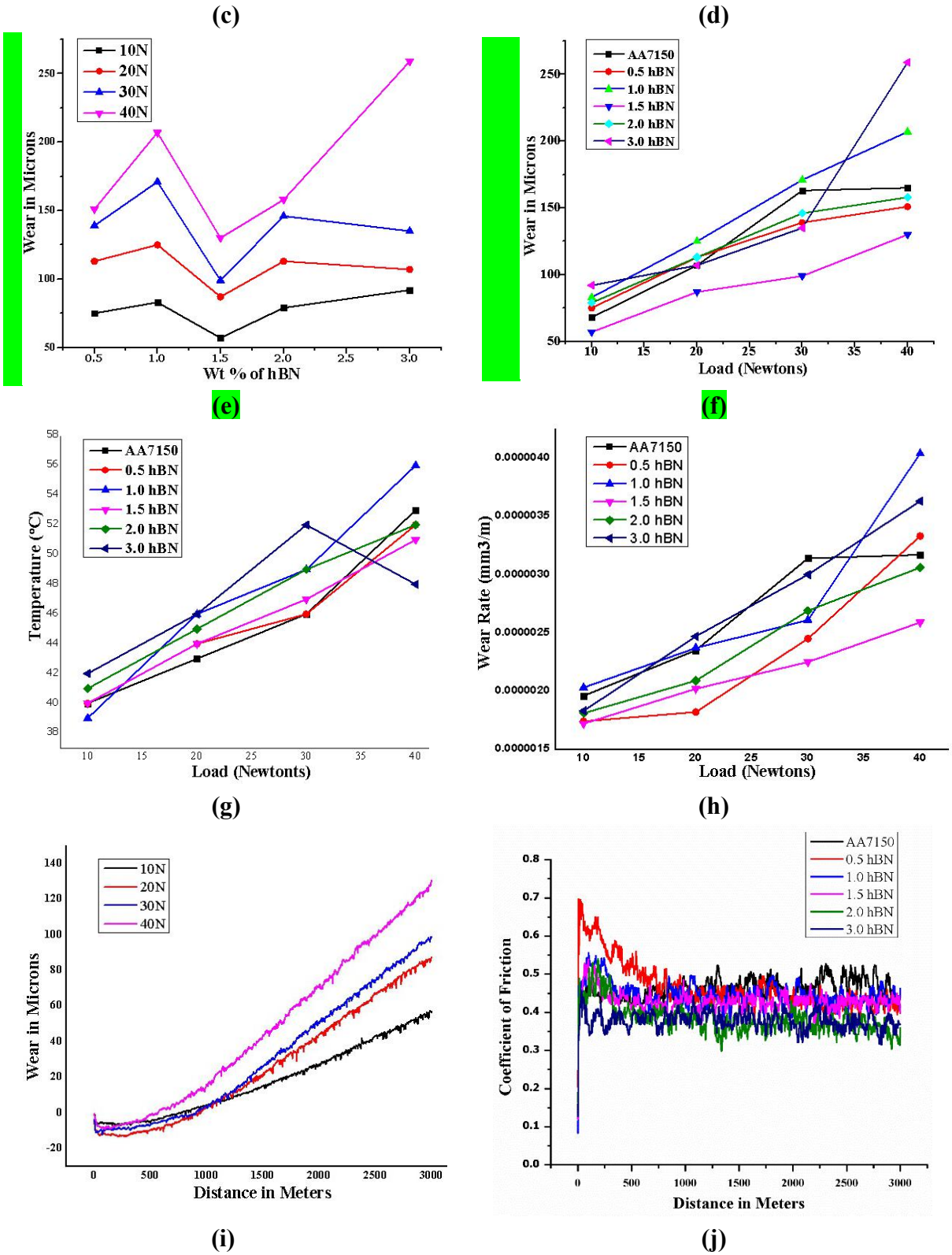

Figure 5.1. 7 (a)-(d) Distance vs wear height loss at each load (e)-(g) Load vs temperature, wear height loss, wear rate (h) wt.% vs wear at each load (i) Distance vs wear at 1.5 wt.%hBN (j) COF at 40 N.

Figure 5.1.7a-d shows the wear loss of sliding distance 3000 m at a load of 10-40 N and it was observed that the wear loss of the monolithic and nanocomposites increases with increasing of sliding distance due to friction between the sliding surfaces hence the higher temperature rise at larger distances leads to soften the pin material and heavy deformation at contact point results in more wear loss. The wear loss of the hBN reinforced nanocomposites was significantly reduced as compared to monolithic material up to 1.5wt.% hBN due to the hardness enhancement, results in seizure and wear resistance improvement of materials. Further higher wt.% of hBN leads to reduce the wear resistance due to lower hardness and the same has been shown in **Figure 5.1.7e**. **Figure 5.1.7f-g** shows the influence of applied load on wear and temperature rise. The graphical trend was confirmed that the load has greatest significant effect and the most influencing tribological parameter. As the load increased, the wear loss also noted to increase and temperature due to higher frictional forces. **Figure 5.1.7h** also shows the wear loss against to wt.% at 25 min time period also attribute that the load increase on the nanocomposites, improves the wear loss respectively. **Figure 5.1.7i** shows that as the load increases, the wear increases with raise in temperature. When the load is low, oxides form on the surfaces of the composites and interact with the metal contact surfaces. These oxides significantly affect the tribo characteristics, results in lower COF and wear rate. Further, when the applied load increased, heat at contact surface is also increased and worn out the oxide layers, therefore the oxide layers are no longer capable of preventing layers at metallic contact surfaces, this frictional heat softens the pin material, resulting in enhancement in the grain size. This is attributed to more contact surface area and increase in wear loss, and further change to delamination with further increase in load. The COF at maximum load at 40 N load, **Figure 5.1.7j** shows that COF decreases with increasing hBN wt.% content as compared to monolithic material due to the interaction of lubricating film with self-mated couples and this leads to smooth contact surface while reducing the COF**.**

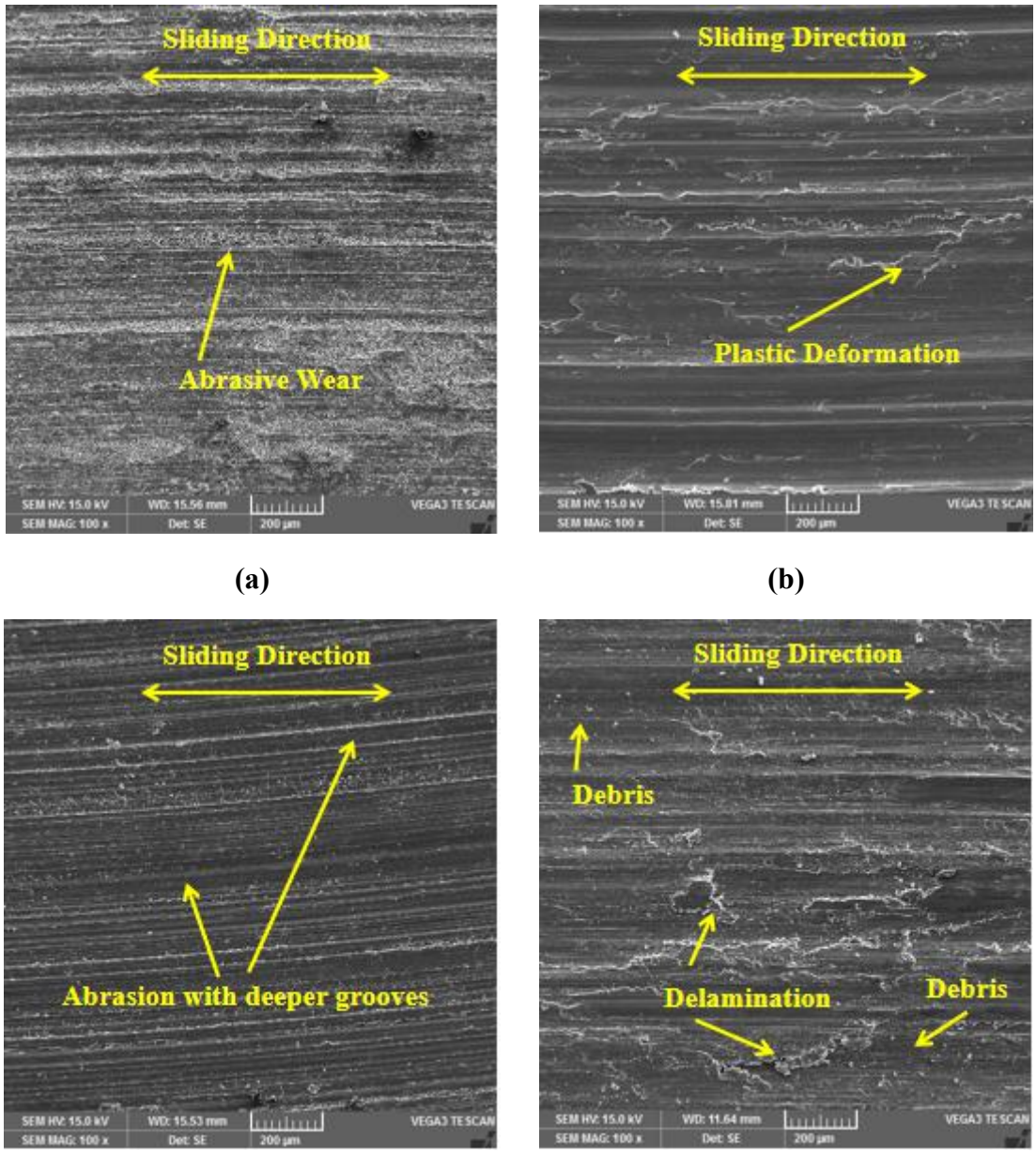

Figure 5.1. 8 SEM images of wear surface (a) AA7150 at 10 N load (b) AA7150 at 40 N load (c) AA7150-1.5 wt.% hBN at 40 N load (d) AA7150-3.0 wt.% hBN at 40 N load.

Figure 5.1.8a-b SEM images display the monolithic worn surface at minimum load 10 N and maximum load 40 N. 10 N image disclose patches of seriously damaged domains, as well as deep abrasion grooves due to lower load and it leads to severe wear. **Figure 5.1.8b** shows the worn surface of the monolithic alloy at a maximum load of 40 N, and reveals more plastic deformation in films as well as deeper grooves due to high frictional temperature, which softens the pin material at coupled region, resulting in massive plastic deformation and

oxide layers. From **Figures 5.1.8a-b**, it is evident that lower loads lead to more delamination as well as abrasive wear; at higher loads heavy plastic deformation results.

Figure 5.1.8c shows the worn surface of 1.5 wt.% hBN nanocomposite at a load of 40 N, and indicates the abrasive wear with deeper grooves due to increase in hBN wt.%; therefore, the plastic deformation is restricted and acts as a protective film, which results in minimum surface damage. **Figure 5.1.8d** displays the worn surface of 3 wt.% hBN nanocomposite at 40 N load, revealing more delamination, debris and oxide layer formation on wear surface.

5.1 Summary of AA7150-hBN nanocomposites

The MMCs of Al7150-hBN nanocomposites were fabricated and the influence of hBN nanoparticles reinforcement was investigated on mechanical, tribological and the following conclusions were inferred. UV assisted double stir casting technique and vortex methods were used to fabricate the novel Al7150-hBN nanocomposites with uniformly distributed hBN nanoparticles.

1. XRD and EDS analysis revealed the major elements of Al7150 alloy and hBN nanoparticles presence in the matrix alloy with no impurities.
2. Increase in hBN wt.%, increased the hardness and strength (151.3-185.2 HV and 141-255 MPa) of the nanocomposites due to uniform distribution, grain refinement and hard phase particles, which promotes load bearing capacity. Further increment in hBN wt.% decreases the hardness and strength (185.2-160.8 HV and 255-216 MPa) due to voids, clusters and agglomerations.
3. Microstructure analysis of Al7150-hBN nanocomposites OM & SEM reveals the grain refinement, uniform nanoparticle distribution and nature of failure in nanocomposites.
4. Wear loss of nanocomposites decreased with the increase in the hBN nanoparticle reinforcement due to hardness enhancement, which leads to seizure and wear resistance.
5. Graphical representation of wear results confirmed that the load has greatest influence on wear loss and temperature due to higher frictional forces.
6. SEM images of wear surface reveals that the wear is an abrasive type with restricted plastic deformation and acted as protective layer at 1.5 wt.% hBN. 3 wt.% hBN reveals more debris, oxide layer and delamination on wear surfaces.

5.2 AA7150-B_4C nanocomposites

5.2.1 Microstructure studies of AA7150-B_4C nanocomposites

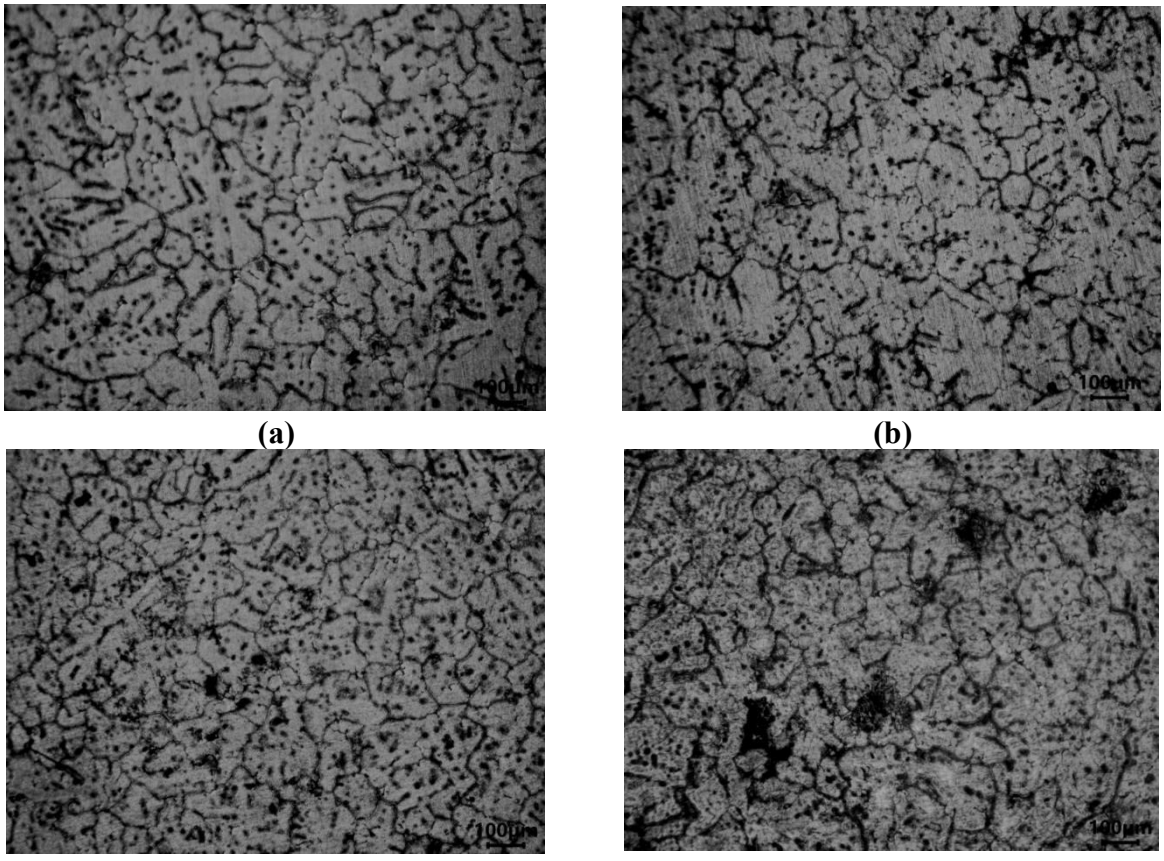

Figure 5.2. 1 OM images of(a)0.5% B_4C (b)1.0% B_4C (c)1.5% B_4C (d)2.0% B_4C.

The strength of the material depends on the grain size and it increases as the grain size reduces as per Hall-Petch theory. Toughness and ductility of material are significantly affected by the grain size. Throughout AA7150-B_4C nanocomposite liquid solidification process, the B_4C nanoparticles act as the centre of non-homogeneous nucleation as well as reinforcement of matrix alloy grains. The main reason for maintaining the ductility of composites even after inclusion of reinforcements is due to the grain refinement and size reduction of the matrix material. Therefore, grain refinement is an attractive mechanism compared to other strengthening mechanisms due to the retention of ductility as well as toughness of the materials.

From the above **Figure 5.2.1a-d**, it is clear that the formation of grain boundaries decreases by up to 1.5 wt.% and then increases to 2.0 wt.% due to high content of cluster

particles along with nanoparticles. Therefore, 1.5 wt.% nanocomposite has higher strength compared to other wt.% reinforcements.

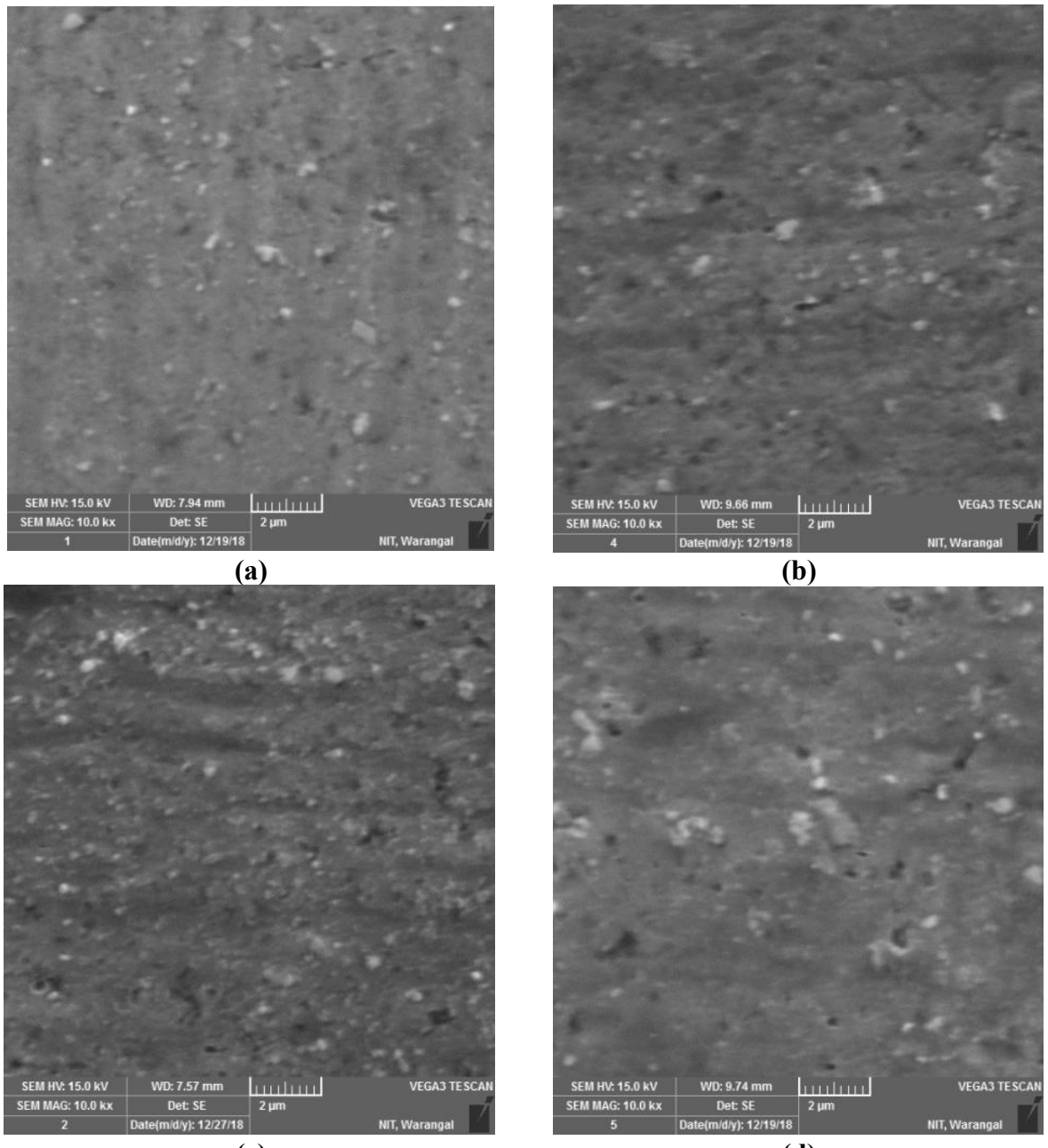

Figure 5.2. 2 SEM for nanoparticles distribution B_4C in AA7150 matrix alloy (a) 0.5% B_4C (b) 1.0% B_4C (c) 1.5% B_4C (d) 2.0% B_4C.

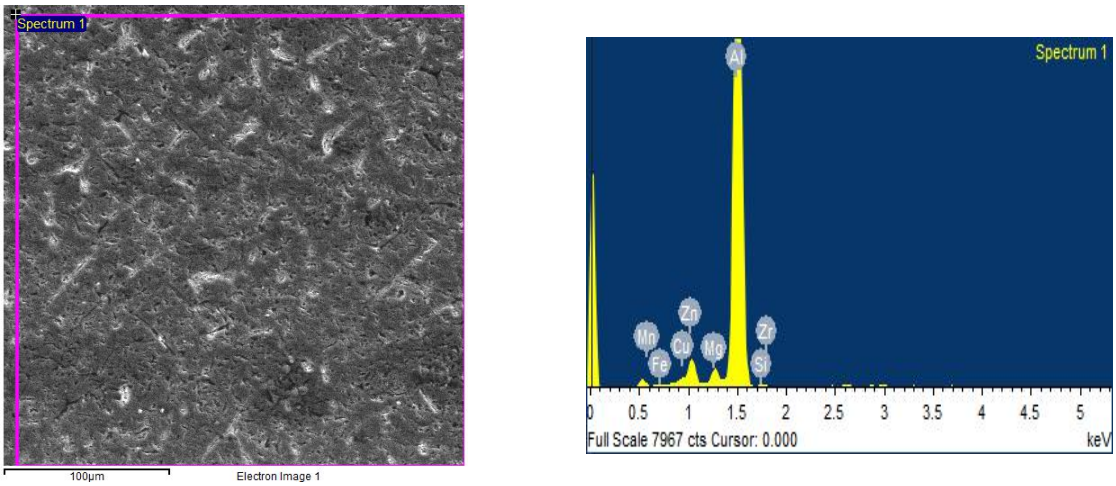

(a)

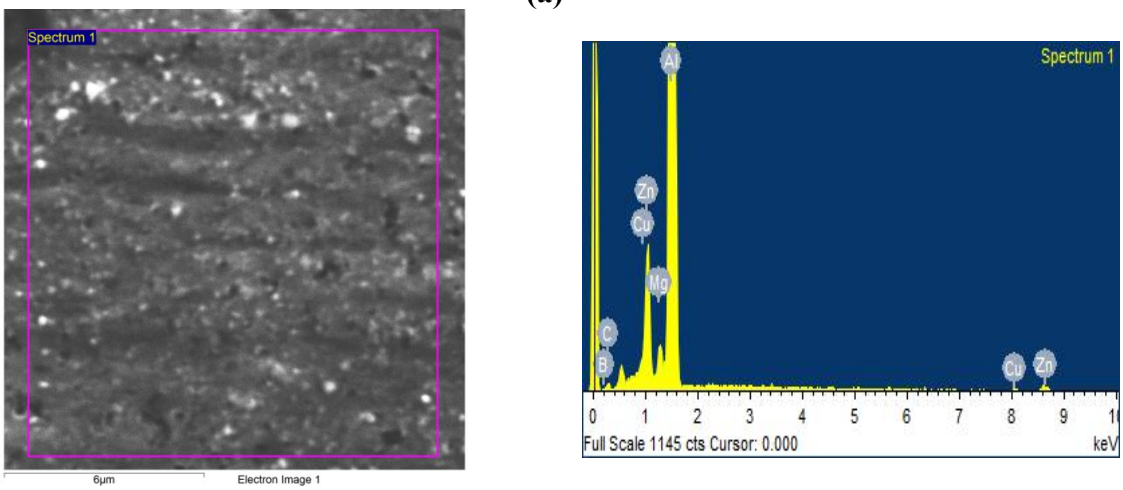

(b)

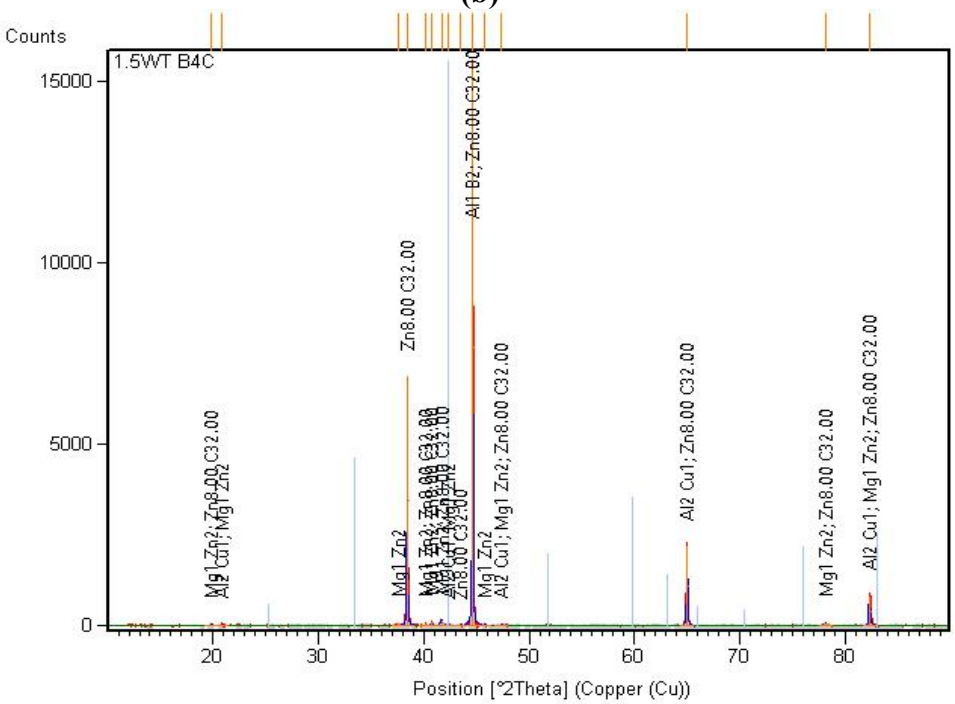

Figure 5.2. 3 EDS for elemental analysis (a) AA7150 (b) 1.5% B_4C (c) XRD for chemical composition at 1.5 wt.% B_4C.

Figure 5.2.2 shows particle distribution of various wt.% of nanocomposites and it is observed that there is uniform distribution of B_4C nanoparticles of 0.5, 1.0, 1.5, & 2.0 wt.%. It is also observed that 1.5 wt.% of B_4C represents more particles and homogeneous distribution throughout the AA7150 matrix alloy. **Figure 5.2.2d** clearly indicates that the number of voids and cluster is increased and the porosity spread around the material which leads to increase in grain sizes. **Figure 5.2.3** shows the elemental analysis of monolithic, optimal wt.% of (1.5% B_4C) nanocomposite using EDS and XRD analysis at 1.5wt.%. It is confirmed with the interaction phases like Aluminium Boride (AlB_2), Magnesium Zinc ($MgZn_2$), Aluminium Copper (Al_2Cu) and ZnC_4 in the composite. EDS confirmed with the presence of the major alloying elements in monolithic material like Al, Cu, Mg, Zn and nanocomposite like Al, Cu, Zn, Mg, B, C.

5.2.2 Mechanical properties of AA7150-B_4C nanocomposites

Figure 5.2.4 shows the experimental results of density and porosity of various nanocomposites as well as base metal. It is observed that the experimental density decreases with the increase of reinforcement content due to lower density of B_4C (2.52 g/cc) particles. Porosity of the nanocomposites decrease first and then increase at 2.0% with increase of B_4C content. Increase of porosity at 2.0% B_4C is mainly due to voids, cluster formation and it is confirmed by **Figures 5.2.1d and 5.2.2d**.

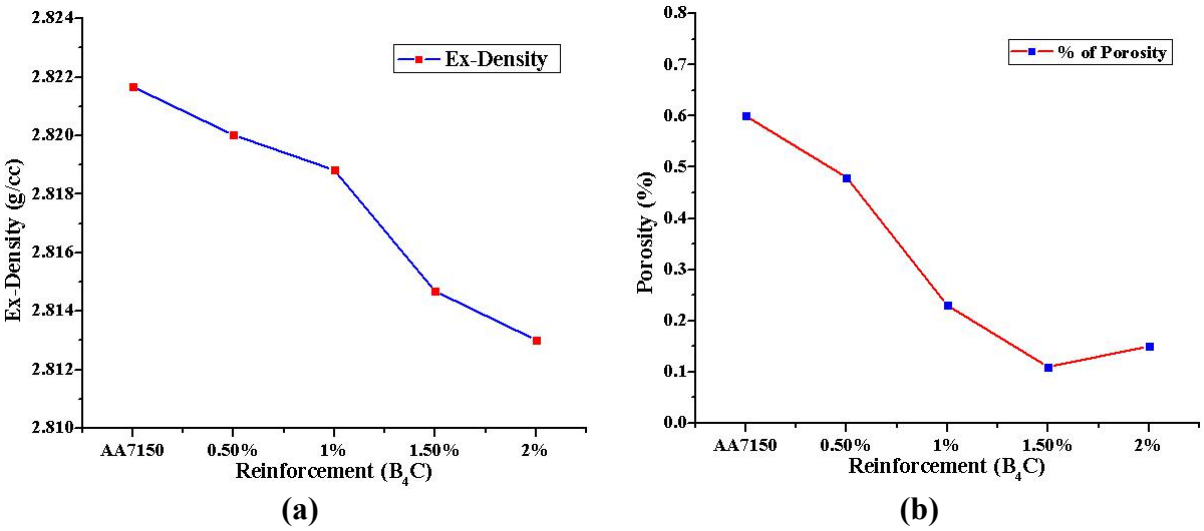

Figure 5.2. 4 (a)Ex-Density and (b) % Porosity graphs against to wt.%.

Figure 5.2.5a shows the results of Vickers hardness test for various nanocomposites. Hardness behavior of B_4C reinforced MMNCs is represented through bar graph and the

corresponding values are shown in **Table 5.2.1**. Hardness increases with increase of particle wt.% gradually due to UV, which in turn leads to homogeneous mixing of B_4C. Movement of dislocation can be prevented by the engulfed B_4C particle as the indentor movement increases when particle congregation increases near the indentor and it leads to an increase in hardness of nanocomposites. There is a reduction in the value of hardness at 2wt.% due to the formation of a large number of clusters compared to other wt.%.

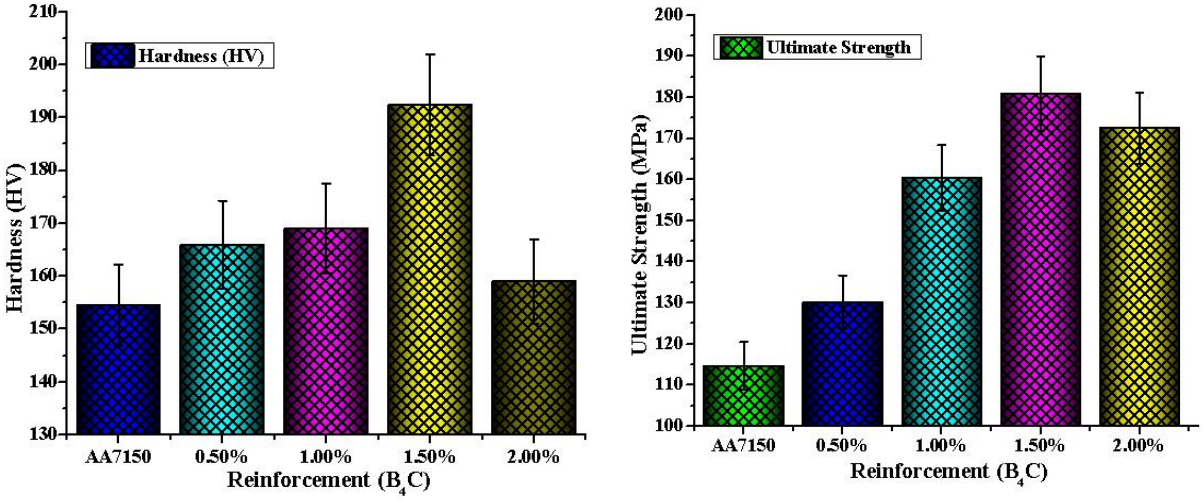

(a) **(b)**

Figure 5.2. 5 Bar chart for (a) Micro-hardness Vs wt.% B_4C (b) UTS Vs wt.% B_4C.

Table 5.2. 1 Mechanical properties of various nanocomposites and monolithic material

Reinforcement (wt.%)	Hardness		Yield Strength	Ultimate Strength		% Elongation
	(HV)	Error	(MPa)	(MPa)	Error	
AA7150	154.5	7.725	35	114.7	5.735	13.34
AA7150+0.5% B_4C	166	8.3	41	130.15	6.5075	13.49
AA7150+1.0% B_4C	169	8.45	66	160.39	8.0195	14.08
AA7150+1.5% B_4C	***192.4***	9.62	***77***	***180.9***	9.045	***16.27***
AA7150+2.0% B_4C	159	7.95	96	172.5	8.625	13.69

Figure 5.2.5b shows the tensile results of the base material and B_4C nanoparticles reinforced composites at room temperature. The effect of B_4C reinforcement in Al-MMNCs was analyzed for tensile values. It was observed that the UTS increases as B_4C wt.% increase by up to 1.5%. average value of UTS of base metal and 1.5 % B_4C reinforced nanocomposites are 114.7 MPa and 180.9 MPa and beyond 1.5% B_4C, Al-MMNCs register an increase in voids, clusters, and agglomeration. Therefore, the strength of 2% B_4C nanocomposite exhibits

grater reduction in properties and the % of elongation follows the same trend as shown in **Figure 5.2.6**. The reason can be rightly attributed to the interaction of ultra-fine B_4C particles which lead to grain refinement that increases the UTS. Large UTS with increased ductility make this material useful for industrial and structure-related application.

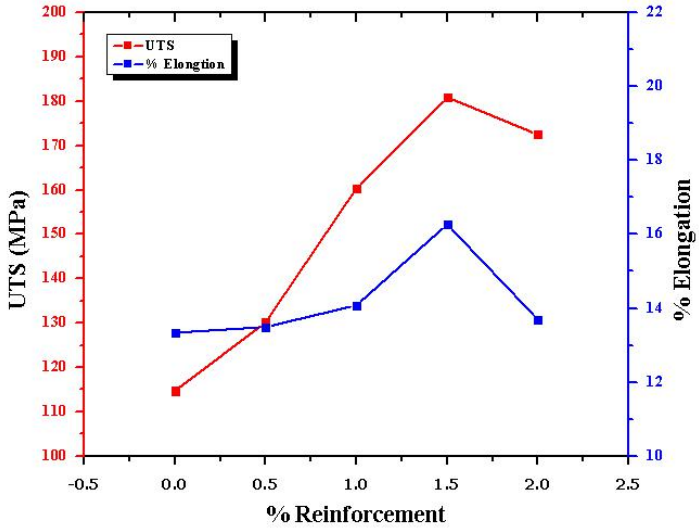

Figure 5.2. 6 Line graph of UTS and % elongation against to % reinforcement.

5.2.3 Fracture studies of AA7150-B_4C nanocomposites

Tensile fracture surface fractographic images at 100X magnification for base metal and different wt.% of reinforcement are shown in **Figure 5.2.7**. The optimal wt.% fractography was enlarged for the fracture surface analysis and it is represented in **Figure 5.2.8**. **Figures 5.2.7a-e**, reveal that the number of cracks, voids, and grape shaped dendrites are more at monolithic material and are moderately increasing, while increasing wt.% of reinforcement particle content. **Figure 5.2.7d** confirms that the voids and cracks are minimized compared to other wt.%. Further increment in wt.% leads to an increase in huge voids and cracks which are of various shapes and sizes as confirmed by **Figure 5.2.7e**. It is also confirmed that facets and dimples are present. A large number of dimples are associated with particulates and the samples failed because of brittle behaviour without any identification of neck formation. Therefore, the nature of the failure of AA7150-B_4C may be said to be semi-brittle.

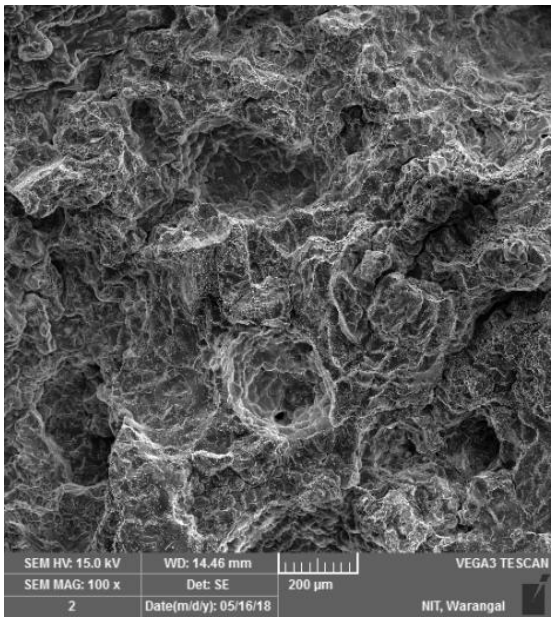
SEM HV: 15.0 kV
WD: 14.46 mm
VEGA3 TESCAN
SEM MAG: 100 x
Det: SE
200 µm
2
Date(m/d/y): 05/16/18
NIT, Warangal

(a)

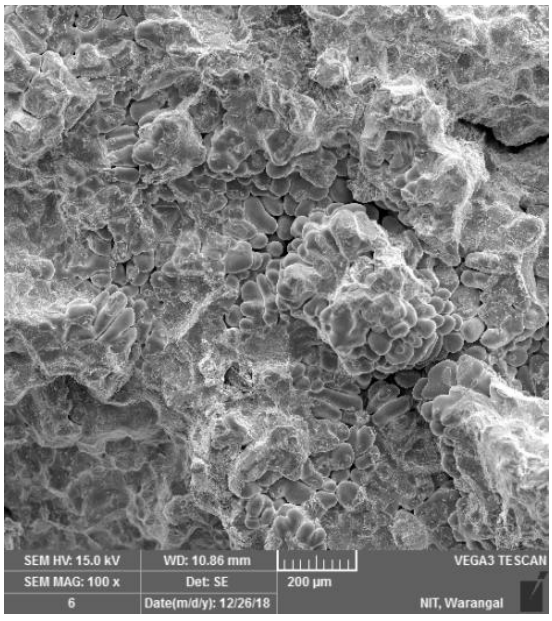
SEM HV: 15.0 kV
WD: 10.86 mm
VEGA3 TESCAN
SEM MAG: 100 x
Det: SE
200 µm
6
Date(m/d/y): 12/26/18
NIT, Warangal

(b)

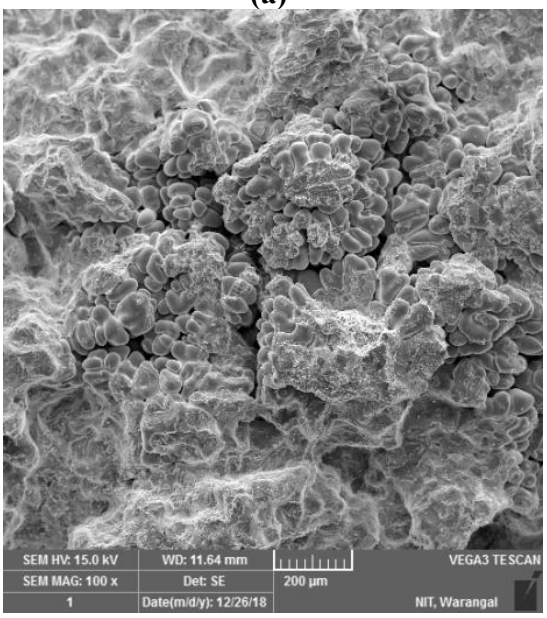
SEM HV: 15.0 kV
WD: 11.64 mm
VEGA3 TESCAN
SEM MAG: 100 x
Det: SE
200 µm
1
Date(m/d/y): 12/26/18
NIT, Warangal

(c)

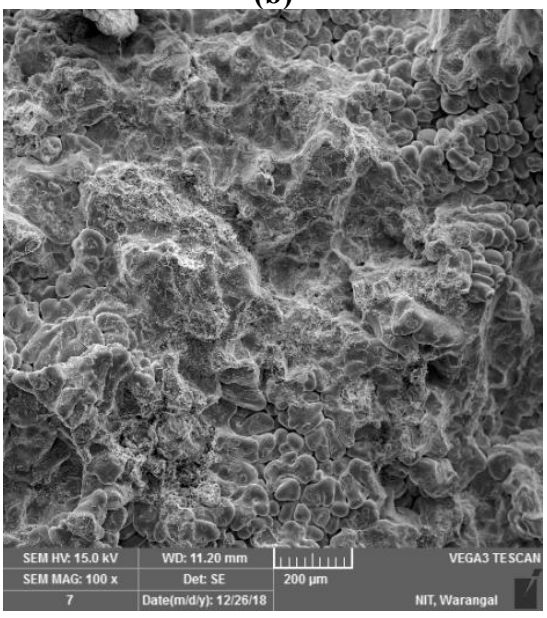
SEM HV: 15.0 kV
WD: 11.20 mm
VEGA3 TESCAN
SEM MAG: 100 x
Det: SE
200 µm
7
Date(m/d/y): 12/26/18
NIT, Warangal

(d)

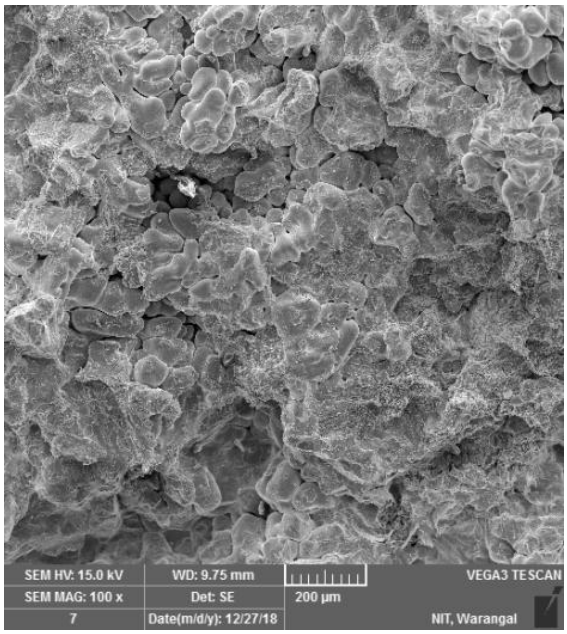

(e)

Figure 5.2. 7 Fracture surface of (a) AA7150 (b) 0.5 wt.% B_4C (c) 1.0 wt % B_4C (d) 1.5 wt % B_4C (e) 2.0% B_4C.

Figure 5.2.8 shows the enlarged photography of 1.5%B_4C nanocomposite at 20µm from a 200µm fractograph. The enlarged photography shows many stepwise dendrites and facets. At the same time, it also reveals the boron-carbide strength of the next crystal layer, which elevates the high surface energy and friction between adjacent interfaces required to detach the particles. Therefore, it leads to optimal strength of nanocomposites.

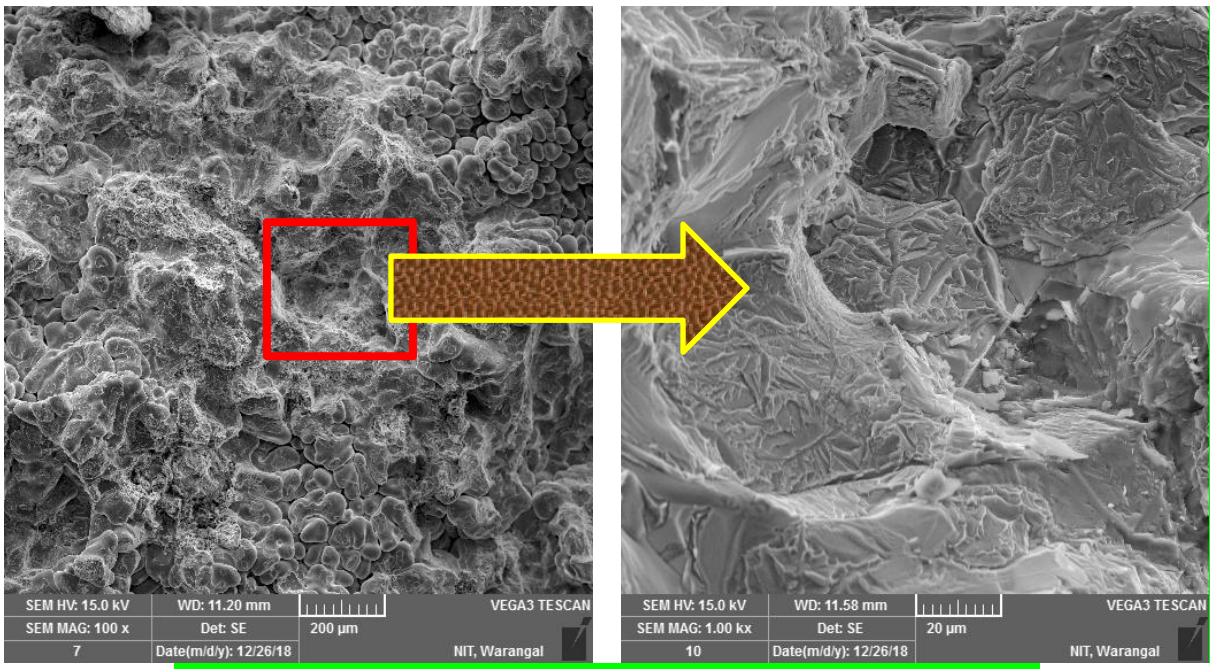

Figure 5.2. 8 Enlarged fracture surface of 1.5%B_4C nanocomposite.

5.2 Summary of AA7150-B_4C nanocomposites

AA7150-B_4C nanocomposites were successfully fabricated through UV assisted double stir casting technique using vortex method. The experiments were conducted in as-cast condition. Mechanical properties were found to increase with increase of B_4C particles reinforcement of up to 1.5 wt.% and any further increase led to reduction in mechanical properties due to the presence of voids, clusters, and agglomeration. Microstructure analysis confirms good bonding, formation of grain boundaries and uniform distribution of nanoparticles at 1.5% B_4C compared to others. Porosity decreases while increasing the nano particle content at the observed minimum of 1.5% B_4C (0.11%). Micro-hardness and UTS significantly improved by 154.5-192.4 HV (57.7%) and 114.7-180.9 MPa (24.5%) and the nanocomposite found to have optimal properties at 1.5%B_4C. Fine ductility of AA7150-B_4C was maintained without compromising its strength, while maximum ductility of 16.27% was reported at optimal wt.% of B_4C. Fractographic studies reveal the brittle nature of failure in nanocomposites.

5.3 AA7150-SiC nanocomposites

5.3.1 Microstructure studies of AA7150-SiC nanocomposites

The grain refinement of a particle reinforced nanocomposite is a crucial strengthening mechanism because it improves the strength and fracture toughness of the composite at low-temperature conditions. The strengthening value is given by Hall-Petch formula ($\sigma_{hp} = \frac{K}{\sqrt{d}}$) where, K is strength coefficient and 'd' is the grain size. Therefore, the strength of the composite material is inversely proportional to the grain size of the material. Strengthening and grain refining takes place because of dislocation interactions with grain boundaries. SiC nanoparticles act as nucleation sites towards the matrix phase and limit the solidification procedure in composite material, which results in grain refinement. Therefore, the grain refinement of AA7150 increases the grain boundary's density and protects the movement of dislocations, which contribute to the strength in composite material. Grain refinement is enhanced with increase in wt.% of ceramic reinforcement particles. **Figures 5.3.1a-d** show the grain refinement of alloy matrix grains and reinforcement magnitude with the addition of second phase ceramic nanoparticles and it increases with an increase of wt.% of SiC nanoparticles by up to 1.5 wt % in nanocomposites. Beyond 1.5 wt.% of SiC, the grain size of the matrix increases as shown in **Figure 5.3.1e,** due to clusters/agglomerations, voids, and these are confirmed with SEM photograph **Figure 5.3.2d.**

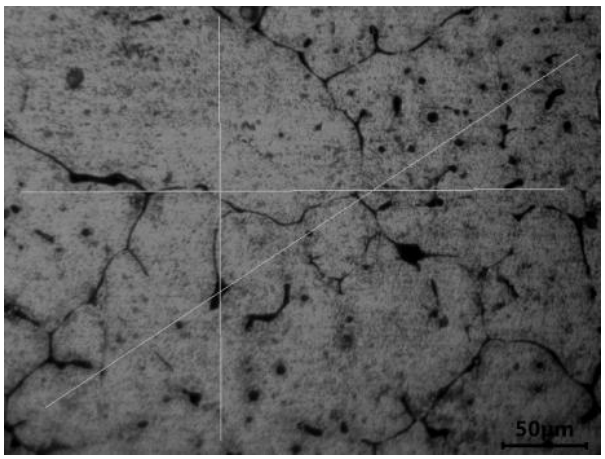

(*a*)

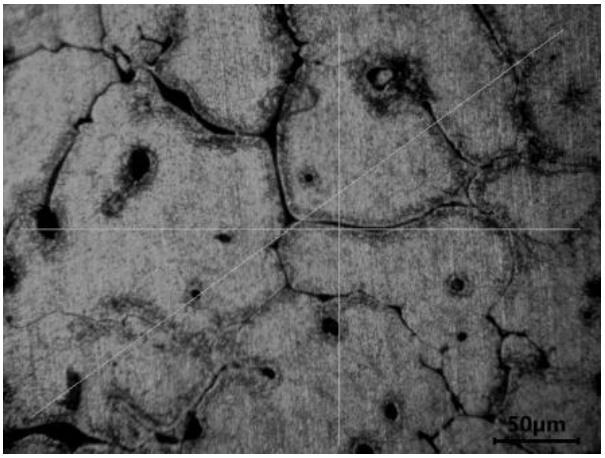

(*b*)

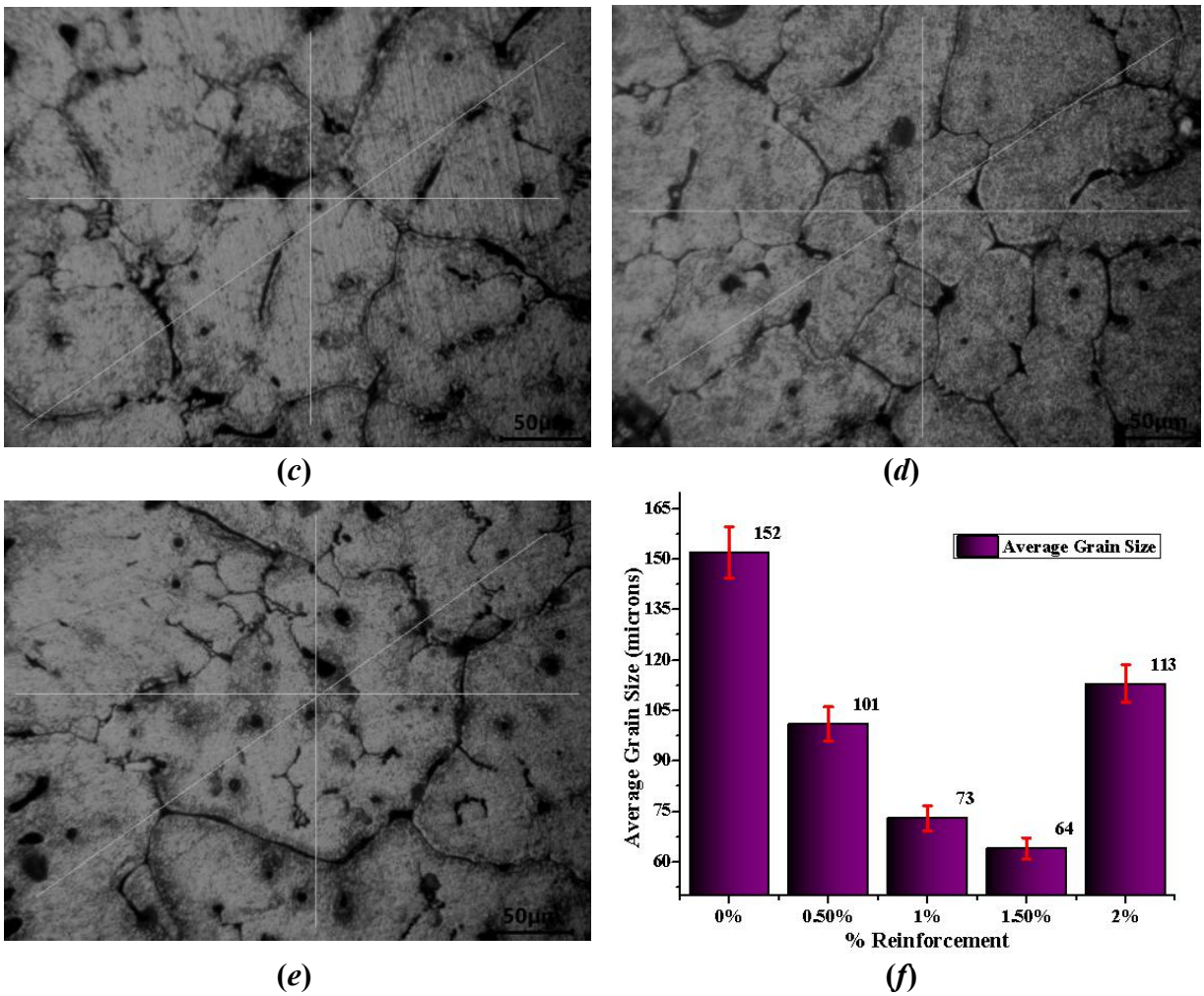

Figure 5.3. 1 Optical microstructure for grain refinement of (a) AA7150, (b) 0.5 wt.% SiC, (c) 1.0 wt.% SiC, (d) 1.5 wt.% SiC, (e) 2.0 wt % SiC, and (f) Graphical representation of AGS

The magnitude of grain refinement size was calculated through LIM and *ImageJ software*. The grain sizes were measured in the direction of principal planes and the values obtained are represented in **Table 5.3.1**., and the corresponding graphs are shown in **Figure 5.3.1f**. From the result, it is observed that the % reduction in grain size is 57.9% compared to alloy matrix.

Figures 5.3.2a-d. show SEM micrographs of particle distribution with various wt.% of SiC nanoparticle reinforced composites at as-cast material conditions. EDS at 1.5 wt.% SiC reveals information about elements and shows nanocomposites with major chemical elements such as Al, Mg, Zn, Cu and Si, C as second phase elements (**Figure 5.3.3**) and also XRD analysis for chemical composition. The phase interaction peaks like Aluminium Magnesium Zinc ($AlMg_4Zn_{11}$), Magnesium Zinc ($MgZn_2$), SiC, Copper Silicade ($Cu_{3.17}Si$), Diamagnesium Silicide (Mg_2Si)have been observed in the composite. A high wt.% of reinforcement mixing

shows more probability of clusters/agglomerations, voids and it is confirmed from **Figure 5.3.2d** at 2 wt.% SiC reinforcement in AA7150. **Figures 5.3.2a-c** demonstrate uniform distribution of nano SiC particles in the Al alloy matrix using the novel fabrication process. The distribution increases with increase in wt.% of SiC. It is also noticed that porosity is decreasing with increasing wt.% of SiC upto 1.5% due to ultrasonic degassing effect and beyond 1.5 wt.%, it shows clusters and porosity due to high surface area to volume ratio. The graphical representation of porosity is shown in **Figure 5.3.2e.** From the result, it is observed that the % reduction in porosity is 83.5% compared to alloy matrix.

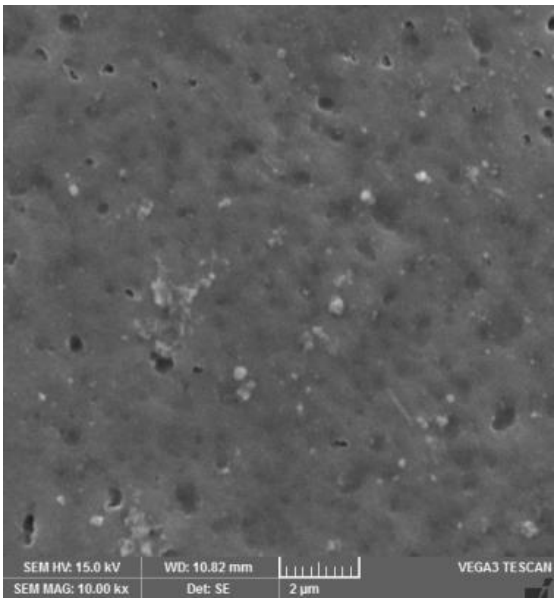

(*a*)

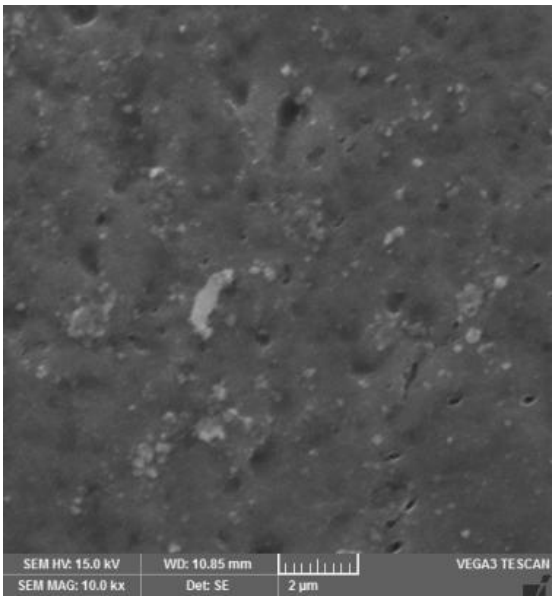

(*b*)

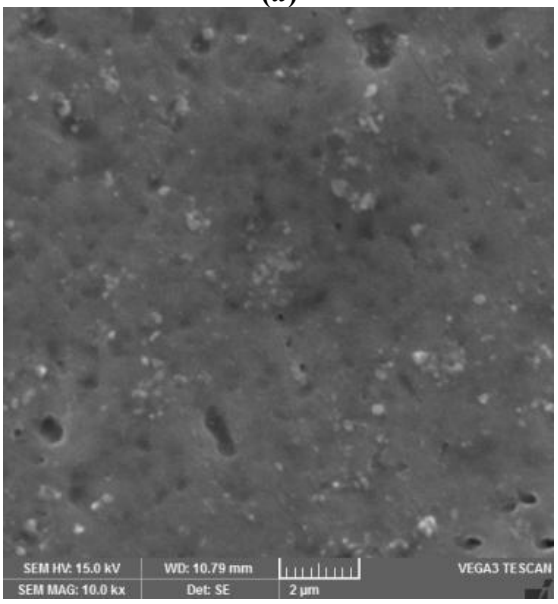

(*c*)

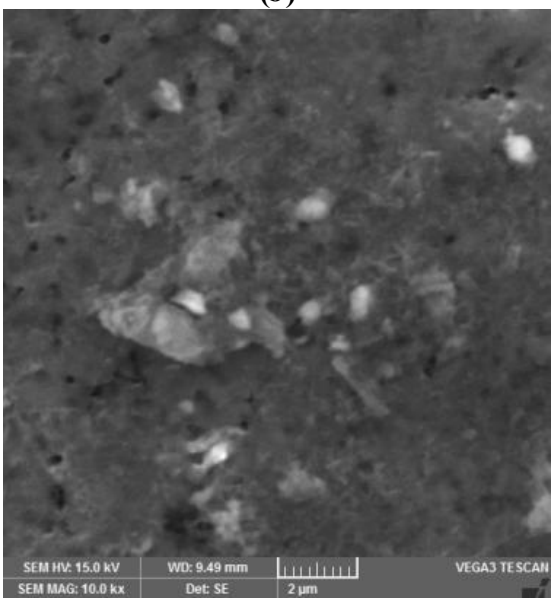

(*d*)

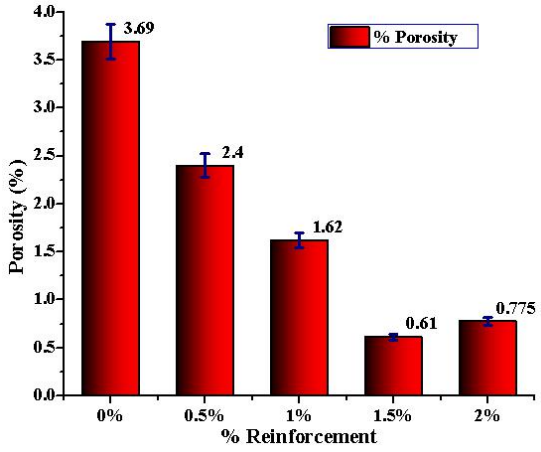

(e)

Figure 5.3. 2 SEM images for particle distribution of (a) 0.5 wt.% SiC, (b) 1.0 wt.% SiC, (c) 1.5 wt.% SiC, (d) 2.0 wt.% SiC, (e) Graphical representation of porosity.

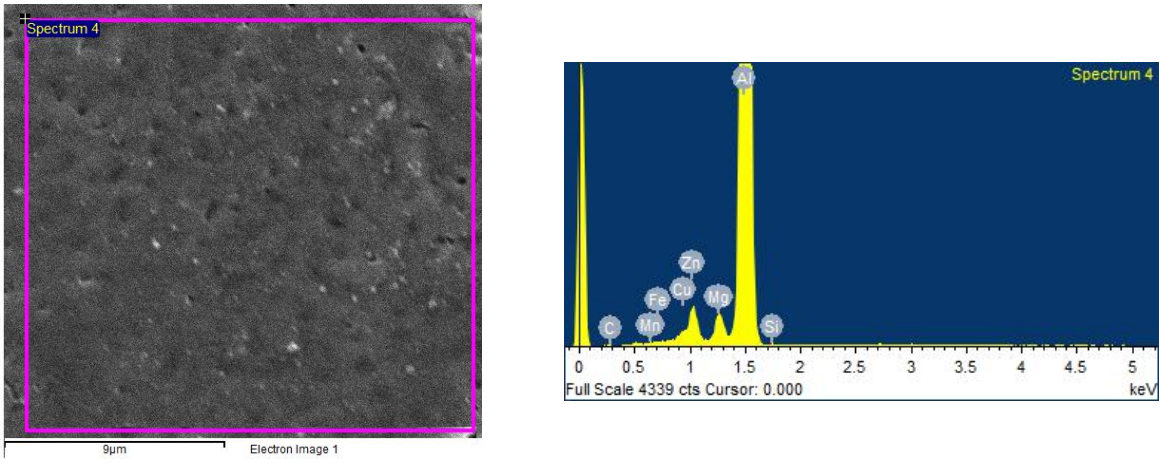

(a)

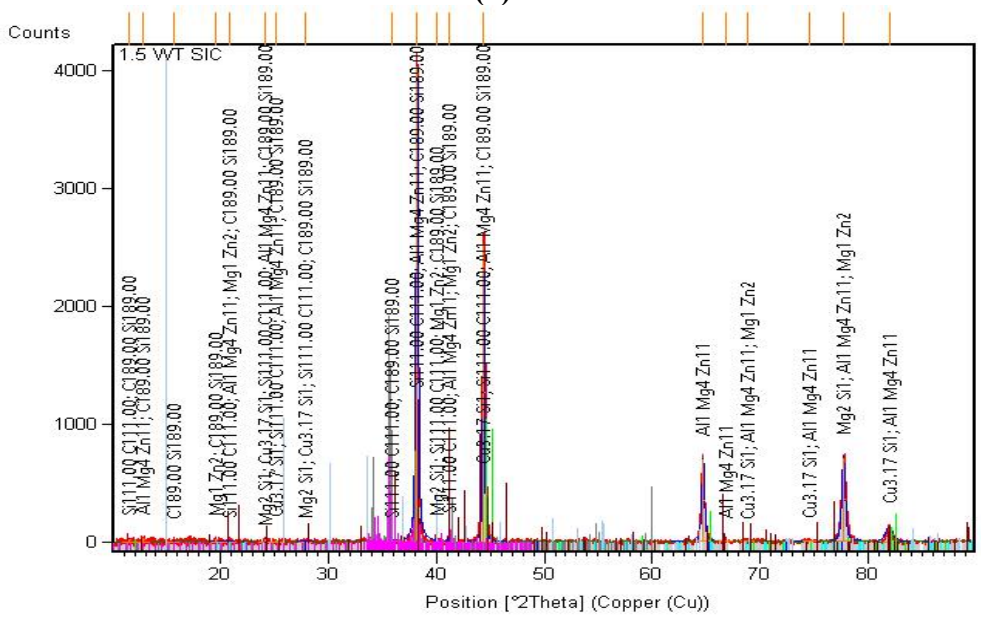

(b)

Figure 5.3. 3 (a) EDS spectrum (b) XRD analysis of AA7150-1.5 wt.%SiC.

5.3.2 Mechanical properties of AA7150-SiC nanocomposites

The densities of nanocomposites were measured by careful experiments to determine the porosity level of the composite material; *Archimedes Principle* was used to calculate density by considering the sample weight in air and its weight in distilled water; the nanocomposites were cut from nanocomposite blocks. Theoretical density of each nanocomposite material was calculated through rule of mixing method. The alloy matrix and SiC nanoparticles had densities of 2.83 g/cc and 3.216 g/cc respectively. It can be observed from the graph that the composite densities were enhanced compared to that of the base matrix. Further, experimental density increased as shown in **Figure 5.3.4,** with increase in wt.% of nano SiC in the nanocomposites. These increments in experimental density of AA7150-SiC nanocomposites are primarily due to higher densities of SiC particles compared to Al7150 alloy material.

Table 5.3. 1 AGS and mechanical properties of nanocomposites and base alloy matrix

Composition	Ex-Density (g/cc)	AGS		Porosity		UTM		Hardness	
		(µm)	Error	(%)	Error	(MPa)	Error	(HV)	Error
AA7150	2.725573	152	7.6	3.69	0.1845	114	5.7	151.8	7.59
AA7150-0.5%SiC	2.763739	101	5.05	2.4	0.12	131	6.55	168.2	8.41
AA7150-1.0%SiC	2.787498	73	3.65	1.62	0.081	143.7	7.185	172.76	8.638
AA7150-1.5%SiC	2.817805	64	3.2	0.61	0.0305	182.5	9.125	188.1	9.405
AA7150-2.0%SiC	2.825773	113	5.65	0.77	0.0387	169	8.45	177.72	8.886

To find the porosity, the densities values based on experiments were tested on base alloy matrix and its reinforced with SiC nanocomposites at as-cast state. The % of porosity after incorporation of SiC nanocomposites is represented in **Figure 5.3.4**. It is observed that the % of porosity decreases with increase of SiC nanoparticles by up to 1.5% weight fraction due to ultrasonic degassing effect and uniform dispersion of nanoparticles. Further increase in reinforcement leads to increase in porosity due to large surface area to volume ratio of nanoparticles. Once the limit is crossed in the molten pool, there is improvement in the formation of clusters and voids resulting in more porosity. It is confirmed by **Figure 5.3.2d.**

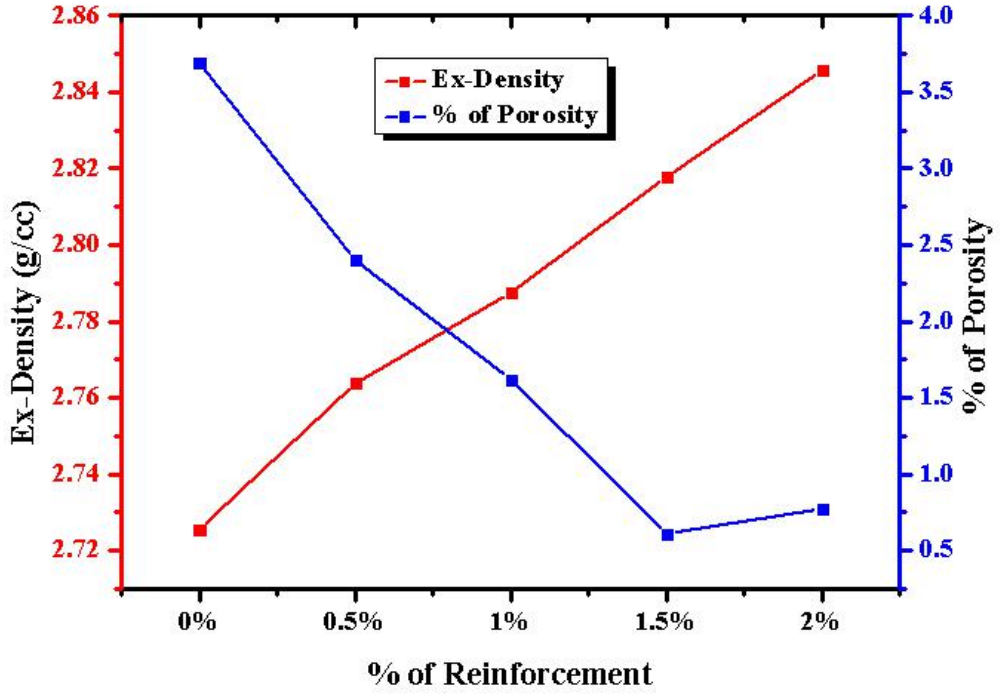

Figure 5.3. 4 Graphical representation of experimental density and porosity.

The microhardness of monolithic and SiC reinforced nanocomposites was carried out through Vickers hardness tester at as-cast state. Each experiment was repeated 8 times and the mean of all the readings was calculated. The microhardness results are represented in a bar chat in **Figure 5.3.5**. It is observed that the microhardness was enhanced and was greater than that of base alloy matrix. Microhardness was found to increase with increase in wt.% of SiC nanoparticles and it can be precisely attributed to ultrasonication, which leads to homogeneous mixing of SiC. The movement of dislocation is prevented by engulfed SiC nanoparticles as the indentor movement increases particle congregation near the indentor. Hence, there is increase in hardness of nanocomposites and it is also due to good adhesion between SiC ceramic nanoparticles and alloy matrix. Beyond 1.5% SiC, the microhardness of nanocomposite decreases due to higher grain size and clusters formation. It is confirmed in **Figures 5.3.1e & 5.3.2d.**

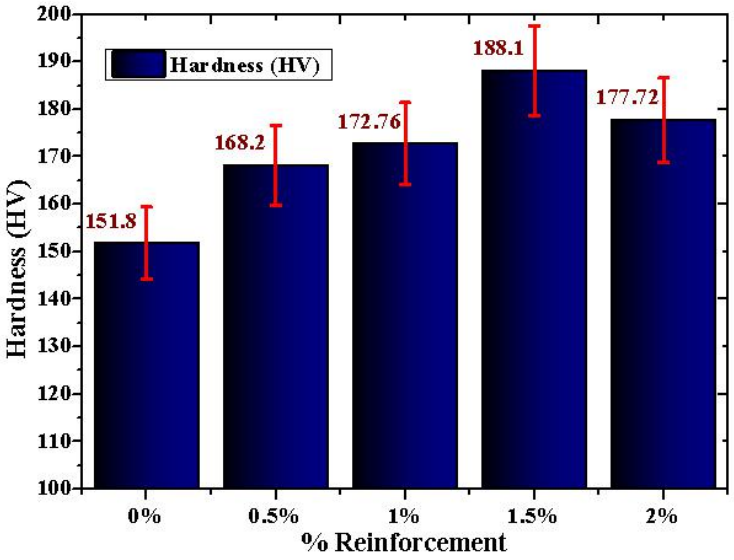

Figure 5.3.5 Graphical representation of microhardness.

Tensile test was carried out on Instron UTM for reinforced and unreinforced composites. The results are represented in **Table 5.3.1**. **Figure 5.3.6** shows the UTS variations against wt.% of reinforcement and it is noticed to increase with increase in SiC nanoparticles up to 1.5 wt.% due to high dislocation between alloy matrix and nanoparticles, which leads to more dislocation loops around the reinforcement particles and produces back pressure that restricts the movement of dislocations as well as grain refinement, resulting in enhanced strength of nanocomposite. Beyond 1.5 wt.%, there is decrease in the strength of nanocomposite due to clusters/agglomerations, resulting in advancing the failure of nanocomposites and a consequent reduction in mechanical properties. This reduction is attributed to cluster/agglomeration present in the composite and creates high stress concentration which leads to crack formation and further propagation, resulting in advancing the material properties.

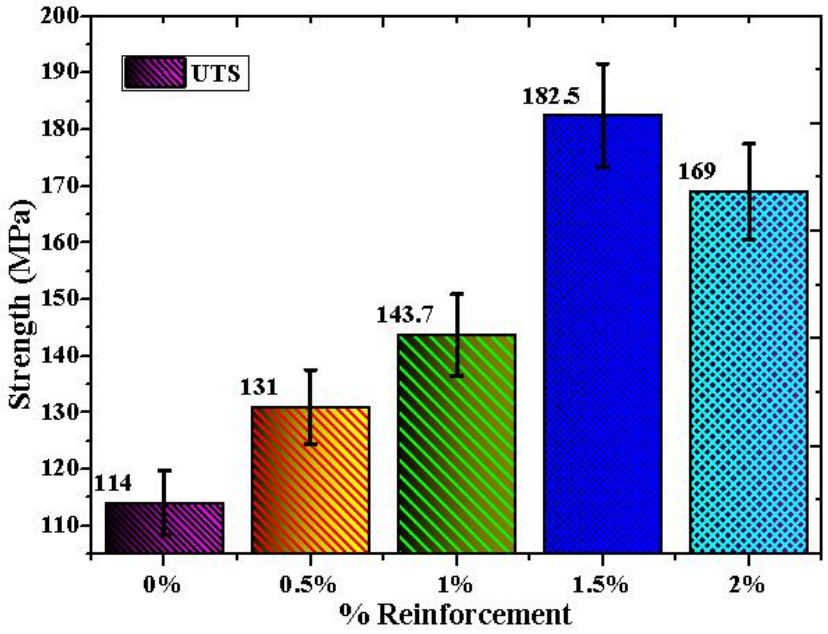

Figure 5.3. 6 Graphical representation of UTS.

5.3.3 Fracture studies of AA7150-SiC nanocomposites

SEM facto-graph images of alloy matrix, at optimal strength was observed in the AA7150-1.5 wt.%SiC and maximum reinforced MMNCs AA7150-2 wt.%SiC, were taken from tensile fracture surface, as shown in **Figure 5.3.7**. These images were captured at 200X magnification as well as the enlarged scale of 1000X magnification. **Figure 5.3.7a** shows the fracture surface of Al7150 alloy matrix sample which shows large grape shape quantities as well as dendritic globules. SiC reinforced nanocomposites (**Figures 5.3.7b-c**) show dendritic microstructure and these act as a weak zone as well as stress riser, leading to crack initiation. These cracks spread around the dendritic boundaries due to alloy matrix and ceramic particle interface, behave like stress concentration spots. Micro-cracks are produced at interfaces as well, which run through soft alloy matrix material and ceramic particles that show stepwise dendritic structure. The failure of SiC reinforced nanocomposites as suitable alloy is confirmed with inter-dendritic, stepwise dendrites and trans-granular cleavage facets on fracture surface facto-graphs as shown in **Figures 5.3.7b-c**. It is also observed that the voids and micro-cracks are minimized at AA7150-1.5 wt.% SiC compared to base alloy and AA7150-2 wt.%SiC nanocomposite.

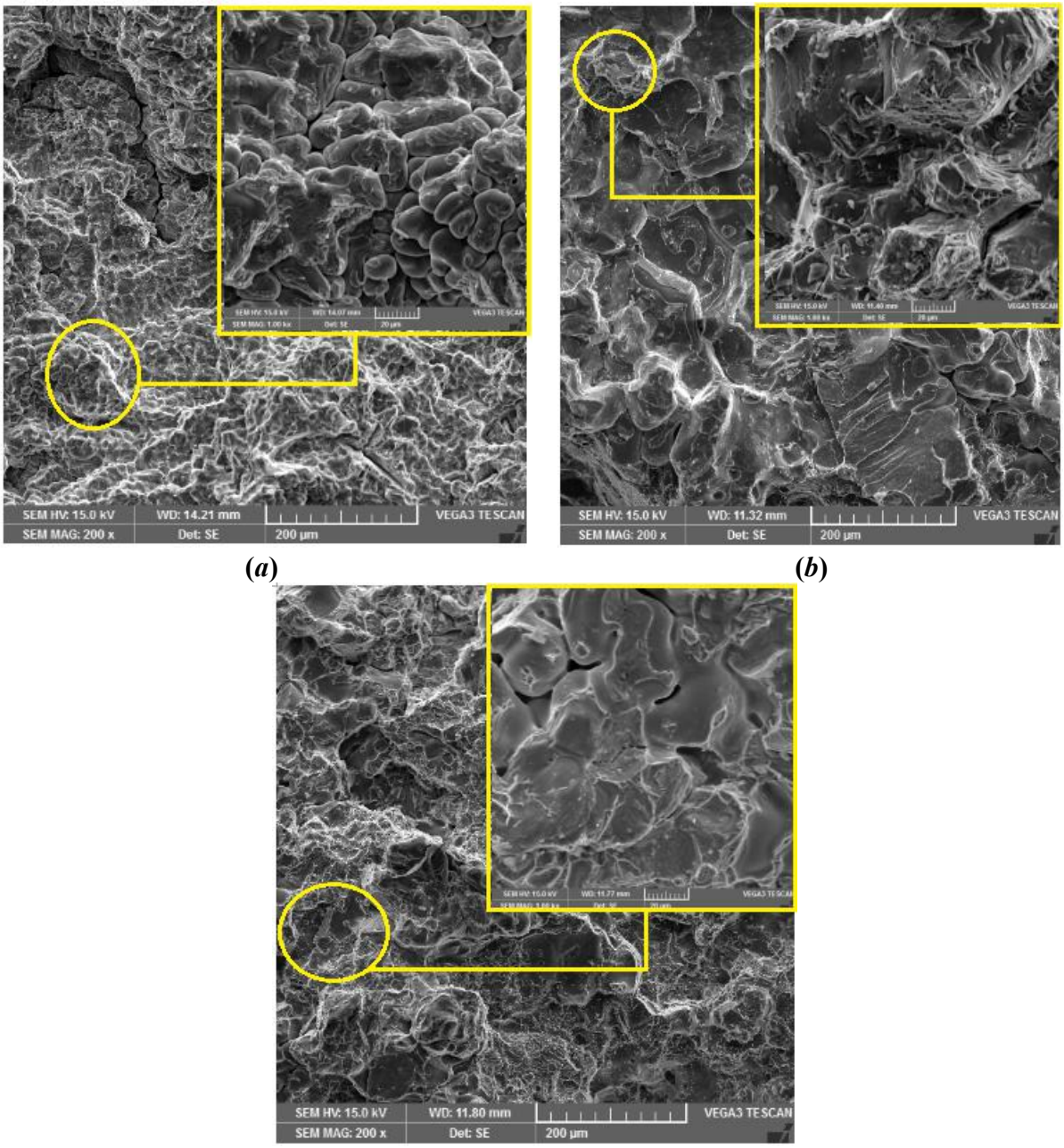

Figure 5.3. 7 SEM images for fracture surface of (a) AA7150, (b) AA7150-1.5wt.%SiC, (c) AA7150-2wt.%SiC.

From the results and analysis, it is confirmed that the mechanical properties of AA7150-1.5 wt.% SiC nanocomposite play a crucial role with respect to porosity, distribution and dispersion of nanoparticles throughout the material. Hence, a novel fabrication process was successfully developed based on a sequence of operations involving vortex, double stir casting, and UV methods to manufacture AA7150-1.5 wt.% SiC nanocomposite and by this

process minimum porosity and maximum homogeneous distribution of SiC nanoparticles was achieved.

5.3 Summary of AA7150-SiC nanocomposites

AA7150-SiC nanocomposites were fabricated successfully with enhanced nanoparticle distribution and improved performance of nanocomposite. The microstructure and mechanical properties were evaluated. The optical microstructure analysis revealed grain refinement and it increased with an increase in SiC nanoparticles and maximum refinement was observed at 1.5 wt.%SiC. SEM photographs confirm uniform distribution of SiC nanoparticles. The mechanical properties of AA7150-1.5 wt.%SiC exhibit significant improvement compared to counter parts and it reveals an enhancement of 23.9% (151.8-188.1 HV) in microhardness, 60.1% (117-182.5 MPa) in UTS and minimum porosity (83.47% reduction) at 1.5 wt.%SiC compared to matrix alloy.

5.4 AA7150-TiC nanocomposites

5.4.1 Microstructure studies of AA7150-TiC nanocomposites

The OM photographs for ceramic TiC nanoparticle reinforced AA7150 alloy composites and unreinforced alloy material are shown in **Figure 5.4.1a-e** followed by AGS graphical representation. It is calculated from LIM and the maximum reduction is 41 μm. SEM graphs for TiC nanoparticle reinforced nanocomposites were used to study particle distribution. EDS for elemental characterization of each nanocomposite and its nanoparticle size distribution graphs are shown in **Figure 5.4.2** and we also investigated the fracture surface for establishing the nature of failure analysis of nanocomposites.

Firstly, microstructural examinations were done on the prepared sample of monolithic and TiC nanoparticles reinforced nanocomposites and the grain boundary photographs are shown in **Figures 5.4.1a-e**. It is observed that fair grain boundary structures were appearing due to reinforcement of TiC nanoparticles. The majority of nanoparticles were repelled to grain boundary areas and beyond 1.5 wt.%, TiC nanoparticles reinforcement formed the cluster/agglomerations and those were trapped between the grain boundaries.

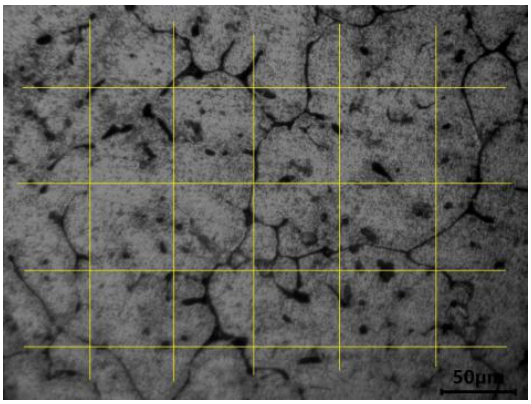

(a)

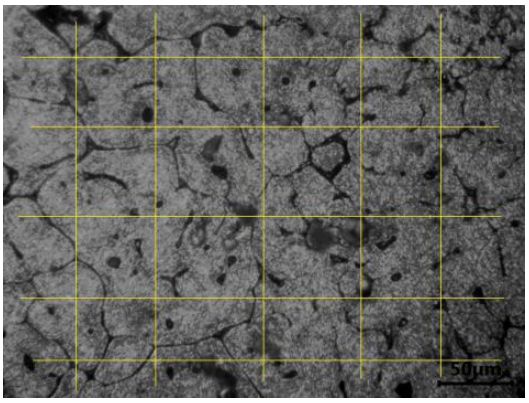

(b)

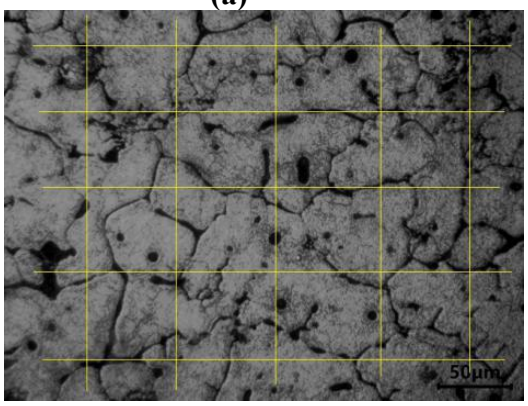

(c)

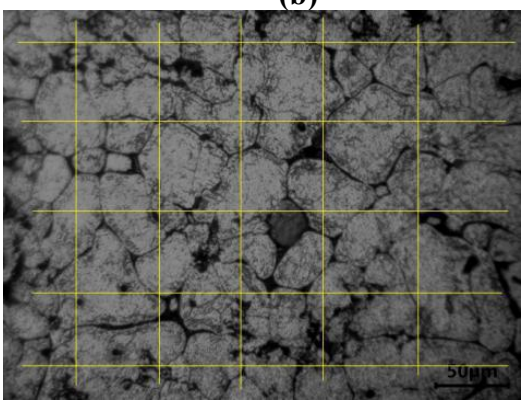

(d)

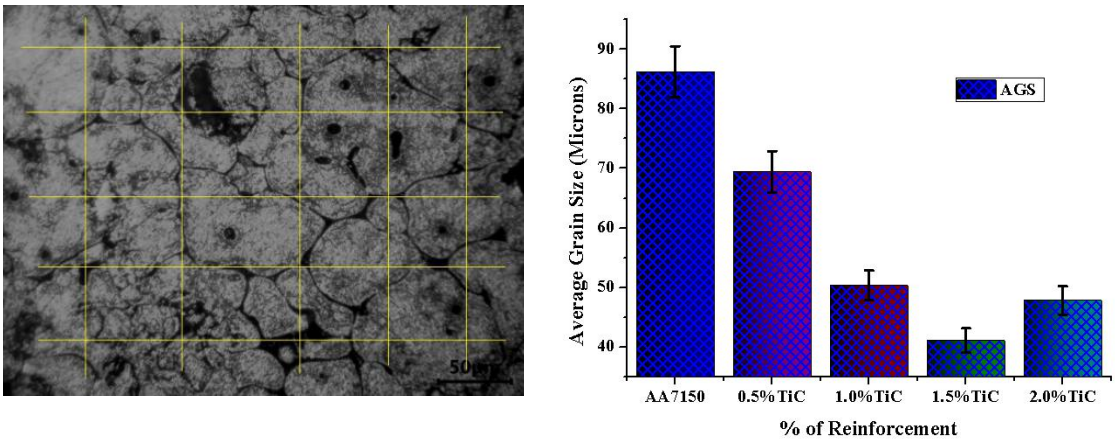

(e) **(f)**

Figure 5.4. 1 Optical microstructure of (a) AA7150 (b) AA7150-0.5 wt.% TiC (c) AA7150-1.0 wt.% TiC (d) AA7150-1.5 wt.% TiC (e) AA7150-2.0 wt.% TiC (f) AGS of each nanocomposite and alloy matrix.

It is noticed that grain size reduces with increase of wt.% of TiC nanoparticles reinforcement due to UV effect. During the UV treatment in molten liquid, the grain size of primary α-Al decreases and the number of grains (α-Al) in composite material increases due to cavitation and acoustic streaming of UV treatment which leads to homogeneous distribution of nanoparticles. The AGS of unreinforced and untreated composite is 86.23 μm and this reduces continuously by adding TiC nanoparticles reinforcement due to UV effect. The optimal refinement of grain size (41.1 μm) for reinforced and UV treated composite is observed at 1.5 wt.% TiC. The reduction of composite grain size has two major reasons. Firstly, TiC nanoparticles interrupt the grain growth of matrix due to accumulation of nanoparticles at grain boundaries. Secondly, grain refinement of nanocomposites is strengthened because of UV effect. This reduction of grain size leads to improvement in the strength of AA7150-TiC nanocomposites according to Hall-Petch theory. Compared to other existing strengthening mechanisms, grain refinement is a beautiful theory because it does not affect the toughness or ductility of the materials. It is proposed to explain that the fabrication process is capable of grain refinement with TiC nanoparticles reinforcement. The grain size of each composite was determined through LIM. Line length was estimated through "*ImageJ Software*". From **Figure 5.4.1f,** it is noticed that the maximum grain size reduction at 1.5 wt.% TiC is 52.37% (86.23 to 41.1 μm) compared to base alloy matrix.

SEM photographs of novel fabrication process (reinforced composites for nanoparticle distribution and respective histogram for nanoparticles size distribution) are shown in **Figure 5.4.2**. It reveals the presence of TiC nanoparticles in Al7150 alloy and uniform distribution of

nanoparticles in 0.5 wt.%, 1.0 wt.%, & 1.5 wt.% TiC except for 2 wt.% TiC. Therefore, improvement in mechanical properties is observed due to uniform distribution of particles as per Orowan strengthening theory but in 2 wt.% TiC, SEM micrographs reveal the formation of cluster/agglomeration. F**igure 5.4.2** confirms uniform distribution of TiC nanoparticles. The corresponding elemental analysis was studied through EDS of each particle distribution photograph. EDS spectroscopy reveals a major element of AA7150 and TiC nanoparticle reinforcement with elemental peak intensities. It is also observed that the porosity of nanocomposites decreases with increase of wt.% of TiC nanoparticles which plays a crucial influence in improving material properties of composites. Minimum porosity and maximum TiC nanoparticle distribution was noticed at AA7150-1.5 wt.% of TiC nanocomposite as shown in **Figure 5.4.2c**. The reduction of porosity and homogeneous dispersion of nanoparticles is mainly due to UV treatment which involves cavitation as well as acoustic streaming. This effect leads to optimal strength of the nanocomposites according to Orowan strengthening mechanism. The histogram representation for nanoparticle size distribution also supports uniform distribution of TiC nanoparticles which increases with increase of wt.% of ceramic nanoparticles by up to 1.5 wt.% TiC. The majority of nanoparticles are dispersed (0-150 nm range) throughout the composite material due to sonication effect and it is confirmed with histogram representation as shown in **Figure 5.4.2.** In **Figure 5.4.2c** histogram shows more nanoparticles dispersed in the range of 30-120 nm compared to counter parts. Further improvement of nanoparticles (2 wt.% TiC) shows fewer particles distribution <200 nm and more clusters/agglomerations in the range of 200-600 nm in histogram **of Figure 5.4.3d.** XRD analysis of optimal weight percentage (1.5 wt.%) is shown **Figure 5.4.3e** and Aluminium Titanium ($Al_{0.48}Ti_{1.52}$), TiC, Magnesium Zinc ($MgZn_2$ and $MgZn_5$), Aluminium Copper ($Al_9Cu_{11.5}$), Aluminium Copper Titanium ($AlCu_2Ti$), Ti_3AlC_2 phases are identified.

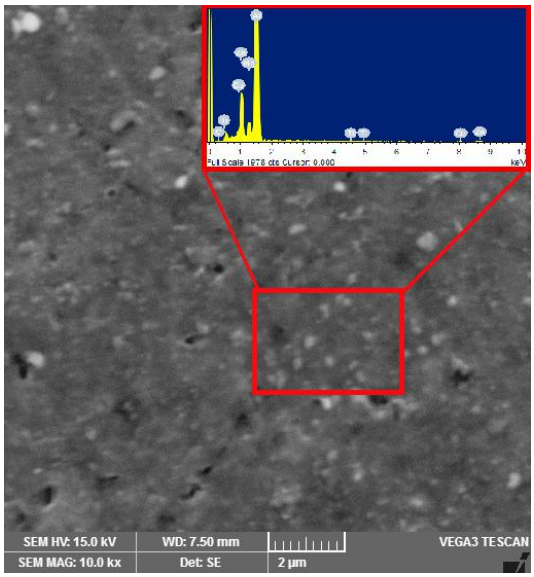
SEM HV: 15.0 kV
WD: 7.50 mm
VEGA3 TESCAN
SEM MAG: 10.0 kx
Det: SE
2 µm

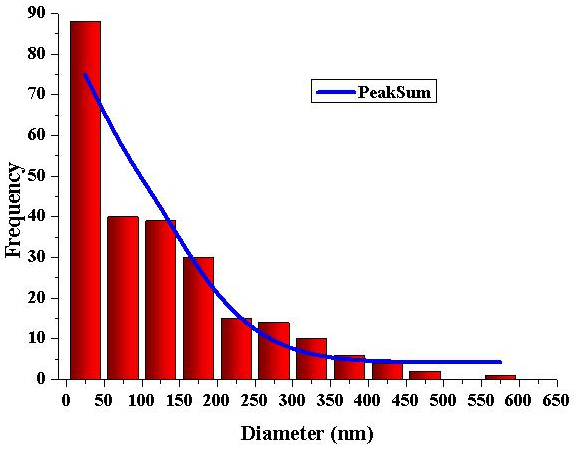
PeakSum
Frequency
Diameter (nm)
0 10 20 30 40 50 60 70 80 90
0 50 100 150 200 250 300 350 400 450 500 550 600 650

(a)

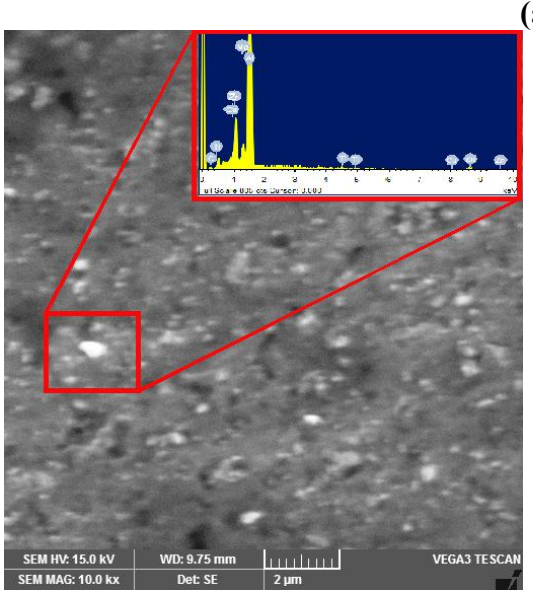
SEM HV: 15.0 kV
WD: 9.75 mm
VEGA3 TESCAN
SEM MAG: 10.0 kx
Det: SE
2 µm

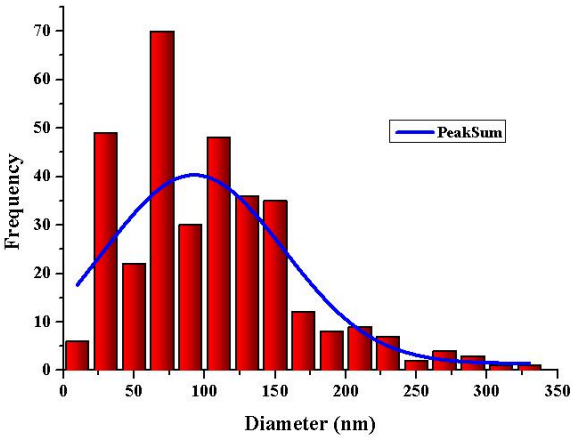
PeakSum
Frequency
Diameter (nm)
0 10 20 30 40 50 60 70
0 50 100 150 200 250 300 350

(b)

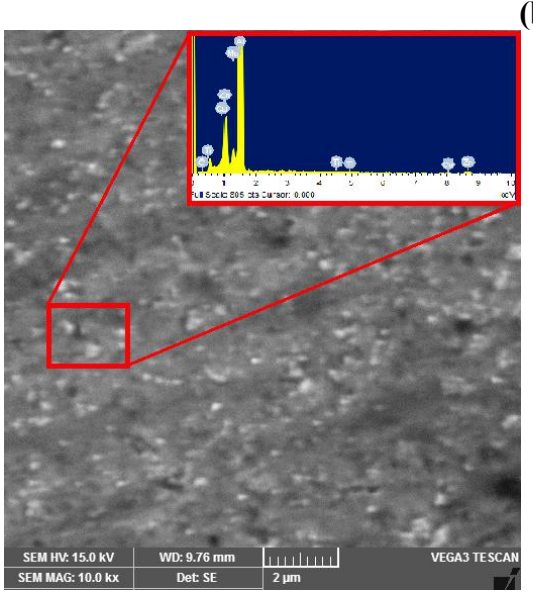
SEM HV: 15.0 kV
WD: 9.76 mm
VEGA3 TESCAN
SEM MAG: 10.0 kx
Det: SE
2 µm

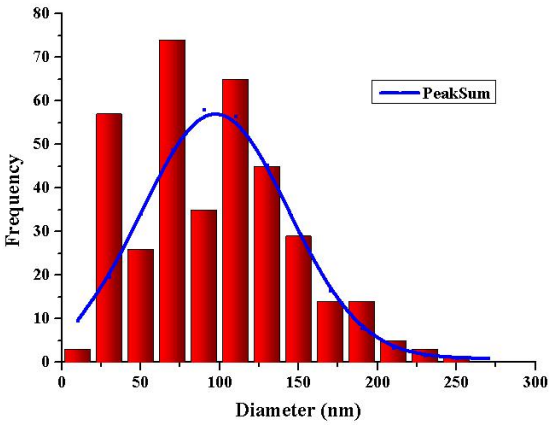
PeakSum
Frequency
Diameter (nm)
0 10 20 30 40 50 60 70 80
0 50 100 150 200 250 300

(c)

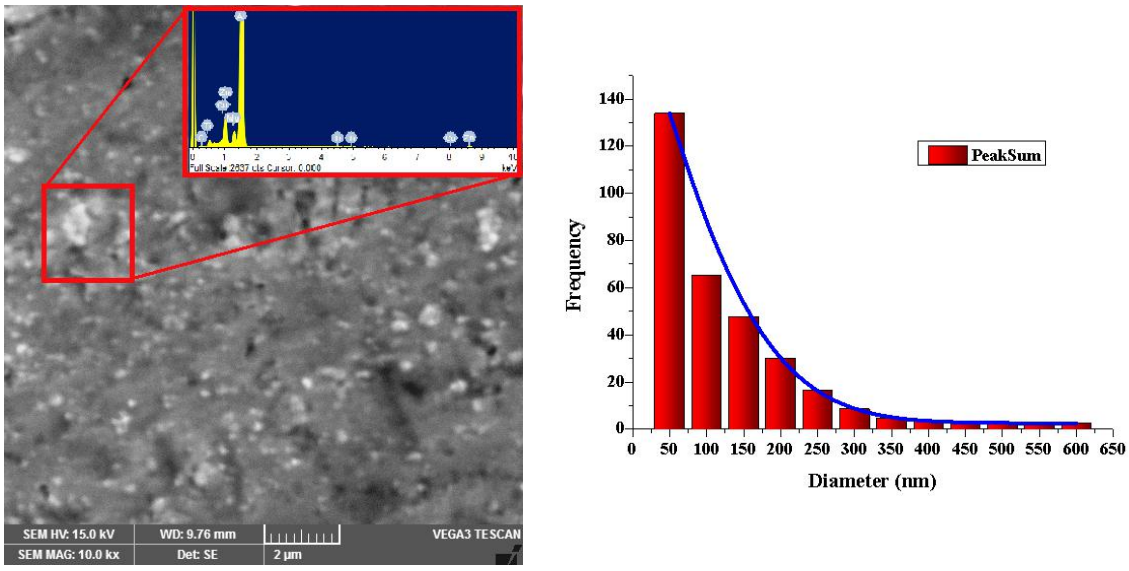

(d)

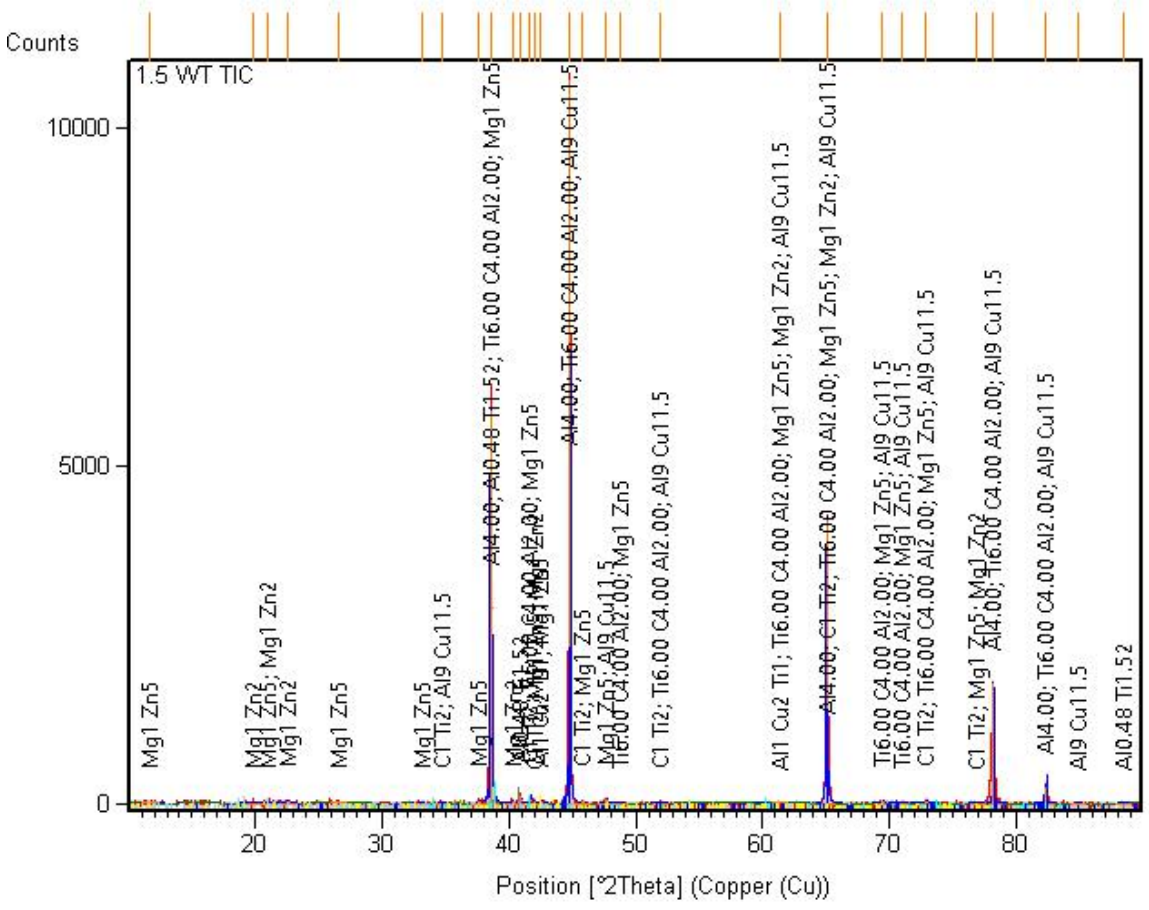

(e)

Figure 5.4. 2 SEM photographs and comparable histogram of nanoparticles distribution of (a) AA7150-0.5 wt.% TiC (b) AA7150-1.0 wt.% TiC (c) AA7150-1.5 wt.% TiC (d) AA7150-2.0 wt.% TiC and (e) XRD analysis at 1.5 wt.% TiC.

5.4.2 Mechanical properties of AA7150-TiC nanocomposites

To investigate the strengthening effect of TiC ceramic nanoparticles, the mechanical properties of AA7150-TiC nanocomposites at room temperature were examined. Al7150 alloy and TiC nanoparticles have densities of 2.83 g/cc and 4.93 g/cc respectively. In order to find the porosity level in fabricated samples, the experimental density and theoretical density of samples were calculated and are represented in **Figure 5.4.3a**. The experimental density of various nanocomposite samples and monolith material was calculated through *Archimedes's* principle. Digital electron weighing balance was used to find the samples weight in air and distilled water. The theoretical densities of the various samples were evaluated through rule of mixing formula. With the help of experimental and theoretical densities, the porosity of monolithic and nanocomposites which is reinforced with TiC nanoparticles of 0.5 to 2.0 wt.%, in the steps of 0.5 wt.% at as-cast state was calculated. The measured values of porosity are represented in **Table 5.4.1**.

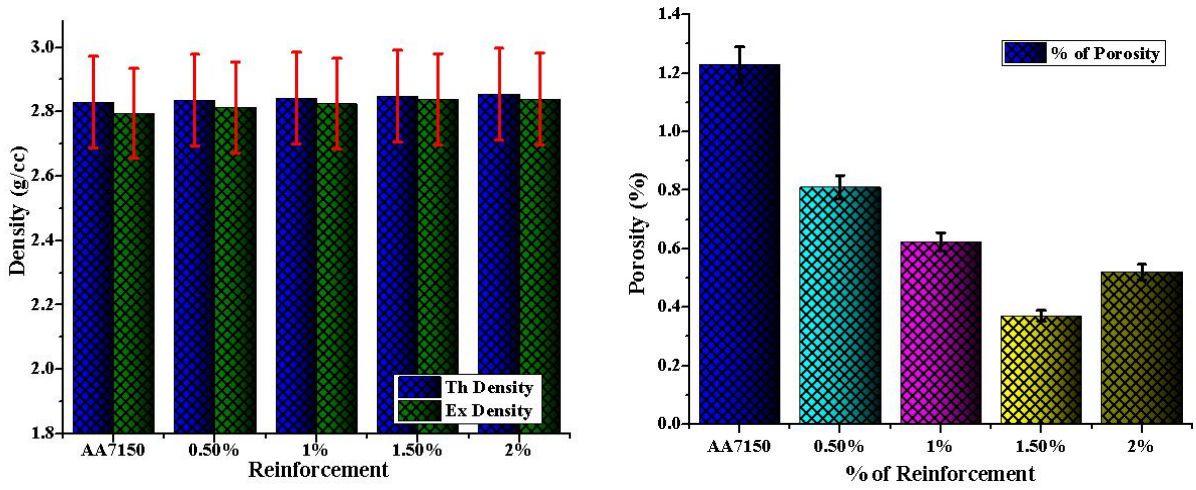

Figure 5.4. 3 Influence of TiC % reinforcement on (a) Experimental and Theoretical densities (b) % of porosity.

The porosity variation with wt.% of TiC reinforced nanocomposites is shown in **Figure 5.4.3b.** It is noticed that the porosity of nanocomposite decreases with increase of wt.% of nanoparticle reinforcement. It is due to the effect of ultrasonic waves which enhance the wetting of molten Al7150 alloy. TiC nanoparticles behave as nucleates to refine the grains of the matrix material. It is also observed that the % of porosity reduction at 1.5 wt.% TiC is 69.87% and this can be attributed to ultrasonic degassing effect of liquid metal, enhancement of fluidity by uniform distribution of nanoparticles and UV effect on liquid homogenization.

Table 5.4. 1 AGS, Mechanical properties of base alloy and nanocomposites

Composition	Ex-Density		Porosity		AGS		UTM	Hardness	
	g/cc	Error	%	Error	µm	Error	MPa	HV	Error
AA7150	2.79524	0.13976	1.23	0.06141	86.23	4.3114	118	150.81	7.5405
AA7150-0.5%TiC	2.81304	0.14065	0.81	0.04048	69.44	3.47189	137	158.56	7.928
AA7150-1.0%TiC	2.82437	0.14122	0.62	0.0312	50.35	2.51768	154	163.86	8.193
AA7150-1.5%TiC	2.83766	0.14188	0.37	0.0185	41.07	2.05355	***175***	***177.05***	8.8525
AA7150-2.0%TiC	2.83946	0.14197	0.52	0.026	47.83	2.39133	158	160.5	8.025

Hardness test was carried out on Vickers microhardness tester at a load of 200 g and 15 sec of dwell period. Specimens were subjected to indentation at various locations and 10 readings were taken. The microhardness values of AA7150 and AA7150-TiC nanocomposites are graphically represented in **Figure 5.4.4**. The test results of Vickers hardness value with TiC reinforced nanocomposites were higher than unreinforced matrix alloy. It is noticed that the inclusion of ceramic TiC nanoparticles to Al7150 alloy matrix significantly increased the microhardness of nanocomposite material. It is confirmed in **Figure 5.4.4**, that the microhardness value of the nanocomposite material was enhanced with enhancement in ceramic nanoparticle wt.%. It also reveals that hardness increases by up to 1.5 wt.% but it decreases on further increase of TiC nanoparticles. The optimal magnitude value of microhardness for AA7150-TiC nanocomposites which has 1.5 wt.% of TiC ceramic nanoparticles is 177.05 HV because of the existence of hard phase TiC nanoparticles, Hall-Petch and Orowan strengthening mechanism, as well as uniform particle distribution. The reason for increase in microhardness of AA7150-TiC nanocomposites can be attributed to the fact that the presence of TiC nanoparticles which are harder than Al7150 alloy and they prevent the movement of dislocation which ultimately increases microhardness as well as strength of composite. Another thing which also contributes to the increase in microhardness of the nanocomposite is the large surface to volume ratio of ceramic nanoparticles. This large surface area increased the particle to matrix interface area, which leads to an increase in the microhardness of the nanocomposites.

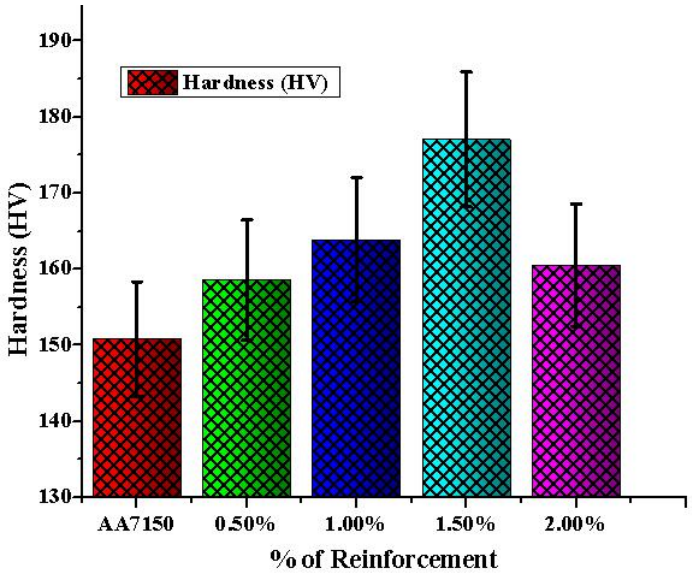

Figure 5.4. 4 Effect of reinforcement on AA7150 alloy hardness.

The reason for decrease in hardness value at 2 wt.% TiC can be rightly attributed to the formation of agglomeration of nano reinforcement and increased porosity content due to low nanoparticle percolation threshold effect. It can be confirmed from **Figures 5.4.1e** and **Figure 5.4.2d.**

UTS was tested on AA7150-TiC nanocomposite and the tests were done according to ASTM E8M standard. UTM (INSTRON – 10 KN Load cell) was used in tensile experiments. The specimens were clamped between the fixed cross-head and the moving cross-head of the universal machine. The strength of different specimens was evaluated at 0.5 mm/min cross head speed. The influence of TiC nanoparticles reinforcement on the tensile strength of AA7150-TiC nanocomposites was analyzed through tensile results and the graphical representation is shown in **Figure 5.4.5** and it was compared with monolithic material. The stress-strain graph showed the fracture surface of each AA7150-TiC based composite respectively. It is realized that the ultimate strength values of TiC nanoparticles reinforced composites are higher than unreinforced metal matrix alloy. It is noticed that that the material strength enhanced with enhancement in ceramic reinforcement. However, a marked improvement in strength was noticed when 1.5 wt.% TiC nanoparticle reinforcements were added. This is due to fact that porosity was estimated by ultrasonic degassing effects and Hall-Petch grain refinement and strengthening mechanism. The grains were refined and equated to Al7150 alloy matrix grains which promote the enhancement of UTS of Al7150-TiC nanocomposites. Moreover, it is a known fact that Orowan strengthening mechanism is

substantial while the size of the particle reinforcements is <1 μm and when there is homogeneous dispersion throughout the alloy matrix.

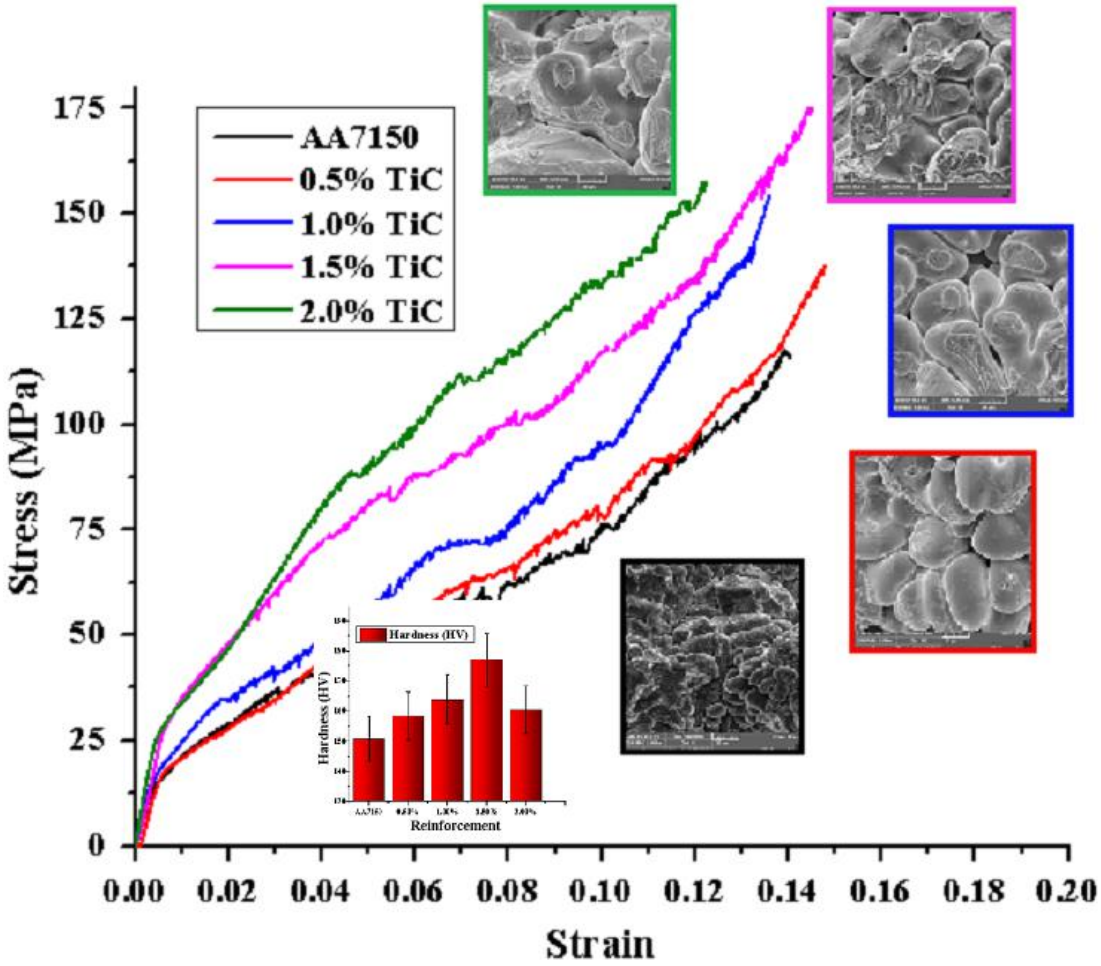

Figure 5.4. 5 Stress-Strain curves, Vickers hardness (inset) and fracture surface (inset) of unreinforced and reinforced nanocomposites at room temperature.

The average particle size of TiC was 30-50 nm and these nanoparticles contribute to dislocation moment which leads to enhancement in the ultimate strength of nanocomposites. The influence of load sharing effect is minimum and improvement of UTS is primarily due to grain refinement according to Hall-Petch theory. 1.5 wt.% TiC showed superior tensile strength value compared to monolithic and other counter parts of the composites. The reason for improvement in tensile strength (175 MPa) can be suitably attributed to uniform distribution of TiC nanoparticles, which act as a barrier to dislocation movement. Under externally applied load, alloy matrix distributes the applied load to ceramic particle reinforcement when there is solid interfacial bonding strength between two material phases. This strengthening is attained by distribution of reinforcement particle strengthening,

dislocation and grain refinement strengthening. The homogeneous dispersion of TiC nanoparticles provides marked improvement of distribution strengthening in AA7150-TiC nanocomposites through accommodating most of the applied forces which leads to improvement in load bearing capacity of matrix alloy to ceramic particles. There is decrease in tensile strength value for 2 wt.% TiC (158 MPa). The reason can be attributed to the formation of porosity and increased agglomeration of particles due to the limit on the threshold value of larger surface to volume ratio in the molten liquid.

5.4.3 Fracture studies of AA7150-TiC nanocomposites

Fracture surface of Al7150 alloy was observed at 100X magnification. **Figure 5.4.6a** shows the elliptical shaped molecules of matrix alloy that are clearly visible at 1000X magnification and it is also observed that the fracture is ductile in nature due to shearing effects and it in turn is brittle in nature while adding TiC nanoparticles to the content. Increasing TiC wt.% reduces the voids and elastic deformation due to UV effect in the metal pool. This deformation can be observed along fracture surface of TiC reinforced composites (**Figures 5.4.6b-e**).

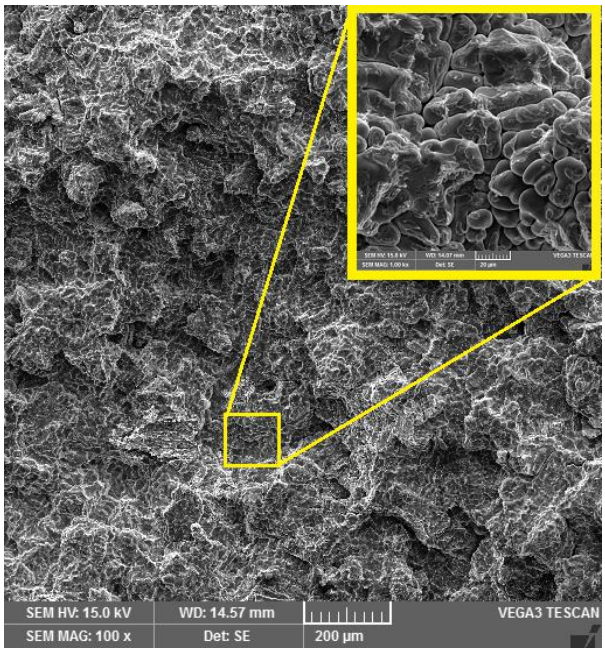

(a)

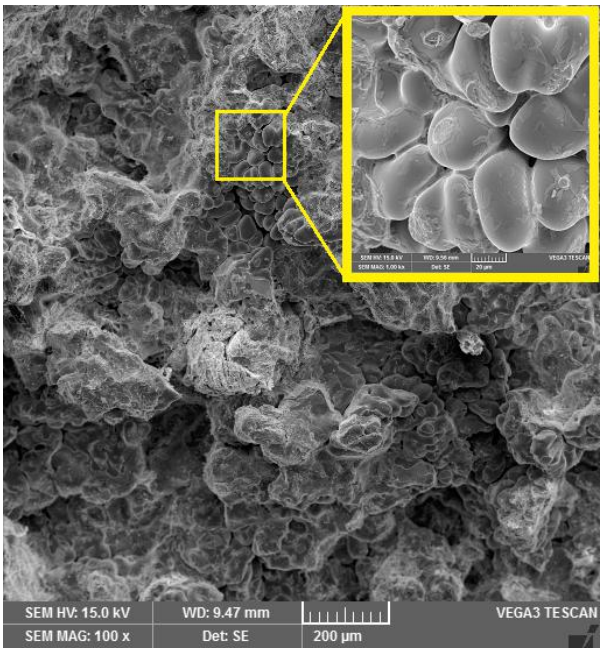

(b)

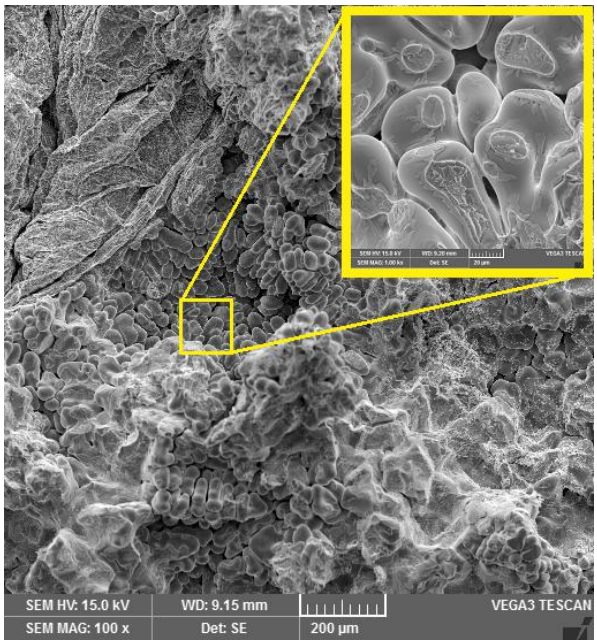

(c)

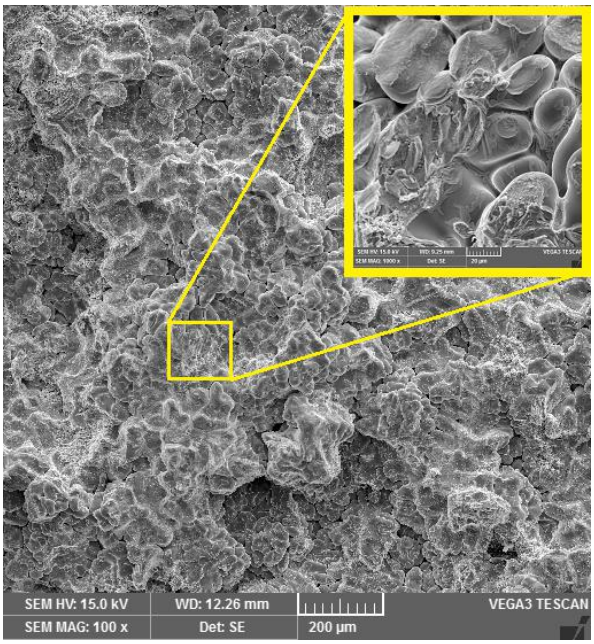

(d)

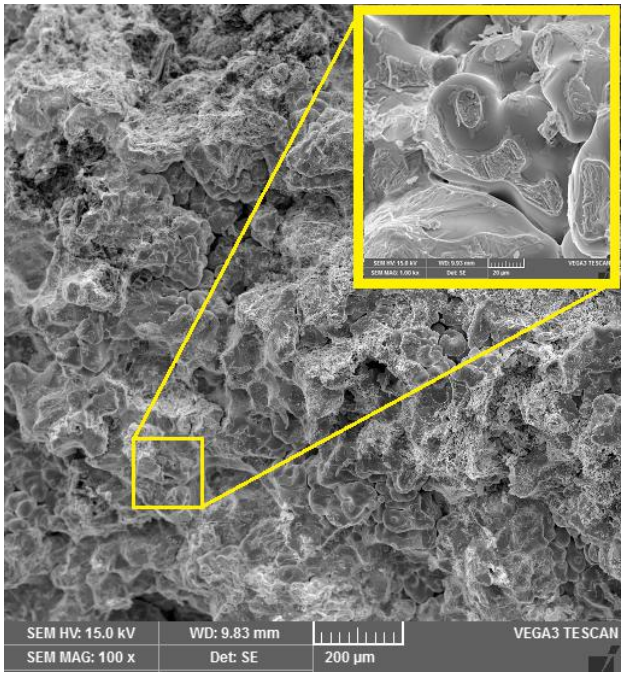

(e)

Figure 5.4. 6 SEM photographs for fracture surface of (a) AA7150 (b) AA7150-0.5 wt.% TiC (c) AA7150-1.0 wt.% TiC (d) AA7150-1.5 wt.% TiC (e) AA7150-2.0 wt.% TiC.

At higher TiC nanoparticle reinforcement, micro cracks are observed due to the cluster/agglomeration supported by **Figure 5.4.2d,** which initiate and propagate the crack for the continuous loading and the surface shows brittle fracture mode of **Figure 5.4.6e.** It is also due to the strong interface between the matrix alloy and TiC nanoparticles. Therefore, the

failure of AA7150-TiC nanocomposite is in mixed mode with partially ductile and partially brittle in nature.

5.4 Summary of AA7150-TiC nanocomposites

Novel AA7150-TiC nanocomposites were fabricated successfully which enhanced the homogeneous distribution of TiC nanoparticles in AA7150 based composites. The material properties improved with increased TiC nanoparticle reinforcement of upto 1.5 wt.% due to sonication effect and then decreased due to clusters/agglomerations. Based on optical and SEM analysis, it was concluded that the grain size refinement, good bonding between matrix and reinforcement particulates, and homogeneous distribution of TiC nanoparticles in AA7150-TiC nanocomposite was due to UV effect. The maximum grain refinement of the nanocomposite was 41.07 μm and minimum porosity was 0.37% which decreased by 52.37% (86.23-41.04 μm) and 69.87% (1.23-0.37%) compared to AA7150 material. The microhardness and tensile strength of AA7150-TiC nanocomposites at as-cast case were enhanced due to novel fabrication process followed by UV treatment. The microhardness and tensile strength of AA7150-TiC nanocomposites properties of are 177.05 HV and 175 MPa, which are enhanced by 17.40% (150.81-177.05 HV) and 48.31% (118-175 MPa) compared to AA7150 alloy matrix respectively.

CHAPTER -6

MICROSTRUCTURE AND MECHANICAL EVALUATION OF HYBRID NANOCOMPOSITE

This chapter deals with microstructure and mechanical properties of hybrid nanocomposites fabricated through novel fabrication process. Microstructure of nanocomposites were analyzed by OM and SEM. The mechanical characterization was done using microhardness tester and UTM. The results are discussed through graphical, tabular and microstructure in detailed.

6.1 Results and discussions of hybrid nanocomposites

6.1.1 Microstructure analysis of hybrid nanocomposites

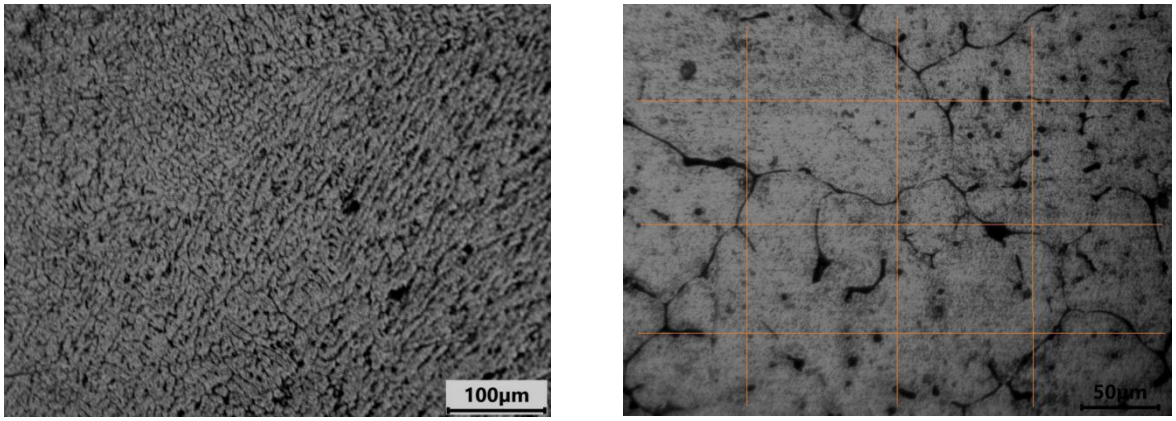

(a)

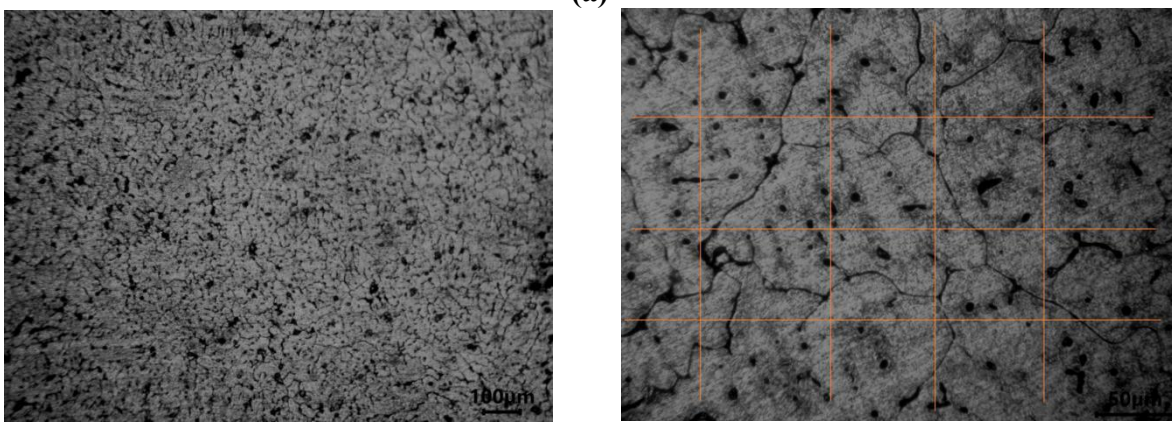

(b)

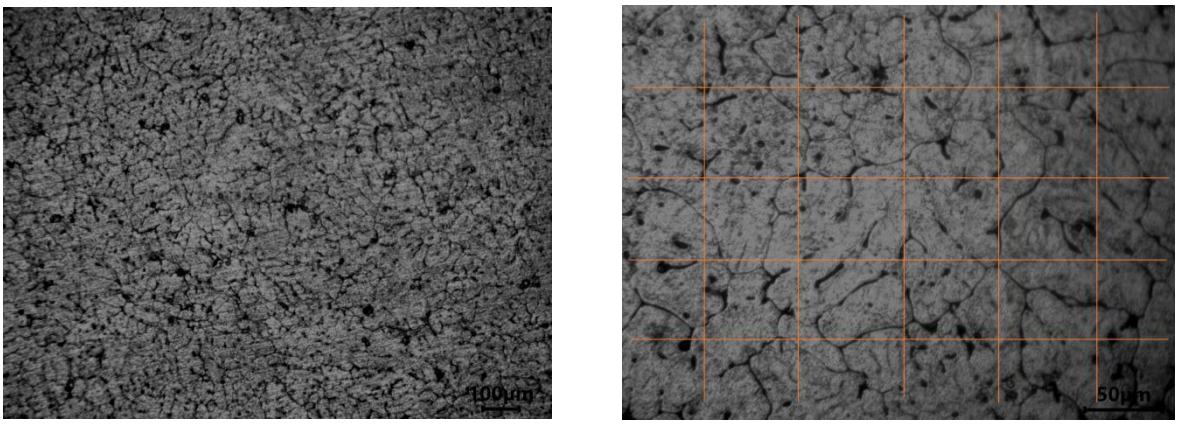

(c)

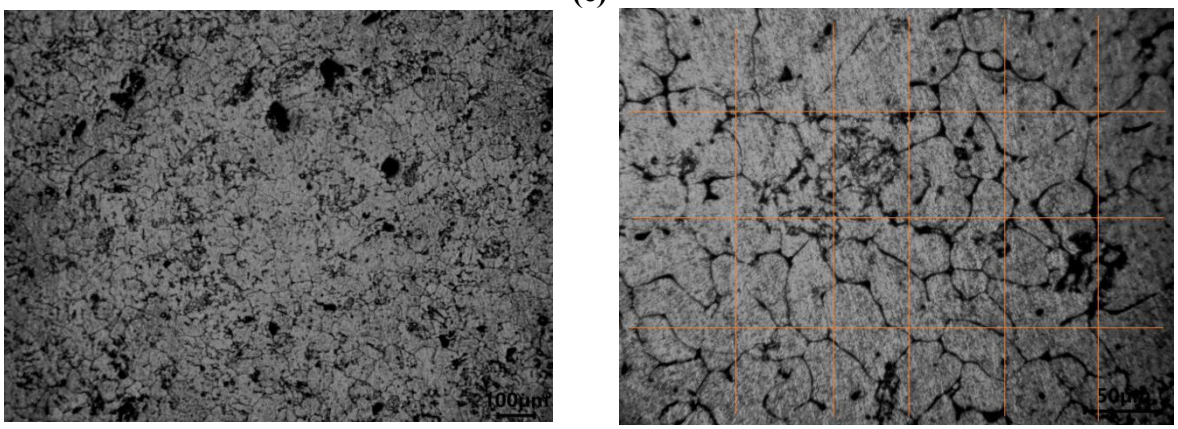

(d)

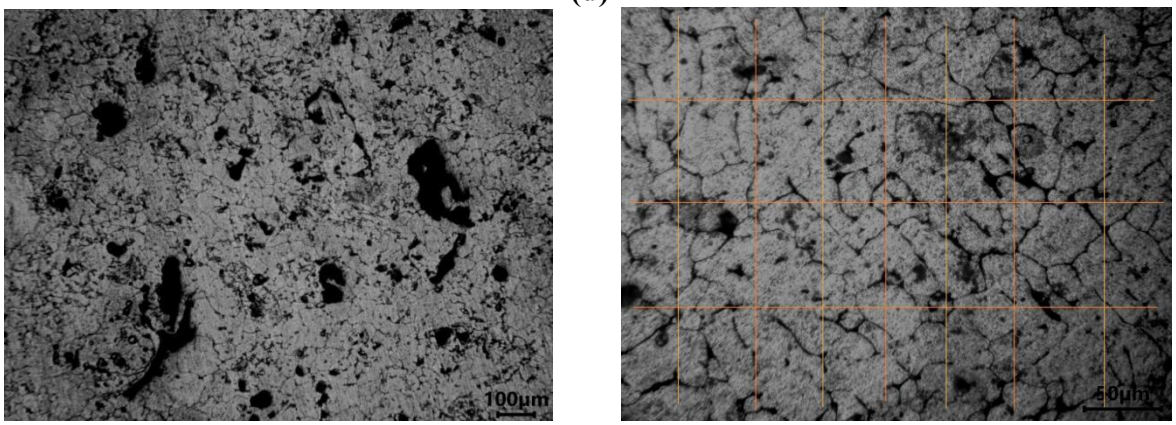

(e)

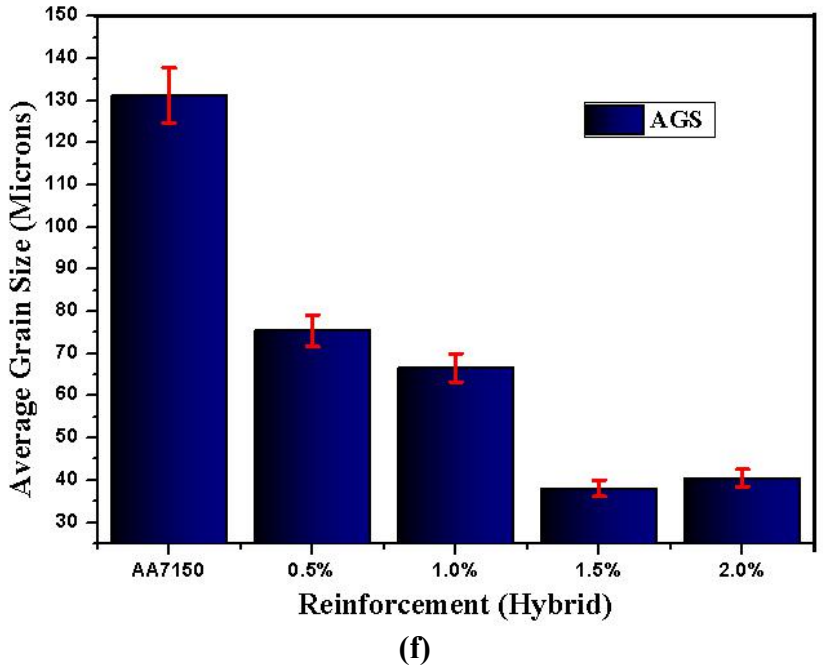

Figure 6. 1 OM images with 100X and 400X of (a) AA7150 (b) 0.5 wt.% (B_4C-hBN) (c) 1.0 wt.% (B_4C-hBN) (d)1.5 wt.% (B_4C-hBN) (e) 2.0 wt.% (B_4C-hBN) (f) AGS.

The strength of the material depends on the grain size and it increases as the grain size reduces as per Hall-Petch phenomena. Toughness and ductility of material are significantly affected by grain size. Throughout the AA7150-B_4C-hBN nanocomposite liquid solidification process, the hybrid nanoparticles act as a center of non-homogeneous nucleation as well as reinforcement of matrix alloy grains. Grain refinement is an attractive mechanism compared to other strengthening mechanisms due to the retention of ductility as well as toughness of the materials.

From the above **Figures 6.1a-e** show lower magnification (100X) to higher magnification (400X) for better understanding of grain refinement and it is clear that the formation of grain boundaries decreases by up to 1.5 wt.% and then increases to 2.0 wt % due to high content of cluster particles along with the nanoparticles. The AGS of each nanocomposite were calculated through LIM. The measured values for the AGS are represented in **Table 6.1** and corresponding bar chart is shown in **Figure 6.1f**. Therefore, it is noticed that the % of reduction of AGS at AA7150-1.5% (B_4C-hBN) is 70.99% compared to base metal. Hence, AA7150-B_4C-hBN hybrid nanocomposite at 1.5 wt.% has higher strength (192 MPa) compared to base metal.

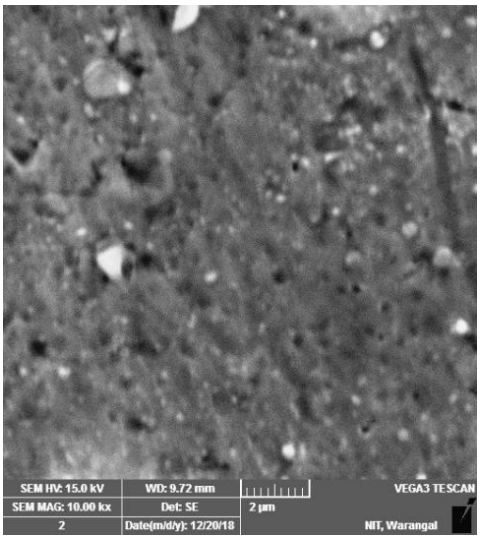
SEM HV: 15.0 kV
WD: 9.72 mm
VEGA3 TESCAN
SEM MAG: 10.00 kx
Det: SE
2 µm
2
Date(m/d/y): 12/20/18
NIT, Warangal

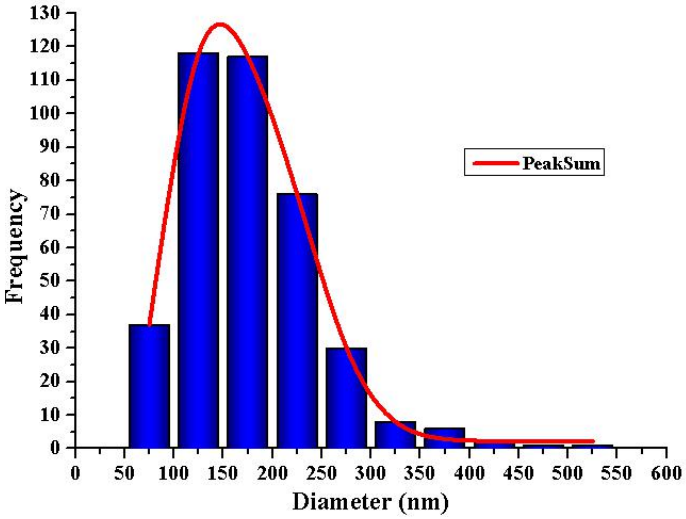
Frequency
Diameter (nm)
PeakSum

(a)

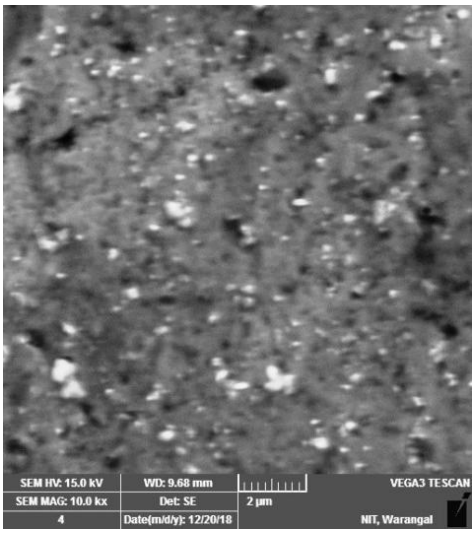
SEM HV: 15.0 kV
WD: 9.68 mm
VEGA3 TESCAN
SEM MAG: 10.0 kx
Det: SE
2 µm
4
Date(m/d/y): 12/20/18
NIT, Warangal

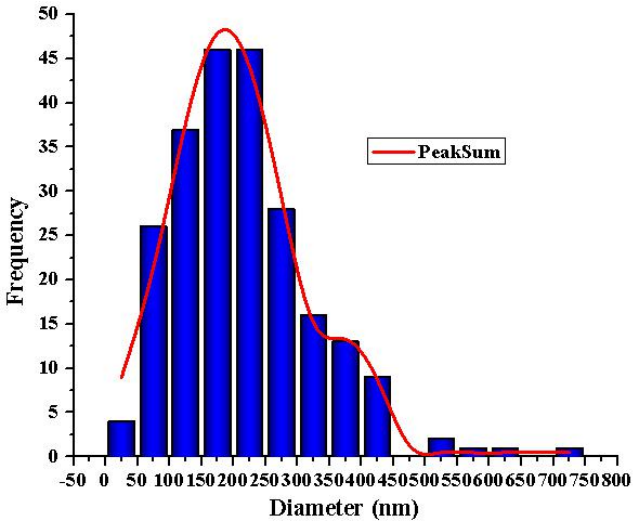
Frequency
Diameter (nm)
PeakSum

(b)

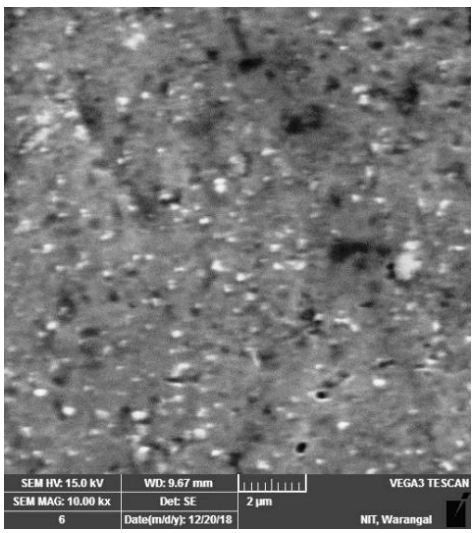
SEM HV: 15.0 kV
WD: 9.67 mm
VEGA3 TESCAN
SEM MAG: 10.00 kx
Det: SE
2 µm
6
Date(m/d/y): 12/20/18
NIT, Warangal

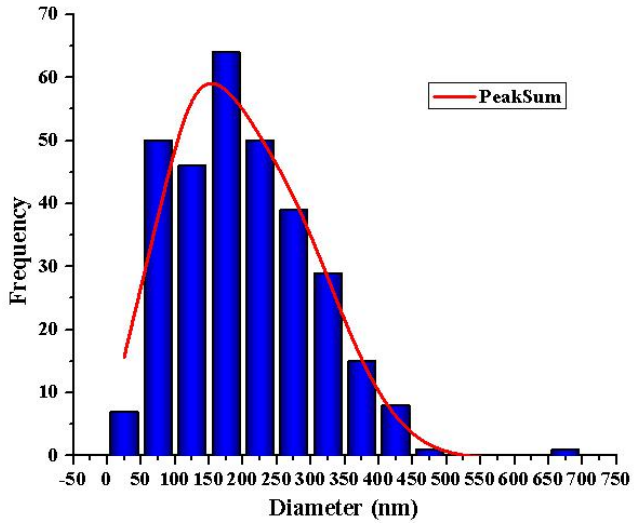
Frequency
Diameter (nm)
PeakSum

(c)

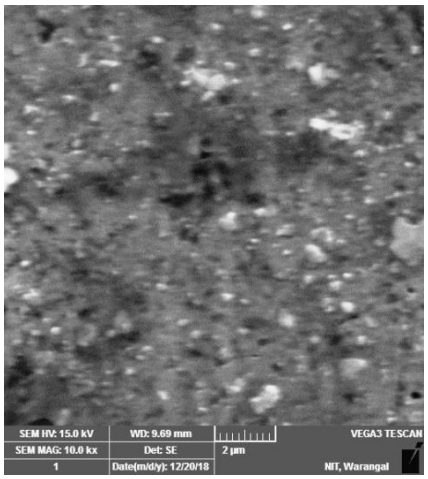

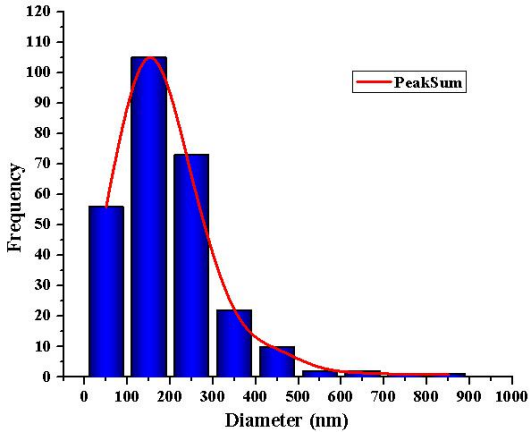

(d)

Figure 6. 2 SEM for hybrid nanoparticles distribution (a) 0.5 wt.% (B_4C-hBN) (b) 1.0 wt.% (B_4C-hBN) (c) 1.5 wt.% (B_4C-hBN) (d) 2.0 wt.% (B_4C-hBN).

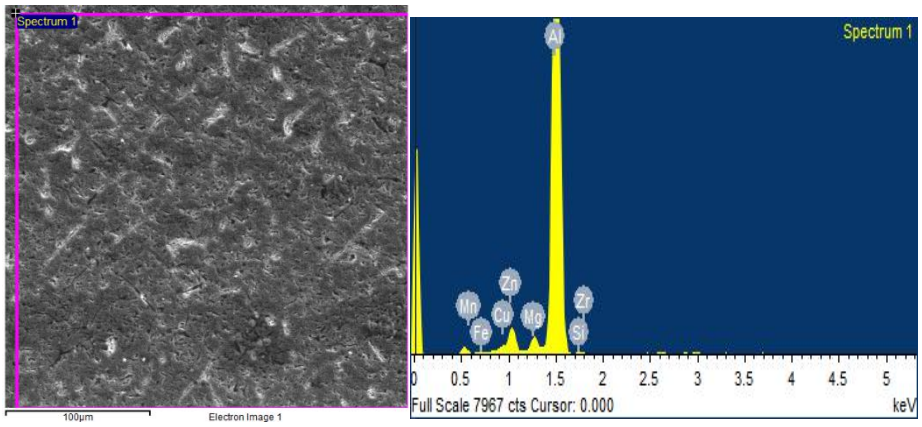

(a)

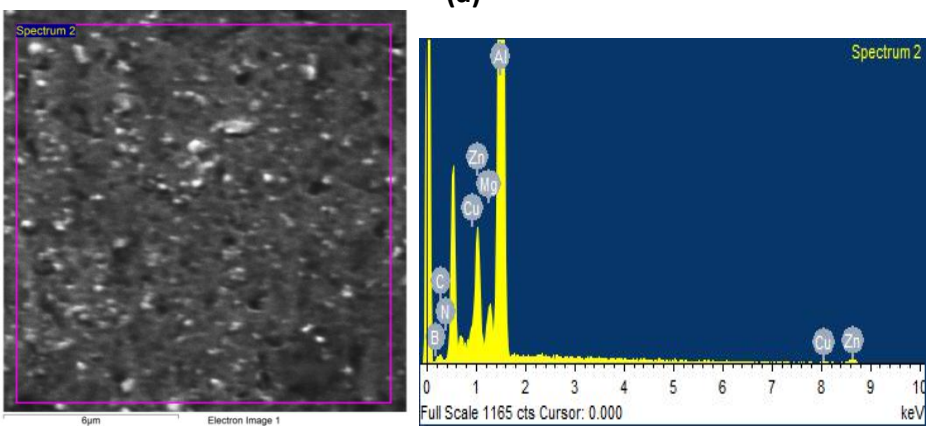

(b)

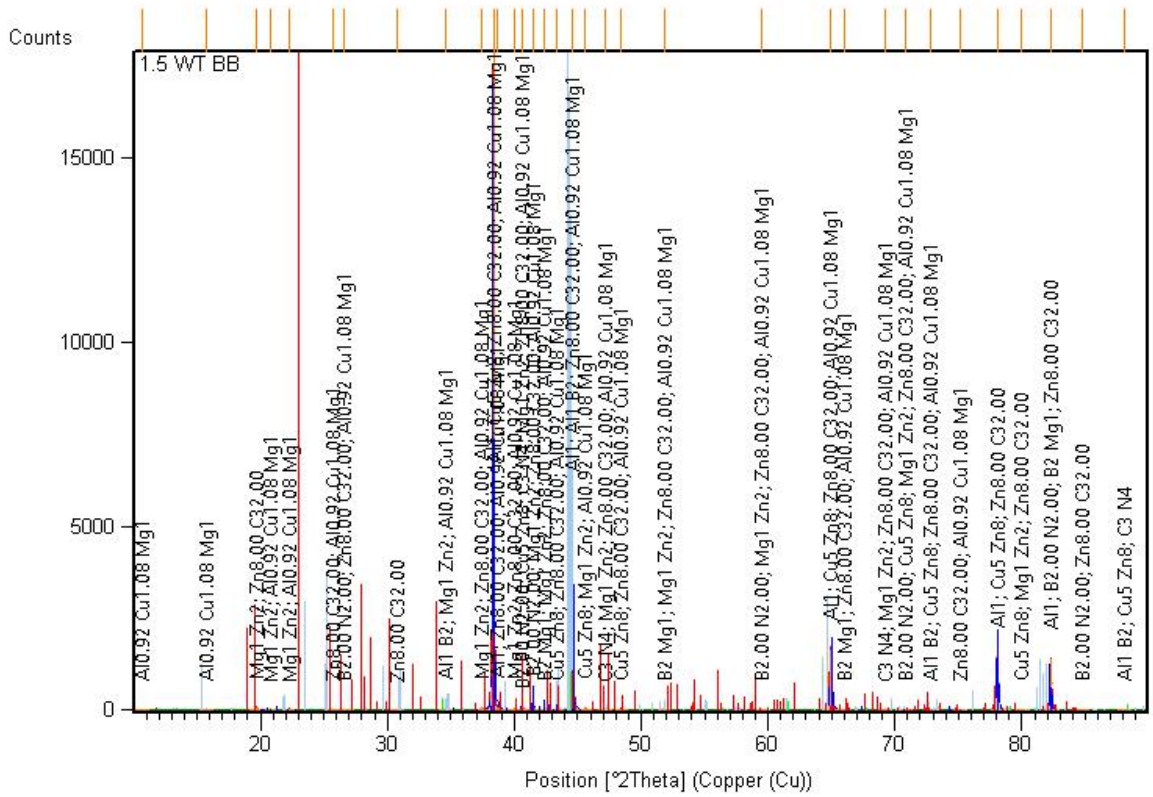

(c)

Figure 6. 3 EDS for elemental analysis of (a) AA7150 (b) 1.5 wt.% (B_4C-hBN) (c) XRD for chemical composition at 1.5 wt.% (B_4C-hBN).

Figure 6.2 shows particle distribution of various weight percentages of hybrid nanocomposites and it is observed that there is uniform distribution of hybrid nanoparticles of B_4C-hBN in 0.5, 1.0, 1.5, and 2.0 wt.%. It is also observed that 1.5 wt.% of B_4C-hBN represents more particles and enjoys better homogeneous distribution throughout the nanocomposite compared to other reinforcements. **Figure 6.2d** clearly indicates that the number of voids and cluster formations are increased and the porosity spread around the material, which leads to increase in grain sizes as well as reduces the strength of composite material. **Figure 6.3** shows the elemental analysis of monolithic and optimal weight percentage of (1.5% B_4C-hBN) hybrid nanocomposite. It is confirmed with the presence of major elements in monolithic material like Al, Cu, Mg, Zn and nanocomposite like Al, Cu, Zn, Mg, along with reinforced elements such as B, C, N. **Figure 6.3c** shows the XRD analysis of 1.5 wt.% composite, **and** observed the phase interactions like Al, Aluminium Boride (AlB2), BN, Magnesium Boride (B_2Mg), Magnesium Zinc ($MgZn_2$), Copper Zinc(Cu_5Zn_8), Aluminium Copper Magnesium ($Al_{0.92}Cu_{1.08}Mg$), Tricarbon Tetranitride (C_3N_4) in the composite.

6.1.2 Mechanical properties of hybrid nanocomposites

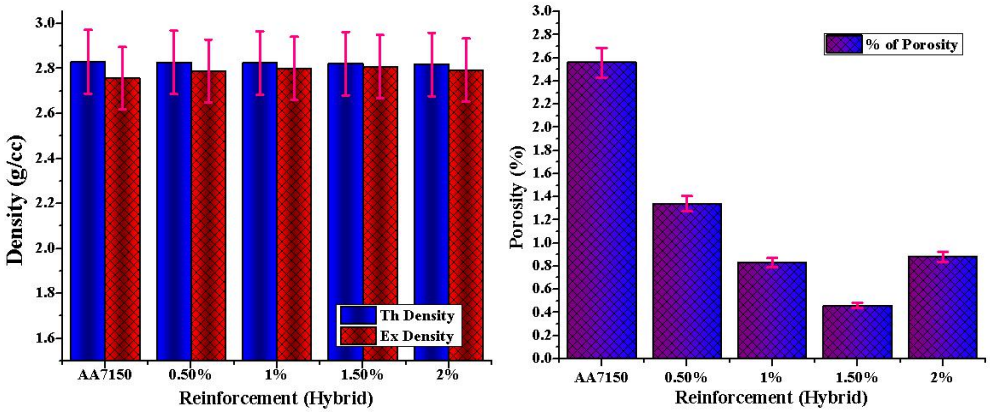

(a) **(b)**

Figure 6. 4 (a) Density and (b) Porosity graphs against to hybrid reinforcement.

The theoretical and experimental densities of AA7150-B_4C-hBN hybrid nanocomposites and alloy matrix material were measured by rule of mixing and *Archimedes principle* respectively. According to the results obtained, the graphical representation of density and % of porosity against to wt.% of hybrid reinforcement is shown in **Figure 6.4**. From the results, it was noticed that the experimental density of AA7150-B_4C-hBN hybrid nanocomposites decreases with increase of hybrid reinforcement content due to lower densities of reinforcements and the effect of ultrasonic degassing phenomena, which plays a vital role in minimizing the porosity because of cavitation effect and closely packed dispersion of hybrid ceramic nanoparticles due to acoustic streaming effect. The existence of porosity in AA7150-B_4C-hBN hybrid nanocomposites and monolithic material was attributed to theoretical and experimental difference. From the porosity results, it was noticed that the % of porosity decreases with increase of hybrid nanoparticle content of up to 1.5 wt.% and maximum reduction at 1.5% due to degassing effect of UV as well as homogeneous distribution of hybrid nanoparticles throughout composites as compared to counter parts. Further reinforcement of hybrid nanoparticle content leads to enhancement of % of porosity due to large surface area to volume ratio of nanoparticles, voids and cluster formation.

Vickers hardness test for various nanocomposites was performed. Microhardness behavior of hybrid nanocomposites is represented through bar graph (**Figure 6.5a**). Microhardness of hybrid nanoparticles reinforced composites was positively enhanced increasing nanoparticle weight percentage by up to 1.5% due to hard B_4C, hBN ceramic particles which strengthened the composite material. It is also due to better interaction

between AA7150 matrix and hybrid nanoparticles, Orowan strengthening (uniform distribution of nanoparticles due to UV effect) mechanism, and Hall-Petch (grain refinement) mechanism, which restrict the deformation and crystal movement during the indentation.

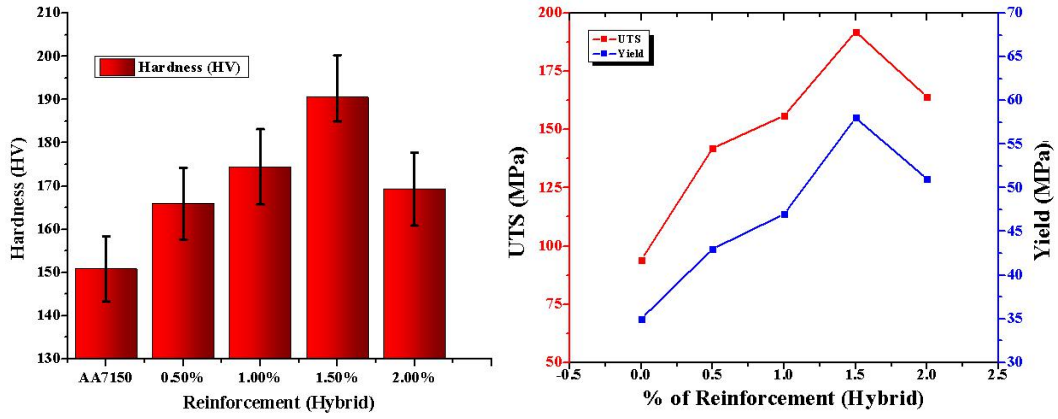

(a) **(b)**

Figure 6. 5 Graph for (a) Micro-hardness Vs hybrid reinforcement (b) Ultimate strength Vs hybrid reinforcement.

Tensile strength results of the base material and hybrid nanoparticles reinforced composites at room temperature are shown in **Figure 6.5b** and the corresponding stress-strain curves are shown in **Figure 6.6**. The effect of hybrid reinforcement in Al nanocomposites was analyzed for UTS values. It was observed that the UTS enhanced positively with (B_4C-hBN) hybrid nanoparticles up to 1.5 wt.% due to nanoparticle load bearing effect, inter-facial distance between the nanoparticles as well as CTE mismatch strengthening mechanism. CTE variation in AA7150 (23.2 X 10^{-6}/ ^oC), hBN nanoparticles (1 X 10^{-6}/ ^oC in $\parallel$ and 4 X 10^{-6}/ ^oC in $\perp$ directions) and B_4C nanoparticles (5 X 10^{-6}/ ^oC) influenced the results because of thermally developed residual stresses and high dislocation density, which act as a barrier to movement of dislocation in the nanocomposite material. The reason can also be rightly attributed to the uniform distribution of ultra-fine hybrid particles in the nanocomposites is due to UV effect in the Al melt bath, which causes homogeneous distribution of nanoparticles and grain refinement during the solidification process. This phenomenon promotes the enhancement of tensile strength in the nanocomposite material. Hence, AA7150-B_4C-hBN nanocomposites strength increases with hybrid nanoparticle content of up to 1.5 wt.% (value of UTS for base metal and 1.5 wt.% of nanoparticles reinforced nanocomposites of 94.7 MPa and 192 MPa) and then decreases further. This decrement of ultimate strength in AA7150-

2wt.% hybrid nanocomposites mainly due to clusters/agglomerations and micro voids which promote stress concentration in the nanocomposites.

Table 6. 1 AGS and material properties of alloy matrix and nanocomposites

Composition	Ex-Density		Porosity		AGS		Hardness	
	g/cc	Error	%	Error	µm	Error	HV	Error
AA7150	2.75755	0.13788	2.56	0.128	131.17	6.5584	150.8	7.541
AA7150-0.5%Hybrid	2.78926	0.13946	1.34	0.067	75.42	3.771	165.9	8.295
AA7150-1.0%Hybrid	2.80086	0.14004	0.83	0.0415	66.62	3.331	174.4	8.720
AA7150-1.5%Hybrid	2.81848	0.14042	0.46	0.023	38.05	1.9025	189.1	9.735
AA7150-2.0%Hybrid	2.79345	0.13967	0.88	0.044	40.49	2.0245	169.3	8.465

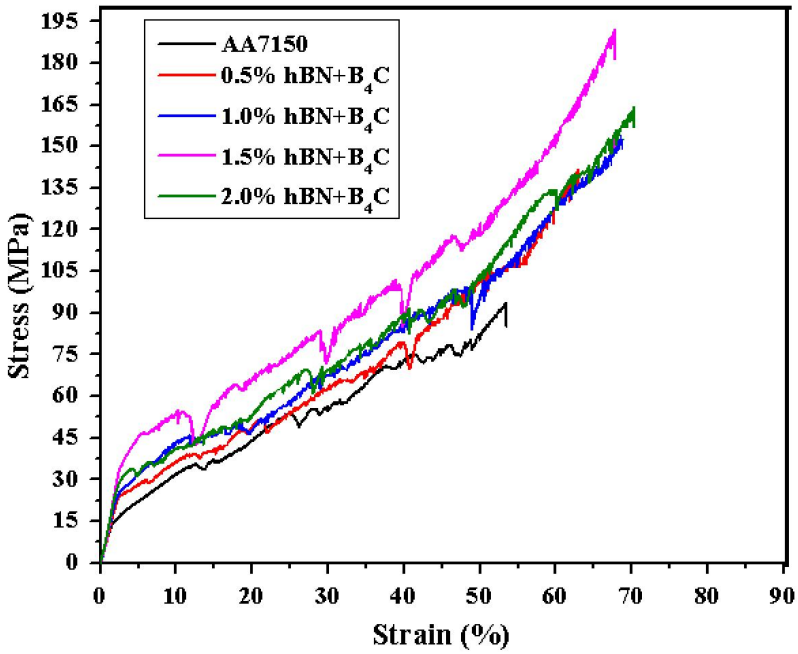

Figure 6. 6 Stress-Strain graph for monolithic and hybrid nanocomposites.

6.1.3 Fracture surface of hybrid nanocomposites

Tensile fracture surface fractographic images at 100X and 1000X magnification for base metal and different weight percentages of hybrid reinforcement are shown in **Figure 6.7**. **Figures 6.7a-e**, reveal that a number of cracks, voids, and grape shaped dendrites globules act as stress riser and lead to cracks. These are moderately increasing, while increasing of wt.% of reinforcement particle content is increasing. **Figure 6.7d** confirms that the voids and cracks are minimized compared to other weight percentages. Further increment in weight percentages leads to an increase in huge voids and cracks which are of various shapes and sizes as confirmed by **Figure 6.7e**. It is also confirmed that facets and dimples are present.

Therefore, the nature of the failure of AA7150-B_4C-hBN is mixed kind, being partially brittle and partially ductile.

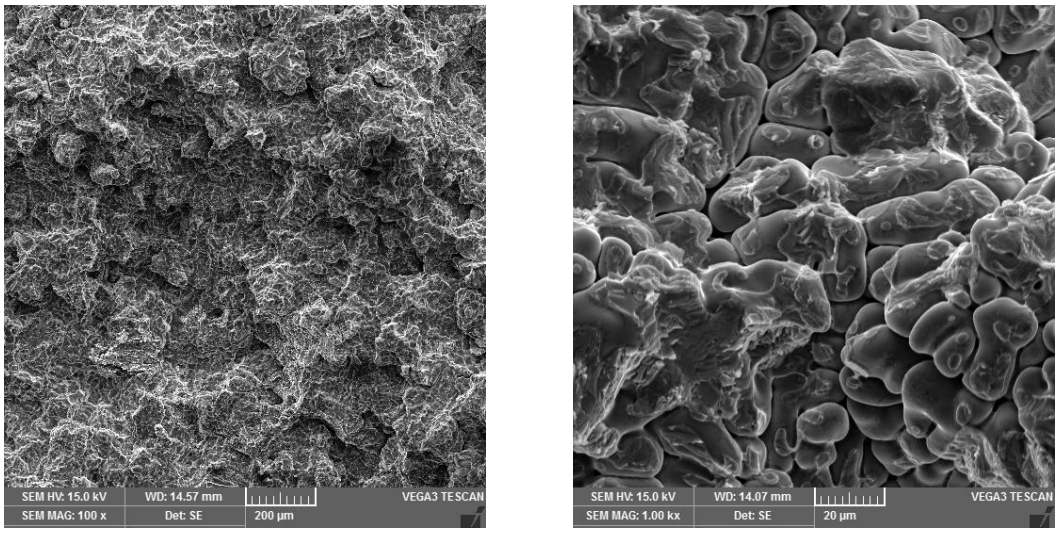

(a)

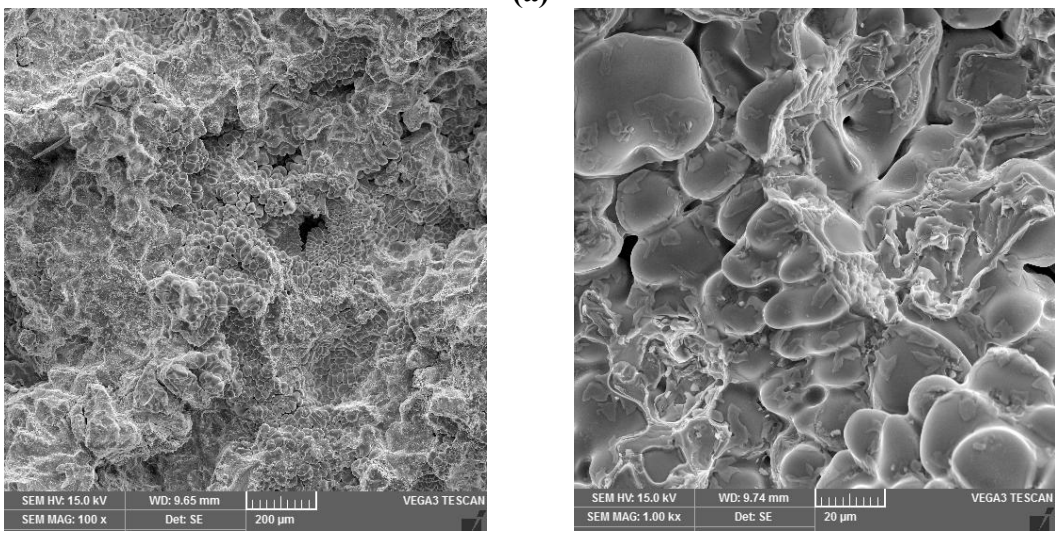

(b)

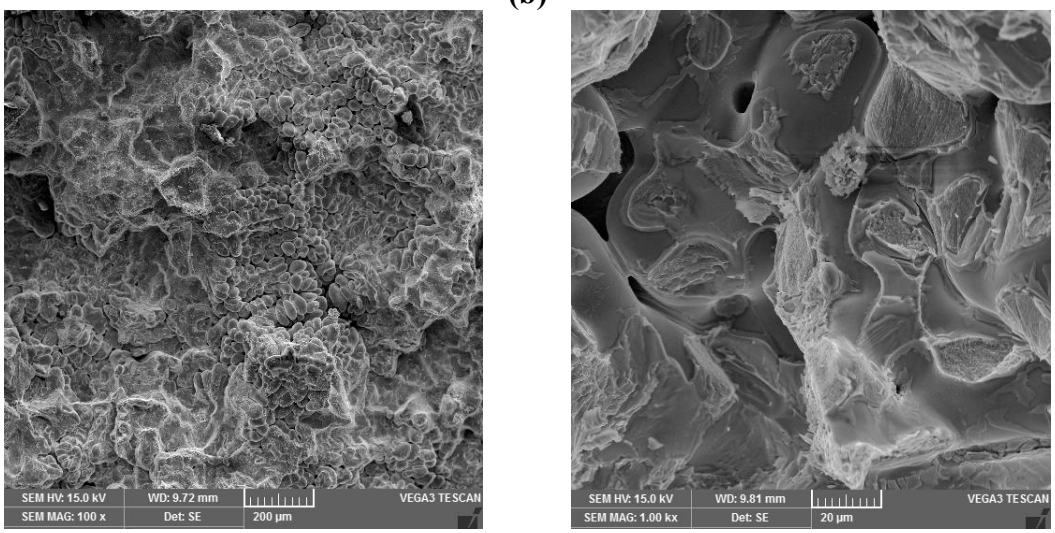

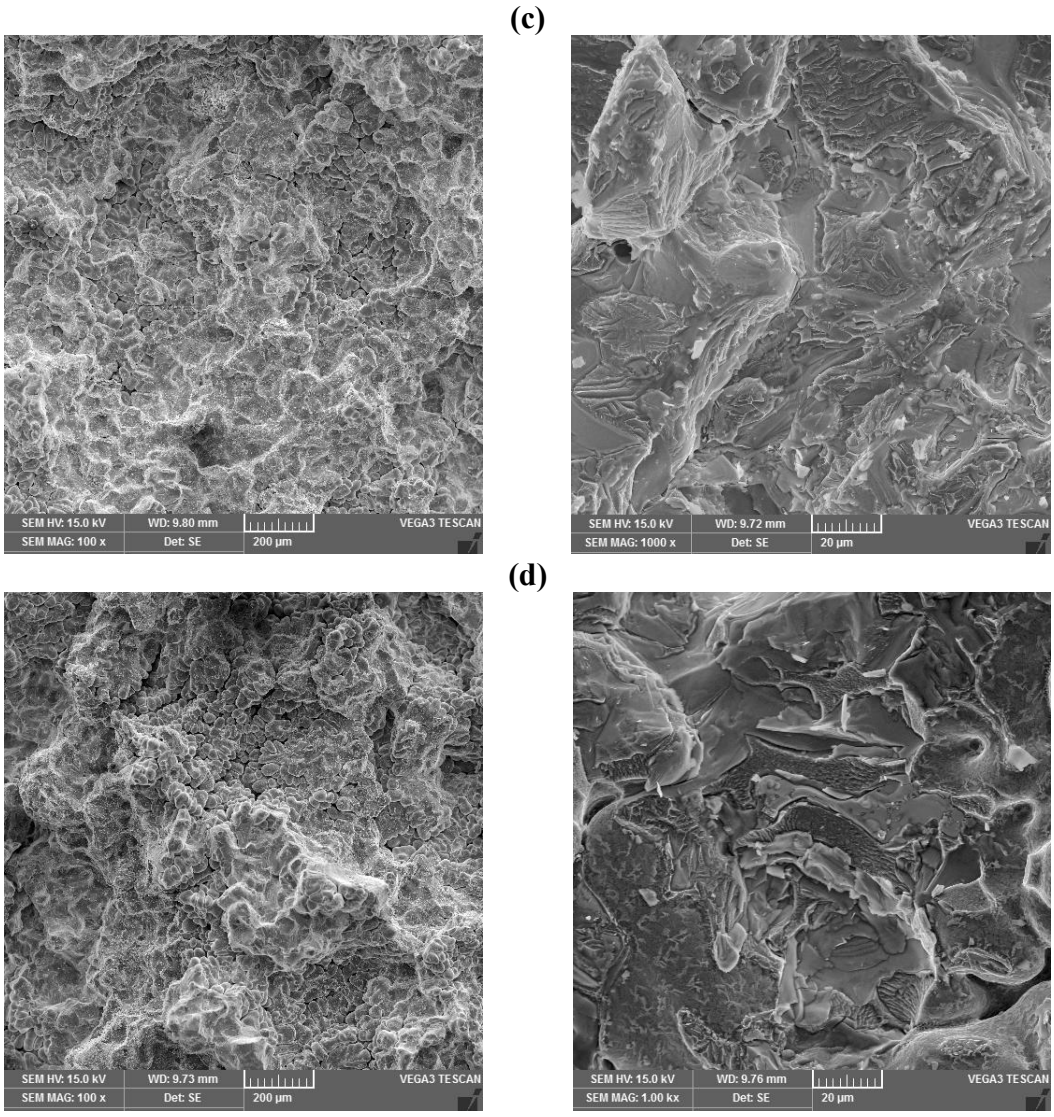

Figure 6. 7 Fracture surfaces of (a) AA7150 (b) 0.5 wt.% (B_4C-hBN) (c) 1.0 wt.% (B_4C-hBN) (d) 1.5 wt.% (B_4C-hBN) (e) 2.0 wt.% (B_4C-hBN).

Figure 6.7 also shows the enlarged photography of hybrid nanocomposites at 20 µm (100X) from a 200 µm (1000X) fractography. The enlarged photography shows detailed clarification of fracture phenomena and 1.5 wt.% hybrid composites show many stepwise dendrites and facets compared to other counter parts. At the same time, it is also revealing the B-C and B-N strength of the next crystal layers, which reveals the high surface energy and friction between adjacent interfaces required to detach the particles. Therefore, it leads to optimal strength of nanocomposites.

6.2 Summary of hybrid nanocomposites

AA7150-B_4C-hBN hybrid nanocomposites were successfully fabricated through a novel fabrication method. All the experiments were conducted at ambient temperature. Mechanical properties were found to increase with increase of hybrid nanoparticle reinforcement of up to 1.5 wt.% and further increment led to reduction in mechanical properties due to the presence of voids, clusters, and agglomeration. Microstructure analysis confirms good formation of grain boundaries and uniform distribution of nanoparticles at 1.5 wt.% compared to counter parts. Porosity decreases while increasing the particulates content at the observed minimum of 1.5 wt.% B_4C-hBN (82.03%). Microhardness, UTS, and yield strength significantly improved by 150.81-189.1 HV (25.40%), 94-192 MPa (104.25%), and 35-58 MPa (68.7%) and the hybrid nanocomposite was found to have optimal properties at 1.5 wt.% (B_4C-hBN). Fractographic studies reveal the semi-brittle nature of failure in hybrid nanocomposites.

CHAPTER -7
CONCLUSIONS

AA7150 based nanocomposites were successfully fabricated through a novel fabrication process by combining vortex, double stir casting, and UV techniques. Microstructure and mechanical properties were investigated for novel fabrication process and compared base material. The following conclusions for the individual nanocomposites reinforced with hBN, B_4C, SiC, TiC, and hBN-B_4C hybrid nanocomposites are stated below:

➢ hBN

1. XRD and EDS analysis revealed the major elements of Al7150 alloy and hBN nanoparticles presence in the matrix alloy with no impurities.
2. Percentage of porosity reduces from 2.056-0.1776 (i.e., 93.36% reduction at 1.5 wt.%)
3. Increase in hBN wt.%, increased the hardness and strength (151.3-185.2 HV and 141-255 MPa) of the nanocomposites due to uniform distribution, grain refinement and hard phase particles, which promotes load bearing capacity. Further increment in hBN wt.% beyond 1.5 wt%, decreases the hardness and strength (185.2-160.8 HV and 255-216 MPa) due to voids, clusters and agglomerations.
4. Microstructure analysis of Al7150-hBN nanocomposites reveals the grain refinement, more uniform nanoparticle distribution and exact nature of failure in nanocomposites.
5. Wear loss of nanocomposites decreased with the increase in the hBN nanoparticles reinforcement due to hardness enhancement, which leads to seizure and wear resistance.
6. Graphical representation of wear results confirmed that the load has greatest influence on wear loss and temperature due to higher frictional forces.
7. SEM images of wear surface reveals that the wear is an abrasive type with restricted plastic deformation and acted as protective layer at 1.5 wt.% hBN., 3 wt.% hBN reveals more debris, oxide layer and delamination on wear surfaces.

➢ B_4C

1. Porosity decreases while increasing the B_4C nano particulate content and observed minimum at 1.5% B_4C (0.11%).

2. Microhardness improved by 154.5-192.4 HV (57.7%)

3. UTS significantly improved by114.7-180.9 MPa (24.5%) and found to have optimal properties at 1.5%B_4C.

4. Maximum ductility of 16.27% was reported at optimal weight percentage of B_4C. Fractographic studies reveal the brittle nature of failure in nanocomposites.

➢ SiC

1. The optical microstructure analysis revealed grain refinement and it increased with an increase in SiC nanoparticles and maximum refinement was observed at 1.5 wt.% SiC. SEM photographs confirm uniform distribution of SiC nanoparticles in Al7150 matrix alloy.

2. The mechanical properties of AA7150-1.5 wt.% SiC nanocomposites exhibit significant improvement as compared to base alloy and it reveals an enhancement of 23.9% (151.8-188.1 HV) in microhardness, 60.1% (117-182.5 MPa) in UTS and minimum porosity (83.47% reduction) at 1.5 wt.% SiC as compared to matrix alloy.

➢ TiC

1. The maximum grain refinement of the TiC reinforced nanocomposite is 41.07 μm and minimum porosity is 0.37% which were decreased by 52.37% (86.23-41.04 μm) and 69.87% (1.23-0.37%) as compared to AA7150.

2. The microhardness and tensile strength of AA7150-TiC nanocomposites at as-cast case enhanced due to novel fabrication process followed by UV treatment effect. The properties of nanocomposites are 177.05 HV and 175 MPa, which are enhanced by 17.40% (150.81-177.05 HV) and 48.31% (118-175 MPa) as compared to AA7150 base alloy.

➢ Hybrid

1. Porosity decreases while increasing the (hBN-B_4C) hybrid nanoparticle content and observed minimum at 1.5% B_4C-hBN (82.03%). Microhardness, UTS, and yield strength significantly improved by 25.40% (150.81-189.1 HV), 104.25% (94-192 MPa), and 65.714% (35-58 MPa) and found to have optimal properties at 1.5 wt% B4C-hBN non-reinforcements.

2. SEM Fractographic studies all individual and hybrid nanocomposites reveal semi-brittle nature of failure.

FUTURE SCOPE

- The microstructure model can be applied to predicting grain size of individual and hybrid reinforced nanocomposites at high temperature.
- Strength prediction models can be applied for nanocomposites.
- Wear characterization of individual nanocomposites reinforced with hBN, B_4C, SiC TiC, and hBN-B_4C hybrid nanocomposites can be carried out.
- For the developed nanocomposites and hybrid nanocomposites, machinability studies can be also performed by using Laser assisted machining.
- Modeling can be possible using soft computing techniques like Artificial Neural Networks, Genetic Algorithm, Genetic Program, Particle Swarm Optimization.

REFERENCES

1. Abu-Warda A, Utrilla MV, Escalera MD, Otero E, Lopez MD. The effect of TiB2 content on the properties of AA6005/TiB2 nanocomposites fabricated by mechanical alloying method. Powder Technol, 2018, 28, 235-244.
2. Akhlaghi, F., & Mahdavi, S. Effect of the SiC content on the tribological properties of hybrid Al/Gr/SiC composites processed by in situ powder metallurgy (IPM) method. In Adv Mater Research, 2011, 264, 1878-1886.
3. Alaneme K K, Olubambi PA, Afolabi AS, Bodurin MO, Corrosion and tribological studies of bamboo leaf ash and alumina reinforced Al-Mg-Si alloy matrix hybrid composites in chloride medium, Int J Electrochem Sci, 2014, 9, 5663 - 5674.
4. Alaneme KK, Akintundea IB, Olubambib PA, Adewalec TM. Fabrication characteristics and mechanical behaviour of rice husk ash-Alumina reinforced Al–Mg–Si alloy matrix hybrid composites. J Mater Res Technol, 2013, 2(1), 60–67.
5. Alaneme, K. K., Ademilua, B. O., & Bodunrin, M. O. Mechanical properties and corrosion behaviour of aluminium hybrid composites reinforced with silicon carbide and bamboo leaf ash. Tribolo Ind, 2013, 35(1), 25-35.
6. Alexandru Sergiu Nanu, Niculae Ion Marinescu, Daniel Ghiculescu, Nanu, Study on ultrasonic stepped horn geometry design and FEM simulation. Nonconventional Technol Review, 2011, 4, 25-30.
7. Arun Kumar M. B and R. P. Swamy, Evaluation of Mechanical Properties of Al6061, Flyash And e-Glass Fiber Reinforced Hybrid Metal Matrix Composites .ARPN J En Applied Sci, 2011, 6(5), 40-44.
8. Arun Premnath A, Studies on Machining Parameters While Milling Particle Reinforced Hybrid (Al6061/Al2O3/Gr) MMC, Part Sci Technol, 2015, 33(6), 682-692.
9. Attharangsan, S., Ismail, H., Bakar, M. A., & Ismail, J. Carbon Black (CB)/Rice Husk Powder (RHP) Hybrid Filler-Filled Natural Rubber Composites: Effect of CB/RHP Ratio on Property of the Composites. Polymer-Plastics Technol Eng, 2012, 51(7), 655–662.
10. Basavarajappa, S., Chandramohan, G., Davim, J. P., Prabu, M., Mukund, K., Ashwin, M., & PrasannaKumar, M. Drilling of hybrid aluminium matrix composites. Int J Adv Manuf Technol, 2008, 35(11-12), 1244-1250.

11. Blaža Stojanović, Miroslav Babić, Sandra Veličković & Jasmina BlagojevićTo, Tribological behavior of aluminum hybrid composites studied by application of factorial techniques, Tribol Tran, 2016, 59(3), 522-529.
12. Boopathi M, Arulshri KP, Iyandurai N. Evaluation of mechanical properties of aluminium alloy 2024 reinforced with silicon carbide and fly ash hybrid metal matrix composites. Am J Appl Sci, 2013, 10(3), 219–229.
13. Chawla N, Shen Y. Mechanical behavior of particle reinforced metal matrix composites. Adv Eng Mater, 2001, 3, 357–370.
14. Chen Baiming, Bi Qinling, Yang Jun, Xia Yanqiu, Jingcheng Hao. Tribological properties of solid lubricants (graphite, h-BN) for Cu-based P/M friction composites. Tribol Int, 2008, 41, 1145–1152.
15. Chen R, Lwabuchi A, Shimizu T, Shin HS, Mifune H. The sliding wear resistance behavior of NiAI and SiC particles reinforced aluminum alloy matrix composites. Wear, 1997, 213(1–2), 175–184.
16. Courtney TH. Mechanical behaviour of materials. 2nd ed.India: Overseas Press; 2006.
17. Dalmis R, Cuvalci H, Canakci A, Guler O, Celik E. The effect of mechanical milling on graphite–boron carbide hybrid reinforced ZA27 nanocomposites. Arabian J Sci Eng, 2018, 43, 1113–1124.
18. Debdas Roy, Nidhi Khobragade, Koushik Sikdar, Binod Kumar, Supriya Bera, Mechanical and electrical properties of copper-graphene nanocomposite fabricated by high pressure torsion J Alloys Comp, 776, 2019, 123-132.
19. Devaraju, A., Kumar, A., & Kotiveerachari, B. Influence of addition of Grp/Al2O3p with SiCp on wear properties of aluminum alloy 6061-T6 hybrid composites via friction stir processing. Tran Nonferrous Met Soc China, 2013, 23(5), 1275-1280.
20. Devaraju, A., Kumar, A., & Kotiveerachari, B. Influence of rotational speed and reinforcements on wear and mechanical properties of aluminum hybrid composites via friction stir processing. Mater Des, 2013, 45, 576-585.
21. Dhandapani S, Rajmohan T, Palanikumar K & Charan M, Synthesis and characterization of dual particle (MWCT+B4C) reinforced sintered hybrid aluminum matrix composites, Part Sci Technol, 2015, 34(3), 255-262.
22. Dinesh Kumar Kolia, Geeta Agnihotri, Rajesh Purohit, Influence of Ultrasonic Assisted Stir Casting on Mechanical Properties of Al6061-nano Al2O3 Composites, Mater Today: Proc, 2015, 2, 3017-3026.

23. Dora Siva Prasada, Chintada Shobab, Nallu Ramanaiahc,Investigations on mechanical properties of aluminum hybrid composites, J Mater Res Technol, 2014, 3(1), 79–85.
24. Du Yuan, Xiong Yang, Shusen Wu, Shulin Lü, Kun Hu, Development of high strength and toughness nano-SiCp/A356 composites with ultrasonic vibration and squeeze casting, J Mater Process Technol, 292, 2019, 1-9.
25. Duan, X., Yang, Z., Chen, L., Tian, Z., Cai, D., Wang, Y., & Zhou, Y. Review on the properties of hexagonal boron nitride matrix composite ceramics. J Eur Ceram Soc, 2016, 36(15), 3725-3737.
26. Elkady Omayma A, Abolkassem Shimaa A, Elsayed Ayman H, Hussein Walaa A, Hussein Khalid FA. Microwave absorbing efficiency of Al matrix composite reinforced with nano-Ni/SiC particles Results in. Phys, 2019, 12, 687–700.
27. Escalera-Lozano, R., Gutiérrez, C. A., Pech-Canul, M. A., & Pech-Canul, M. I. Corrosion characteristics of hybrid Al/SiCp/MgAl2O4 composites fabricated with fly ash and recycled aluminum. Mater Char, 2007, 58(10), 953-960.
28. Essam R.I. Mahmoud, Makoto Takahashi, Toshiya Shibayanagi, Kenji Ikeuchi, Wear characteristics of surface-hybrid-MMCs layer fabricated on aluminum plate by friction stir processing, Wear, 2010, 268, 1111–1121.
29. Ezatpour HR, Torabi Parizi M, Sajjadi SA. Microstructure and mechanical properties of extruded Al/Al2O3 composites fabricated by stir-casting process. Trans Nonferrous Metals Soc China 2013, 23, 1262–1268.
30. Fadavi Boostania A, Yazdania S, Azari Khosroshahia R, Jiangb ZY, Wei D. A novel graphene-stimulated semi-solid processing to fabricate advanced aluminum matrix nanocomposites. Mater Sci Eng A, 2018, 736, 316–328.
31. Fink, A., Camanho, P. P., Andrés, J. M., Pfeiffer, E., & Obst, A. Hybrid CFRP/titanium bolted joints: Performance assessment and application to a spacecraft payload adaptor. Comp Sci Technol, 2010, 70(2), 305-317.
32. Firestein, K. L., Steinman, A. E., Golovin, I. S., Cifre, J., Obraztsova, E. A., Matveev, A. T., & Golberg, D. Fabrication, characterization, and mechanical properties of spark plasma sintered Al–BN nanoparticle composites. J Mater Sci Eng A, 2015, 642, 104-112.
33. Fogagnolo JB, Robert MH, Torralba JM. Mechanically alloyed AlN particle- reinforced Al-6061 matrix composites, powder processing, consolidation and mechanical strength and hardness of the as-extruded materials. J Mater Sci Eng A, 2006, 426, 85–94.
34. Ganeshan pandi, Sarvanan Muthusamy, A review on machining and tribological behaviors of aluminium hybrid composites, Procedia Eng, 2012, 38, 1399-1408.

35. Guo, H., Zhao, Y., Xu, S., Li, J., Liu, N., Zhang, Y., & Zhang, Z. Influence of high B4C contents on structural evolution of Al-B4C nanocomposite powders produced by high energy ball milling. Ceram Int,. 2018, 45(5), 5436-5447.
36. Hanada K, Murakoshi Y, Negishi H, Sano T. Microstructures and mechanical properties of Al–Li/SiCp composite produced by extrusion processing. J Mater Process Technol, 1997, 63, 405–410.
37. Harichandran, R., & Selvakumar, N. Effect of nano/micro B4C particles on the mechanical properties of aluminium metal matrix composites fabricated by ultrasonic cavitation-assisted solidification process. Arc Civil Mech Eng, 2016, 16(1), 147-158.
38. Harish K.Garg, Ketan Verma, Alakesh Manna, Rajesh Kumar, Hybrid metal matrix composites and further improvement in their machinability– A Review, Int J Latest Res Sci Techno, 2012, 1(1), 36-44.
39. Hutching IM. Wear by particulates. Chem Eng Sci, 1987, 42(4), 869–878.
40. Jaswinder Singha, Amit Chauhan, Characterization of hybrid aluminum matrix composite for advance applications- a review, J Mater Res Techno, 2016, 5(2), 159-169.
41. Javad Nasr Isfahani Mohammad, Payami Fereidoun, Asadi Asadabad Mohsen, Asghar Shokri Ali. Investigation of the effect of boron carbide nanoparticles on the structural, electrical and mechanical properties of Al-B4C. J Alloy Comp 2019, 797, 1348–1358.
42. Jeyasimman D, Narayanasamy R, Ponalagusamy R, Anandakrishnan V, Kamaraj M. The effects of various reinforcements on dry sliding wear behaviour of AA 6061 nanocomposites. Mater Des, 2014, 64, 783–93.
43. Jianyu Li, Gaozhan Zhao, Shusen Wu, Zhiwei Huang, Shulin Lü, Qiang Chen, and Fei Li. Preparation of hybrid particulates SiCnp and Mg2Si reinforced Al-Cu matrix composites. Mater Sci Eng A, 2019, 751, 107-114.
44. Jin Ho Bang and Kenneth S. Suslick, Applications of Ultrasound to the Synthesis of Nano structured Materials. Adv Mater, 2010, 22, 1039-1059.
45. Jufu Jiang, Ying Wang, Microstructure and mechanical properties of the semisolid slurries and rheoformed component of nano-sized SiC/7075 aluminum matrix composite prepared by ultrasonic-assisted semisolid stirring, Mater Sci Eng A, 2015, 639, 350-358
46. Károly, Z., Balázsi, C., Balázsi, K., Petrik, A., Lábár, J., & Dhar, A. Hybrid aluminum matrix composites prepared by spark plasma sintering (SPS). Eur Chem Bull, 2014, 3(3), 247-250.
47. Kenneth Kanayo Alaneme, Peter Apata Olubambi, Corrosion and wear behaviour of rice husk ash—Alumina reinforced Al–Mg–Si alloy matrix hybrid composites. J Mater Res

Technol, 2013, 2(2), 188–194.

48. Kenneth Kanayo Alaneme, Tolulope Moyosore Adewale, Peter Apata Olubambi, Corrosion and wear behavior of Al-Mg-Si alloy matrix hybrid composites reinforced with rice husk ash and silicon carbide. J Mater Res Technol, 2014, 3(1), 9–16.
49. Khakbiz M, Akhlaghi F. Synthesis and structural characterization of Al–B4C nanocomposite powders by mechanical alloying. J Alloy Compd, 2009, 479, 334–341.
50. Khalid F.A. Hussein, Microwave absorbing efficiency of Al matrix composite reinforced with nano-Ni/SiC particles, Results in Phys, 2019, 12, 687–700.
51. Krishnamurthy, L., Sridhara, B. K., & Abdul Budan, D. Comparative study on the machinability aspects of aluminium-silicon carbide and aluminium-graphite-silicon carbide hybrid composites. Int J Mach Mach Mater, 2011, 10(1-2), 137-152.
52. Kumaran, S. T., Uthayakumar, M., Slota, A., Aravindan, S., & Zajac, J. Machining behavior of AA6351–SiC–B4C hybrid composites fabricated by stir casting method. Part Sci Technol, 2016, 34(5), 586-592.
53. Lan J., Yang Y., Li X., Microstructure and Microhardness of SiC Nanoparticles Reinforced Magnesium Composites Fabricated by Ultrasonic Method, Mater Sci Eng A, 2004, 386, 284-290.
54. Leigang Zhang, Xi Luo, Jinling Liu, Yongxiang Leng, Linan An, Dry sliding wear behavior of Mg-SiC nanocomposites with high volume fractions of reinforcement, Mater Lett, 2018, 228, 112–115.
55. Li Jianyu, Zhao Gaozhan, Wu Shusen, Huang Zhiwei, Shulin Lü, Chen Qiang, Li Fei. Preparation of hybrid particulates SiCnp and Mg2Si reinforced Al-Cu matrix Composites. Mater Sci Eng A, 2019, 751, 107–114.
56. Li X., Duan Z., Cao G., Roure A. Ultrasonic Cavitation Based Solidification Processing of Bulk Mg Matrix Nanocomposite, AFS Tran, 2007, 107- 135.
57. Li, J., Zhao, G., Wu, S., Huang, Z., Lü, S., Chen, Q., & Li, F. Preparation of hybrid particulates SiCnp and Mg2Si reinforced Al-Cu matrix composites. Mater Sci Eng A, 2019, 751, 107–114.
58. Manivannan I, Ranganathan S, Gopalakannan S, Suresh S. Mechanical properties and tribological behavior of Al6061–SiC–Gr self-lubricating hybrid nanocomposites. Trans Indian Inst Met, 2018, 71,1897–1911.
59. Mehrdad Shayan, Beitallah Eghbali, Behzad Niroumand, Synthesis of AA2024-(SiO2np+TiO2np) hybrid nanocomposite via stir casting Process, Mater Sci Eng A, 2019, 756 484–491.

60. Mitrović, S., Babić, M., Stojanović, B., Miloradović, N., Pantić, M., & Džunić, D. Tribological potential of hybrid composites based on zinc and aluminium alloys reinforced with SiC and graphite particles. Tribol Ind, 2012, 34(4), 177-185.
61. Miyajima T, Iwai Y. Effects of reinforcements on sliding wear behavior of aluminium matrix composites. Wear, 2003, 255(1–6), 606–616.
62. Mohammad Javad Nasr Isfahani Fereidoun Payami, Mohsen Asadi Asadabad, Ali Asghar Shokri, Investigation of the effect of boron carbide nanoparticles on thestructural, electrical and mechanical properties of Al-B4C J Alloys Compd 797, 2019, 1348-1358.
63. Mohapatra, S., Bankoti, A. K. S., Mondal, A. K., & Thirugnanam, A. Dry Sliding Wear and Corrosion Behaviour of Al-Based Hybrid Composites Reinforced with Micro-Tip and Micro/Nano-Al_2O_3p. Trans Indian Inst Met, 2016, 69(6), 1155-1167.
64. Nayak, D., Ray, N., Sahoo, R., & Debata, M. Analysis of tribological performance of Cu hybrid composites reinforced with graphite and TiC using factorial techniques. Tribolo Trans, 2014, 57(5), 908-918.
65. Oluwagbenga Babajide Fatile, Joshua Ifedayo Akinruli and Anthony Akpofure Amori2, Microstructure and Mechanical Behaviour of Stir-Cast Al-Mg-Sl Alloy Matrix Hybrid Composite Reinforced with Corn Cob Ash and Silicon Carbide, Int J Eng Technol Innov, 2014, 4(4), 251.
66. Omayma A. Elkady, Shimaa A. Abolkassem, Ayman H. Elsayed, Walaa A. Hussein, Palanivel, R., Dinaharan, I., Laubscher, R. F., & Davim, J. P. Influence of boron nitride nanoparticles on microstructure and wear behavior of AA6082/TiB2 hybrid aluminum composites synthesized by friction stir processing. Mater Des, 2016, 106, 195-204.
67. Pallav Gupta, Devendra Kumar, Om Parkash, A.K. Jha, Kishor Kumar Sadasivuni Dependence of wear behavior on sintering mechanism for Iron-Alumina Metal Matrix Nanocomposites, Mater Chem Phys, 220, 2018, 441–448.
68. Pardeep Sharma, Satpal Sharma & Dinesh Khanduja, Production and Characterization of AA6082- (Si3N4+Gr) Stir Cast Hybrid Composites, Part Sci Techno, 2017, 35(2), 158-165.
69. Pillari, L. K., Umasankar, V., Elamathi, P., & Chandrasekar, G. Synthesis and characterization of nano hexagonal boron nitride powder and evaluating the influence on aluminium alloy matrix. Mater Today: Proc, 2016, 3(6), 2018-2026.
70. Poovazhagan L Thomas H. J, Selvaraj M, Microstructure and Abrasive Wear Behavior of Copper–Boron Carbide Nanocomposites, Advan Mater Metall, 2019, 43-55.

71. Poovazhagan.L, Kalaichelvan.K, Rajadurai.A and Senthilvelan.V, Fabrication characteristics and mechanical behaviour of rice husk ash – Alumina reinforced Al-Mg-Si alloy matrix hybrid composites, Procedia Eng, 64, 2013, 681 – 689.
72. Popov Vladimir A, Burghammer Manfred, Rosenthal Martin, Kotov Anton. In situ synthesis of TiC nano-reinforcements in aluminum matrix composites during mechanical alloying. Composites Part B, 2018, 145, 57–61.
73. Prakash C.H. and Pruthviraj R.D, Microstructural Studies of Cast Zinc - Aluminum-Sic-Graphite Hybrid Composites, Resear J Chem Sci, 2011, 1(6), 88-90.
74. Puga H, Barbosa J, Seabra E, The influence of processing parameters on the ultrasonic degassing of molten $AlSi_9Cu_3$ aluminium alloy, Mater Lett, 63, 2009, 806–808.
75. Qi Wu, Weixing Xu, Liangchi Zhang, Microstructure-based modelling of fracture of particulate reinforced metal matrix composites, Composites Part B, 163, 2019, 384–392.
76. Radhika, N., & Subramanian, R. Effect of reinforcement on wear behaviour of aluminium hybrid composites. Tribology-Materials, Surfaces & Interfaces, 2013, 7(1), 36-41.
77. Rajmohan T & Palanikumar K, Optimization of Machining Parameters for Surface Roughness and Burr Height in Drilling Hybrid Composites, Mater Manuf Process, 2012, 27(3), 320-328.
78. Rajmohan, T., Palanikumar, K., & Arumugam, S. Synthesis and characterization of sintered hybrid aluminium matrix composites reinforced with nanocopper oxide particles and microsilicon carbide particles. Composites Part B, 2014, 59, 43-49.
79. Rajmohan, T., Palanikumar, K., & Ranganathan, S. Evaluation of mechanical and wear properties of hybrid aluminium matrix composites. Tran nonferrous met soc China, 2013, 23(9), 2509-2517.
80. Ravindra Singh Rana, Rajesh Purohit, Anil kumar Sharma, Saraswati Rana, Optimization of Wear Performance of Aa 5083/10 Wt. % SiC nano Composites Using Taguchi Method, Procedia Mater Sci, 2014, 6, 503-511.
81. Ravindran, P., Manisekar, K., Kumar, S. V., & Rathika, P. Investigation of microstructure and mechanical properties of aluminum hybrid nano-composites with the additions of solid lubricant. Mater Des, 2013, 51, 448-456.
82. Reddy G. Chandrakanth & K. Rajkumar & Sivanandam Aravindan Fabrication of copper–TiC–graphite hybrid metal matrix composites through microwave processing,Int J Adv Manuf Technol, 2010, 48, 645–653.
83. Riaz Ahamed A& Asokan A & Aravindan S, EDM of hybrid Al–SiCp–B4Cp and Al–SiCp–Glassp MMCs, Int J Adv Manuf Technol, 2009, 44, 520–528.

84. Roy Debdas, Khobragade Nidhi, Sikdar Koushik, Kumar Binod, Bera Supriya. Mechanical and electrical properties of copper-graphene nanocomposite fabricated by high pressure torsion. J Alloy Compd, 2019, 776,123–132.
85. Samal, S. K., Mohanty, S., & Nayak, S. K. Banana/glass fiber-reinforced polypropylene hybrid composites: Fabrication and performance evaluation. Polym Plasti Technol Eng, 2009, 48(4), 397-414.
86. Sandra Veličković Blaža Stojanović,·Miroslav Babić, Aleksandar Vencl, Ilija Bobić, Gabriella Vadászné Bognár, Filip Vučetić, Parametric optimization of the aluminium nanocomposites wear rate J Braz Soc Mech Sci Eng, 2019, 41, 19-29.
87. Sasimurugan, T., & Palanikumar, K. Analysis of the machining characteristics on surface roughness of a hybrid aluminium metal matrix composite (Al6061-SiC-Al2O3). J Miner Mater Char Eng, 2011, 10(13), 1213-1220.
88. Selvakumar, N., & Narayanasamy, P. Optimization and effect of weight fraction of MoS2 on the tribological behavior of Mg-TiC-MoS2 hybrid composites. Tribol Trans, 2016, 59(4), 733-747.
89. Shin, K. C., Lee, J. J., Kim, K. H., Song, M. C., & Huh, J. S. Axial crush and bending collapse of an aluminum/GFRP hybrid square tube and its energy absorption capability. Compos Struct, 2002, 57(1-4), 279–287.
90. Shulin Lü, Pan Xiao, Du Yuan, Kun Hu, Shusen Wu, Preparation of Al matrix nanocomposites by diluting the composite granules containing nano-SiCp under ultrasonic vibaration, J Mater Sci Technol, 2018, 34, 1609–1617.
91. Singh, Jaswinder, and Amit Chauhan. Characterization of hybrid aluminum matrix composites for advanced applications–A review. Journal of Materials Research and Technology, 2016, 5(2), 159-169.
92. Siva Prasad D, Shoba C. Hybrid composites – a better choice for high wear resistant materials, J Mater Res Technol, 2014, 3(2), 172–178.
93. Song-Li Zhang, Xian-Wei Dong, Yu-Tao Zhao, Man-Ping Liu, Gang Chen, Zhen-kun Zhang, Yu-ying Zhang, Xue-hua Gao, Preparation and wear properties of TiB2/Al−30Si composites via in-situ melt reactions under high-energy ultrasonic field, Trans Nonferrous Met Soc China, 2014, 24, 3894−3900.
94. Songmene V, Balazinski M. Machinability of graphitic metal matrix composites as a function of reinforcing particles. AnnCIRP 1999, 48:77–80.
95. Sudarshan, Surappa MK. Synthesis of fly ash particle reinforced A356 Al composites and their characterization.Mater Sci Eng A, 2008, 480(1–2),117–124.

96. Sudip Banerjee, Suswagata Poria, Goutam Sutradhar, Prasanta Sahoo, Dry sliding tribological behavior of AZ31-WC nano-composites, Article in Press J Magnesium Alloys, 2018, https://doi.org/10.1016/j.jma.2018.11.005.
97. Suresh S, Harinath Gowd G, Deva Kumar M. L. S, Mechanical and Wear Characterization of Al/Nano-SiC NMMCs by Liquid State Process J Bio- and Tribo-Corrosion 5, 2019, 43-53.
98. Suresha, S, Sridhara, BK, Wear characteristics of hybrid aluminium matrix composites reinforced with graphite and silicon carbide particulate, Compos Sci Technol, 70, 2010, 1652–1659.
99. Tan MJ, Zhang X. Powder metal matrix composites: selection and processing. J Mater Sci Eng A, 1998, 244, 80–85.
100. Thakur SK, Dhindaw BK, Hort N, And Kainer KU, Some Studies on the Thermal-Expansion Behavior of C-Fiber, SiCP, and In-Situ Mg2Si-Reinforced AZ31 Mg Alloy–Based Hybrid Composites, Metall Mater Trans, 2004, 35(3), 1167-1176.
101. Thakur SK, Dhindaw BK. The influence of interfacial characteristics between SiCp and Mg/Al metal matrix onwear, coefficient of friction and microhardness. Wear, 2001, 247(2), 191–201.
102. Thirumalai T, Subramanian R, Kumaran S, Dharmalingam S, Ramakrishnan SS, production and characterization of hybrid aluminium matrix composites reinforced with B4C and Gr, Journal of scintific and Industrial research, 2014, http://nopr.niscair.res.in/bitstream/123456789/29452/1/JSIR%2073%2810%29%20667-670.pdf.
103. Tjong, S. C., Lau, K. C., & Wu, S. Q. Wear of Al-based hybrid composites containing BN and SiC particulates. Metallurgical And Materials Transactions, 1999, 30(9), 2551-2559.
104. Tuo Xu, Guirong Li, Menglei Xie, Ming Liu, De Zhang, Yutao Zhao, Gang Chen, Xizhou Kai Microstructure and mechanical properties of in-situ nano γ-Al2O3p/A356 aluminum matrix composite J Alloys and Comp, 787, 2019, 72-85.
105. Uvaraja VC, Natrajan N. Optimization of friction and wear behavior in hybrid metal matrix composites using Taguchi technique. J Miner Mater Charact Eng, 2012, 11, 757–768.
106. Vara Prasad Kaviti, R, Jeyasimman, D, Gururaj Parande, Manoj Gupta, Narayanasamy, R, Investigation on dry sliding wear behavior of Mg/BN nanocomposites, J Magnesium Alloys, 2018, 6, 263–276.

107. Veeresh Kumar GB, Rao CSP, Selvaraj N. Studies on mechanical and dry sliding wear of Al6061–SiC composites. Composites Part B, 2012, 43, 1185–1191.
108. Venkat Prasat, S., & Subramanian, R. Tribological properties of AlSi10Mg/fly ash/graphite hybrid metal matrix composites. Indust Lubric Tribol, 2013, 65(6), 399-408.
109. Vladimir A. Popov, Manfred Burghammer, Martin Rosenthal, Anton Kotov, In situ synthesis of TiC nano-reinforcements in aluminum matrix composites during mechanical alloying, Composites Part B, 2018, 145, 57–61.
110. Wang Y, Rainforth WM, Jones H, Lieblich M. Dry wear behaviour and its relation to microstructure of novel 6092 aluminium alloy–Ni3Al powder metallurgy composite. J Wear, 2001, 251, 1421–1432.
111. Wang, X. J., Wang, N. Z., Wang, L. Y., Hu, X. S., Wu, K., Wang, Y. Q., & Huang, Y. D. Processing, microstructure and mechanical properties of micro-SiC particles reinforced magnesium matrix composites fabricated by stir casting assisted by ultrasonic treatment processing. Mater Des, 2014, 57, 638-645.
112. Wong, W. L. E., Karthik, S., & Gupta, M. Development of hybrid Mg/Al2O3 composites with improved properties using microwave assisted rapid sintering route. J Mater Sci, 2005, 40(13), 3395-3402.
113. Wu H F, WuL L, A study of tension test specimens of laminated hybrid composites,Part II Size and alignment effects. I J Mater Sci, 1994, 29, 5847-5851.
114. Wu, H. F., & Wu, L. L. A study of tension test specimens of laminated hybrid composites. 1: Methods of approach. Composites Part A, 1996, 27(8), 647-654.
115. Xia Zhou, Shangyu Song, Li Li, Wuming M, Numerical simulation and experimental validation of SiC nanoparticle distribution in magnesium melts during ultrasonic cavitation based processing of magnesium matrix nanocomposites, J Mater Res Technol,. 2014, 3(4), 296–302.
116. Xu Tuo, Li Guirong, Xie Menglei, Liu Ming, De Zhang, Zhao Yutao, Chen Gang, Kai Xizhou. Microstructure and mechanical properties of in-situ nano γ-Al2O3p/ A356 aluminum matrix composite. J Alloy Comp 2019, 787, 72-85.
117. Yang Xuan, Laurentiu Nastac, The role of ultrasonic cavitation in refining the microstructure of aluminum based nanocomposites during the solidification process, Ultrasonics, 2018, 83, 94-102.
118. Yang Y, Li X. Ultrasonic cavitation based nano-manufacturing of bulk aluminum matrix nanocomposites. J Manuf Sci Eng, ASME 2007, 129(2), 252–5.

119. Zhan, Y. Z., Shi, X. B., & Xie, H. F. Microstructural investigation on antifriction characteristics of self-lubricating copper hybrid composite. Mater Sci Technol, 2006, 22(3), 368-374.

120. Zhang ZY, Yang R, Li Y, Chen G, Zhao YT, Liu MP. Microstructural evolution and mechanical properties of friction stir processed ZrB2/6061Al nanocomposites. J Alloy Comp, 2018, 762, 312–318.

121. Zhang, X. X., Wei, H. M., Li, A. B., Fu, Y. D., & Geng, L. Effect of hot extrusion and heat treatment on CNTs–Al interfacial bond strength in hybrid aluminium composites. Compos Interfaces, 2013, 20(4), 231-239.

Composites Part B 175 (2019) 107136

Contents lists available at ScienceDirect

Composites Part B

journal homepage: www.elsevier.com/locate/compositesb

Tribological behavior of ultrasonic assisted double stir casted novel nano-composite material (AA7150-hBN) using Taguchi technique

Pagidi Madhukar [a,*], N. Selvaraj [a], C.S.P. Rao [b], Veeresh Kumar G.B. [c]

[a] Department of Mechanical Engineering, National Institute of Technology, Warangal, Telangana, India
[b] National Institute of Technology - Andhra Pradesh, Tadepalligudem, Andhra Pradesh, India
[c] Department of Mechanical Engineering, National Institute of Technology - Andhra Pradesh, Tadepalligudem, Andhra Pradesh, India

ARTICLE INFO

Keywords:
Al7150 alloy
Ultrasonication
Stir casting
Nanocomposites
Hardness
Tribological characteristics

ABSTRACT

A novel Al-7150 nanocomposite material was fabricated with various weight percentages of Hexagonal Boron Nitride from 0.5 to 2 wt% in steps of 0.5 wt% by liquid metallurgy route via ultrasonic assisted double stir casting method. The tribological properties were tested and carried out on pin-on-disc tribometer considering various input parameters like weight percentage of reinforcement, applied load, sliding distance and speed to study the tribological characterization. Taguchi technique using MiniTab 17 software was used to analyse the wear rate of nanocomposites. Different experiments were conducted using Taguchi technique and the regression equations were developed through Analysis of Variance (ANOVA) to investigate the influence of various test parameters such as applied load, sliding distance, sliding speed and the material parameter such as weight percentage of reinforcements. The applied load had the greatest influence on statistical and physical properties of nano-composites while, the sliding speed exercised its impact on the Coefficient of Friction (COF) of nanocomposite on dry sliding wear and also on the optimal parameters for less wear rate and low COF. The worn-out surface morphology of test specimens was investigated through Scanning Electron Microscope (SEM), Energy-Dispersive X-ray spectroscopy (EDX) system and correlated with the obtained results and conclusions were drawn.

1. Introduction

The majority of researchers aimed for designing lighter materials coupled with high strength to weight ratio, resistance to corrosion for automobile and aerospace applications. To meet this demand, researchers have shifted their focus from monolithic materials to high performance materials like Aluminum (Al) based composite materials owing to its properties like light weight, higher stability at heavier loads, resistance to wear, coupled with good corrosion resistance. The Al-Metal Matrix Composites (MMCs) are produced by various techniques such as squeeze casting, spray deposition, powder and liquid metallurgy route specifically via stir casting method [1]. The liquid casting route is a highly interesting technique due to its flexibility with economics in the fabrication of Al-MMCs [2]. Al-MMCs exhibit better mechanical properties with particulate (p) reinforcements because of its high strength and improved wear resistance than the unreinforced Al alloy [3]. From the recent past the Nanocomposites are attracting the attention of researches because they have low density, high strength and other properties such as high thermal conductivity, low Coefficient of Thermal Expansion (CTE) and dumping properties [4]. The production of nano-composites is a very difficult process and faces several hurdles like random distribution of reinforcement particles, poor wettability, porosity, clusters and agglomerations formation during the fabrication. An ultrasonic-assisted stir casting method may overcome the above-mentioned difficulties and also improve the uniform distribution of particles and wettability [5]. The double stir casting (compo casting) technique was adopted to improve the uniform distribution of nano-particles during the fabrication of Al-Metal Matrix Nano-Composites (MMNCs) [6]. In a study of Al-Graphene MMNCs, the nano-grains during the reheating process significantly enhanced the yield strength. The graphene sheets with onion shape have decreased the agglomeration of Silicon Carbide (SiC) nanoparticles. As a result of wrapping graphene sheets, resulted in lessening the porosity, thereby enhancing the tensile properties of the Al-MMNCs [7]. Shusen Wu et al., studied the microstructure and mechanical properties of nano-SiCp/Al MMNCs by diluting the molten Al under Ultrasonic Vibration (UV) via squeeze casting and noticed that the nano-SiCp are uniformly distributed in the Al-SiCp MMNCs and the tensile strength of the MMNCs improved

* Corresponding author.
E-mail address: pmadhu88@gmail.com (P. Madhukar).

https://doi.org/10.1016/j.compositesb.2019.107136
Received 29 November 2018; Received in revised form 19 June 2019; Accepted 5 July 2019
Available online 6 July 2019
1359-8368/

Ultrasonics - Sonochemistry 58 (2019) 104665

Contents lists available at ScienceDirect

Ultrasonics - Sonochemistry

journal homepage: www.elsevier.com/locate/ultson

Production of high performance AA7150-1% SiC nanocomposite by novel fabrication process of ultrasonication assisted stir casting

Pagidi Madhukar[a], N. Selvaraj[a], Raghavendra Gujjala[a,*], Chilakalapalli Surya Prakasa Rao[b]

[a] Department of Mechanical Engineering, National Institute of Technology – Warangal, Telangana 506004, India
[b] National Institute of Technology – Andhra Pradesh, 534102, India

ARTICLE INFO

Keywords:
AA7150
Silicon carbide
Aluminium metal matrix
Nanocomposite
Ultrasonic
Double stir casting

ABSTRACT

The effect of ultrasonic vibration treatment on nanoparticle distribution was successfully investigated and developed a novel fabrication process to produce nano silicon carbide particle reinforced AA7150-1% SiC nanocomposite through a combination of the vortex, double stir casting, and ultrasonic vibration techniques. Ultrasonic frequency of 20 KHz and with a power capacity of 1000 W was used in the process. Ultrasonic probe was used for proper mixing of the nanoparticles in the molten bath. Microstructure investigation of grain formation, particle distribution, and fracture surface was analyzed through an optical and scanning electron microscope at the as-cast condition. Energy dispersive spectroscopy was used for determining chemical composition of the nanocomposite. In the novel fabrication process, the influence of sonication effect on material properties such as porosity, microhardness, tensile strength were examined and compared with double stir casted nanocomposite material as well as the base material. Mechanical properties of AA7150-1% SiC novel fabrication process were enhanced with a reported increase of 26.05% in tensile strength, and 10.85% in microhardness. 74.1% reduction in porosity as compared to the base alloy. In the double stir casting process, there was 19.6% increase in tensile strength, 2.9% of improvement in microhardness, and 46.96% reduction in porosity as compared to base material properties. The enhancement of material properties with the ultrasonic probe assisted novel fabrication process are attributed to grain refinement of composite and homogeneous distribution of SiC nanoparticles due to the acoustic streaming and cavitation effect.

1. Introduction

Ceramic particle reinforced aluminium alloy matrix composites are widely used in aerospace and automobile industries. Al-Zn-Mg-Cu alloys are used especially in upper and lower wings, fuselage and stringers of aeroplane due to high specific modulus and strength to weight ratio [27,30,32]. Silicon carbide particles are an attractive choice as ceramic reinforcement for lightweight alloy matrix due to their desirable characteristics such as high hardness, high melting point, good thermal stability, low thermal coefficient of expansion, high corrosive resistance and low density [21,29]. The strength of aluminium alloy matrix composite depends on the size of reinforcement and interparticle spacing. The micro ceramic particles, which are incorporated as reinforcement into liquid metal matrix to manufacture the composite material for significant improvement in strength of composite material but decreases the elongation. Recently nano ceramic particles were introduced to fabricate metal matrix composites and proven that the effect of size of ceramic reinforcements is playing a crucial role in the composite material properties and distinctly enhancing the base material properties while maintaining beneficial elongation as well as high resistance to temperature creep [9,12,34]. The quality of metal matrix nanocomposites fully depends on the ceramic nanoparticles distribution and dispersion into the liquid metal.

The material properties of metal matrix composites mainly depending upon the selection of production process and processing methods plays a crucial role to satisfy the demands of industries as well as required functional properties [23]. The main disadvantage of preparing aluminium metal matrix composites is heterogeneous distribution of ceramic nanoparticles in molten liquid, higher cost of nanoparticles and initial investment cost. The cost effective fabrication techniques of nanocomposites are essential for elaborate their field of applications [14]. The leading cost effective methods for fabrication of bulk metal matrix composites are stir casting, infiltration, compo casting and powder metallurgy. However, the major problem with externally adding of the nanoparticles to molten liquid is difficult due to high specific volume ratio and poor wettability between matrix and

* Corresponding author.
E-mail address: raghavendra.gujjala@gmail.com (R. Gujjala).

https://doi.org/10.1016/j.ultsonch.2019.104665
Received 21 May 2019; Received in revised form 29 June 2019; Accepted 29 June 2019
Available online 02 July 2019
1350-4177/

Journal of Alloys and Compounds 815 (2020) 152464

Contents lists available at ScienceDirect

Journal of Alloys and Compounds

journal homepage: http://www.elsevier.com/locate/jalcom

Fabrication and characterization two step stir casting with ultrasonic assisted novel AA7150-hBN nanocomposites

Pagidi Madhukar [a, *], N. Selvaraj [a], C.S.P. Rao [b], G.B. Veeresh Kumar [c]

[a] Department of Mechanical Engineering, National Institute of Technology, Warangal, Telangana State, 506004, India
[b] National Institute of Technology-Andhra Pradesh, Tadepalligudem, Andhra Pradesh, 534102, India
[c] Department of Mechanical Engineering, National Institute of Technology-Andhra Pradesh, Tadepalligudem, Andhra Pradesh, 534102, India

ARTICLE INFO

Article history:
Received 24 June 2019
Received in revised form
24 September 2019
Accepted 25 September 2019
Available online 27 September 2019

Keywords:
Al7150
hBN particulates
Nanocomposite
Ultrasonic
Stir casting
Strength
Wear

ABSTRACT

The Al7150 alloy plays a vital role in aerospace and automotive industry applications due to its extraordinary characteristics like strength to weight ratio, toughness and fatigue resistance. But in the current scenario researchers are looking for significant improvement in wear resistance at various service loads. It is in such a context this paper deals with the fabrication, mechanical and wear resistance properties investigation of the Al7150-hBN nanocomposites, which is fabricated through ultrasonic assisted double Stir casting technique and compared with monolithic material. The microstructure studies were carried out through Optical Microscope (OM) for grain structure, Scanning Electron Microscope (SEM) for particle distribution, ultimate tensile strength including the morphological studies related to fracture surface and Energy Dispersive X-ray (EDX) spectroscopy for elemental analysis. The pin on disc tribometer was used to study the tribological characteristics of the developed nanocomposite materials by varying the applied loads and weight percentage of hBN reinforcement at a constant sliding speed and distance. The SEM images of the worn-out surfaces were studied extensively to study the tribological properties.

1. Introduction

Aluminum (Al) based alloys are highly attractive materials to aerospace and atomic structure applications due to their lightweight properties but they suffer from poor wear resistance. For improving the desired properties of these alloys, Al Metal Matrix Composites (MMCs) were introduced by adding reinforcement particles. These reinforcements act as second phase particles to improve the properties of Al-MMCs and ensure environmental benefits. Therefore, Al-MMCs are widely using in structural applications instead of monolithic and other engineering materials like ferrous and nonferrous alloys. Al-MMCs are playing a major role in aerospace and automotive applications [1] due to their strength to weight ratio and low density. From the last two decades [2], several manufacturing methods are available to produce Metal Matrix Composites (MMCs) which can be classified into two major types. One is solid state fabrication process and another one is liquid state fabrication process. In solid state, mechanical milling and mechanical alloying [3] are used to improve the mechanical properties of MMCs. This enhancement mainly due to re-welding of fractured particle, cold welding and flattering of particles during ball milling. For decreasing porosity and homogeneous distribution of particles, secondary processes are used like extrusion and forging or rolling methods. In case of liquid state, processes classified like stir casting [4], compocasting [5], squeeze casting [6], in-situ synthesis [7] and liquid metal infiltration [8–10]. From the above methods, stir casting is more economical and prominent method to fabricate bulk quantity of MMCs [11]. The reinforcement particles are sorted out into two different sizes: micro and nano. The micro reinforcements enhance engineering properties but lower the ductility. In recent years, nano-sized reinforcements have been introduced and used in place of micro-particles due to its high surface to volume ratio (1000 times more) compared to the micro-particles area [12], which results in superior performance. Few researchers have proved that the alloy has enhanced fatigue life as well as high resistance to temperature creep [5,13], however, the preparation of Al-MMCs with the nano-sized particles in liquid pool is very difficult to distribute homogeneously because of its poor wettability, clusters and agglomerations formation. In such

* Corresponding author.
E-mail address: pmadhu88@gmail.com (P. Madhukar).

https://doi.org/10.1016/j.jallcom.2019.152464
0925-8388/

Materials Research Express

PAPER

Microstructure studies of AA7150-hBN nanocomposites fabricated by ultrasonic assisted stir casting

RECEIVED
9 September 2019

REVISED
26 September 2019

ACCEPTED FOR PUBLICATION
27 September 2019

PUBLISHED
4 October 2019

Pagidi Madhukar[1], **N Selvaraj**[1], **Gurabvaiah Punugupati**[1], **G B Veeresh Kumar**[2], **C S P Rao**[3] and **S K Mishra**[4]

[1] Department of Mechanical Engineering, National Institute of Technology- Warangal, Telangana, 506004, India
[2] Department of Mechanical Engineering, National Institute of Technology- Andhra Pradesh, 534101, India
[3] Director, National Institute of Technology- Andhra Pradesh, 534101, India
[4] CEO, Brahmos Aerospace,110010, India

E-mail: pmadhu88@gmail.com

Keywords: nanocomposites, AA7150, ultrasonic, stir casting, microstructure, hBN

Abstract

For two decades, the Al7XXX series alloys have been playing an extensive role in aerospace and automotive industrial applications due their excellent properties such as toughness, fatigue, strength and low density. However, the current scenario for all these applications, there is a significant improvement at service loads as well as wear resistance properties at elevated temperatures. The main focus of the current investigation is with the microstructure analysis of AA7150-hexagonal Boron Nitride (hBN) nanocomposites which are fabricated through ultrasonic assisted double stir casting process. The Scanning Electron Microscope and Optical Microscope were used to study the particle distribution, grain refinement of the monolithic AA7150 alloy, nanocomposites. The fractured surfaces and wear surfaces were also studied the influence of applied load as well as hBN weight percentage on nanocomposites and compared with base matrix.

1. Introduction

Reinforcement of ceramic nanoparticles in the Metal Matrix Composites (MMCs) are suitable and promising materials for wide range of applications. The fabrication of metal matrix nanocomposites (MMnCs) is facing a crucial problem of low wettability with nano-level fine particles in the molten metal liquid which prone to form agglomeration/clusters during the process. These agglomerations/clusters leads to reduce the uniform distribution of ceramic nanoparticles throughout the molten matrix, result in loss of composite strengthening potential. To avoid this problem during the fabrication process of MMnCs, the ultrasonic assisted stir casting was introduced [1]. Wu *et al* [2], investigated the microstructure as well as mechanical properties of Al356-SiCnp nanocomposites which is fabricated by ultrasonic treatment via squeeze casting. It is noticed that the SiC nanoparticles are homogeneously dispersed and enhancement of tensile strength of the MMnCs compared to base Al356 alloy. Aluminum (Al)-Magnesium (Mg)-Zinc (Zn)-Cupper (Cu) alloy materials are widely used as critical components in automotive and aerospace sectors due to their superior physical and mechanical properties such as strength to weight ratio, higher ductility, high temperature survivability and numerous engineering properties [1, 2]. Yet, they exhibit low abrasive wear under lubricating conditions against the sliding surface making them less futile to tribological applications consequently failure of various components. However, to overcome this problem, solid lubricants were introduced into the aluminium alloys for preparing the MMCs [3–5]. Especially in upper and lower wings, fuselage, stringers and passenger seat tracks of an aircraft. Due to self-lubricating property, the composites accentuated high damping capacity, low thermal expansion [6], low wear and friction [7, 8] an excellent anti-seizure property [9, 10] besides exhibiting reduced temperature rise [11, 12] at mating surface. This research article deals with microstructure analysis of monolithic AA7150 and hBN reinforced nanocomposites for particle distribution through Scanning Electron Microscope (SEM), grain size through Optical Microscope (OM); further, the studies on the surface wear of the AA7150 and hBN

Materials Science Forum
ISSN: 1662-9752, Vol. 969, pp 882-888
doi:10.4028/www.scientific.net/MSF.969.882

Submitted: 2018-11-16
Revised: 2019-02-20
Accepted: 2019-02-23
Online: 2019-08-30

Fabrication of Light Weight Metal Matrix Nanocomposites using Ultrasonic Cavitation Process: A State of Review

Pagidi Madhukar[1*,a] N Selvaraj[1,b] C S P Rao[2,c] S K Mishra[3,d] Gurabvaiah Punugupati[4,e]

[1*,1,4]Department of Mechanical Engineering, National Institute of Technology-Warangal, Telangana, India

[2]Director, National Institute of Technology - Andhra Pradesh, India

[3]CEO, Brahmos Aerospace, India

[a]pmadhu88@gmail.com, [b]selva@nitw.ac.in, [c]csp_rao@rediffmail.com, [d]mishrasudhir@gmail.com, [e]guru.punugupati65@gmail.com

Keywords: Ultrasonic Cavitation. Metal Matrix Nanocomposites, Nanoparticles, Stir Casting

Abstract. Fabrication of nanocomposites is a highly challenging task because of the particles need to be disseminated across the molten liquid. The broad surface area, poor wettability. Homogeneous dispersion is tough in traditional stirring methods leads to cluster and agglomeration formation in high viscous molten metals. In such attempts, the ultrasonic vibration process exhibits the better dispersion and distribution of nanocomposites with enhanced material properties as compared to other fabrication processes. This paper deals with the fabrication process, probe design and effective process parameters of sonication process to the uniform dispersion of nanoparticles.

Introduction

From the last two decades, researchers are aiming for aluminum and magnesium…etc. because of material high strength to weight ratio value. The traditional fabrication methods for lightweight metal matrix composites involve mechanical stirring, powder metallurgy, squeeze casting and semisolid stirring. In recent years the ceramic particles have been scaled up to nano-size such as nano Al2O3, SiC, B4C, BN, TiC, TiB2..etc. have been used to reinforcements to form metal matrix nanocomposite (MMNC). There are several ways to produce MMNCs, the popular methods being powder metallurgy and liquid casting route respectively. The casting process is a liquid phase method to manufacture a component with highly complex in shapes. But getting uniform dispersion and distribution of ceramic particle in a metallic liquid is highly difficult due to its poor wettability, high viscosity as well as a huge ratio of surface to volume.

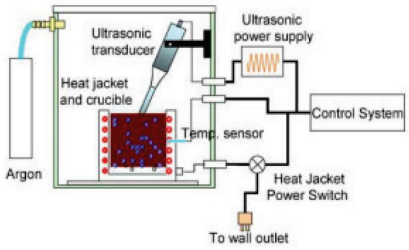

Figure 1. Schematic view of ultrasonic cavitation process set-up

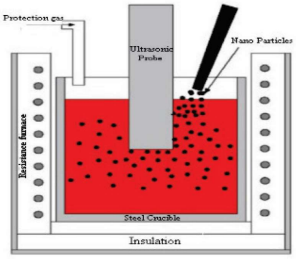

Figure 2. Experimental set-up for fabricating nanocomposites.[11]

With fabrication process, the nano-sized particles creates the problems like clusters and agglomerations during the incorporating, but new sonication and high shearing methods were initiated to help the dispersion, degassing and de-agglomeration of fine as well as nano-sized particles in aluminium and other alloys. Recently some researchers have proven that the

Manufacturing of aluminium nano hybrid composites: a state of review

P Madhukar[1], N Selvaraj[1], C S P Rao[1]

[1]Mechanical Engineering Department, National Institute of Technology, Warangal, Telangana, India-506004

Email: pmadhu88@gmail.com

Abstract. This paper gives the details of hybrid composites, their fabrication methods and evaluation of mechanical, tribological behaviour and machining characteristics. Investigations on the various aspects of Hybrid composites furnish several conclusions regarding the influence of various parameters on the performance of the composites. Mostly micro structures of the hybrid composites fabricated through casting routes have been found to be stable with the distribution of uniformed reinforce particles. therefore, the hybrid composites can be constructed with various combinations of reinforcements to carry out desirable mechanical properties. The density of Hybrid composites increases with increasing reinforcements such as SiC, TiC, B4C....etc, while incorporation of partial reinforcements like fly ash, mica, rice husk, etc. reduces the density of composites. The study also reports that the hybrid composites can be treated as a replacement for regular composite materials in different advanced applications.

1. Introduction

Materials required for the present world are stronger, lighter and cost effective. Present researchers are focusing to develop hybrid composites, which has good strength to weight ratio to meet the requirement. The main advantages[56] of Hybrid Composites over monolithic, alloys and composite materials were high strength to weight ratio, good corrosion/wear resistance, strength/stiffness, low thermal conductivity/coefficient of thermal expansion, light weight, Better impact and flexural properties Reduced overall cost of the composite. The example: aircraft as well as Automobile applications, where the fuel economy plays the key role.Hybrid composites consisting of one matrix and two or more reinforcement. These are bonded due to heterogeneous mixing of one or more particles reinforcement, which has been homogeneous phases at macro level and fabricated through various techniques such as powder metallurgy[3,5,6,19,26,30,33,40,52] route, stir casting[10,13,16,22-24,27,28,36,38,46-48], two step stir casting[41-43,34], squeeze casting[12,31] to aim the mechanical properties and tribological behavior: high specific strength, including stiffness, density, micro hardness, low coefficient of thermal expansion, high thermal resistance, good damping capacities, better wear resistance, and corrosion resistance

Gmail **Madhukar Pagidi <pmadhu88@gmail.com>**

NOIEAS: ACCEPTANCE OF PAPER ID-ME329

1 message

DEBASHIS DUTTA <noieas2019@gmail.com> Thu, Nov 28, 2019 at 10:28 AM
To: Madhukar Pagidi <pmadhu88@gmail.com>

Dear Sir/Madam

I am happy to inform you that your paper entitled "

Optimization of Wear Parameters of AA7150-TiC Nanocomposites by Taguchi Technique

" has been qualified in SPRINGER Check and has been accepted for publication in the Lecture series entitled, **"Advances in Intelligent Systems and Computing" (SCOPUS)**. The Joint Editors of this publication are:

(1) Prof Debashis Dutta, Department of Mathematics, NIT-Warangal &
(2) Prof Biswajit Mahanty, Department of Industrial and Systems Engineering, IIT- Kharagpur

The timeline of the publication is about 10 to 12 weeks. as informed by SPRINGER Office, New Delhi.

I appreciate your contribution towards the conference. Hope that you shall attend with your new research findings in my future conference.

With regards

--
Prof Debashis Dutta
Convenor, NOIEAS-2019
Department of Mathematics
NIT-Warangal, PIN-506004, T.S.
Mobile: +91 8332969450

Gmail **Madhukar Pagidi <pmadhu88@gmail.com>**

NOIEAS: ACCEPTANCE OF PAPER ID-ME327

1 message

DEBASHIS DUTTA <noieas2019@gmail.com> Thu, Nov 28, 2019 at 10:30 AM
To: Madhukar Pagidi <pmadhu88@gmail.com>

Dear Sir/Madam

I am happy to inform you that your paper entitled "

Process Optimization of Digital Conjugate Surfaces : A Review

" has been qualified in SPRINGER Check and has been accepted for publication in the Lecture series entitled, "**Advances in Intelligent Systems and Computing**" (**SCOPUS**). The Joint Editors of this publication are:

(1) Prof Debashis Dutta, Department of Mathematics, NIT-Warangal &
(2) Prof Biswajit Mahanty, Department of Industrial and Systems Engineering, IIT- Kharagpur

The timeline of the publication is about 10 to 12 weeks. as informed by SPRINGER Office, New Delhi.

I appreciate your contribution towards the conference. Hope that you shall attend with your new research findings in my future conference.

With regards

--
Prof Debashis Dutta
Convenor, NOIEAS-2019
Department of Mathematics
NIT-Warangal, PIN-506004, T.S.
Mobile: +91 8332969450